Remote-sensing Indices of Trophic Availability (RITA) for ecosystem status

C. Fuentes-Yaco[1], S.E. Craig[2], C. Caverhill[1], E. Head[1], and W.K.W. Li[1]

[1] Fisheries and Oceans Canada, Science Branch, Ocean and Ecosystem Sciences Division, PO Box 1006, Dartmouth, Nova Scotia B2Y 4A2

[2] CERC. OCEAN, Dept. of Oceanography, Steele Ocean Sciences Building, Dalhousie University, 1355 Oxford Street, P.O. Box 15000, Halifax, Nova Scotia, B3H 4R2

2016

Canadian Technical Report of
Fisheries and Aquatic Sciences 3166

Fisheries and Oceans Canada | Pêches et Océans Canada

Canada

Canadian Technical Report of Hydrography and Ocean Sciences

Technical reports contain scientific and technical information that contributes to existing knowledge but which is not normally appropriate for primary literature. Technical reports are directed primarily toward a worldwide audience and have an international distribution. No restriction is placed on subject matter and the series reflects the broad interests and policies of Fisheries and Oceans Canada, namely, fisheries and aquatic sciences.

Technical reports may be cited as full publications. The correct citation appears above the abstract of each report. Each report is abstracted in the data base *Aquatic Sciences and Fisheries Abstracts*.

Technical reports are produced regionally but are numbered nationally. Requests for individual reports will be filled by the issuing establishment listed on the front cover and title page.

Numbers 1-456 in this series were issued as Technical Reports of the Fisheries Research Board of Canada. Numbers 457-714 were issued as Department of the Environment, Fisheries and Marine Service, Research and Development Directorate Technical Reports. Numbers 715-924 were issued as Department of Fisheries and Environment, Fisheries and Marine Service Technical Reports. The current series name was changed with report number 925.

Rapport technique canadien sur l'hydrographie et les sciences océaniques

Les rapports techniques contiennent des renseignements scientifiques et techniques qui constituent une contribution aux connaissances actuelles, mais qui ne sont pas normalement appropriés pour la publication dans un journal scientifique. Les rapports techniques sont destinés essentiellement à un public international et ils sont distribués à cet échelon. Il n'y a aucune restriction quant au sujet; de fait, la série reflète la vaste gamme des intérêts et des politiques de Pêches et Océans Canada, c'est-à-dire les sciences halieutiques et aquatiques.

Les rapports techniques peuvent être cités comme des publications à part entière. Le titre exact figure au-dessus du résumé de chaque rapport. Les rapports techniques sont résumés dans la base de données *Résumés des sciences aquatiques et halieutiques*.

Les rapports techniques sont produits à l'échelon régional, mais numérotés à l'échelon national. Les demandes de rapports seront satisfaites par l'établissement auteur dont le nom figure sur la couverture et la page du titre.

Les numéros 1 à 456 de cette série ont été publiés à titre de Rapports techniques de l'Office des recherches sur les pêcheries du Canada. Les numéros 457 à 714 sont parus à titre de Rapports techniques de la Direction générale de la recherche et du développement, Service des pêches et de la mer, ministère de l'Environnement. Les numéros 715 à 924 ont été publiés à titre de Rapports techniques du Service des pêches et de la mer, ministère des Pêches et de l'Environnement. Le nom actuel de la série a été établi lors de la parution du numéro 925.

Canada

Canadian Technical Report of
Fisheries and Aquatic Sciences 3166

2016

Remote-sensing Indices of Trophic Availability (RITA) for ecosystem status

César Fuentes-Yaco[1], Susanne E. Craig[2], Carla Caverhill[1], Erica Head[1], and William K.W. Li[1]

[1] Fisheries and Oceans Canada, Science Branch, Ocean and Ecosystem Sciences Division, PO Box 1006, Dartmouth, Nova Scotia B2Y 4A2

[2] CERC. OCEAN, Dept. of Oceanography, Steele Ocean Sciences Building, Dalhousie University, 1355 Oxford Street, P.O. Box 15000, Halifax, Nova Scotia, B3H 4R2

© Her Majesty the Queen in Right of Canada, 2016.
Cat. No. Fs 97-6/3166E-PDF ISBN 978-0-660-05267-0 ISSN 0706-6457

Correct citation for this publication:

Fuentes-Yaco, C., Craig, S., Caverhill, C., Head, E., and Li, W.K.W. 2016. Remote-sensing indices of trophic availability (RITA) for ecosystem status. Can. Tech. Rep. Fish. Aquat. Sci. 3166 : xiii + 87 p.

TABLE OF CONTENTS

TABLE OF CONTENTS iii
LIST OF TABLES v
LIST OF FIGURES vii
ABSTRACT xii
RÉSUMÉ xiii
1. INTRODUCTION 1
1.1 PURPOSE AND OBJECTIVE 1
1.2 STUDY AREA 2
1.2.1 NAFO Convention Area 4
1.2.2 Labrador Sea 5
1.2.3 NAFO Subarea 1 5
2. METHODS 7
2.1 SATELLITE-DERIVED DATA 7
2.1.1 Phytoplankton bloom 8
2.2 ECOLOGICAL INDICES COMPUTATION 9
2.2.1 NAFO divisions 10
2.2.2 Labrador Sea Transect 10
3. RESULTS 14
3.1 COMPARISON OF *IN SITU* AND SATELLITE DATA 14
3.2 NAFO DIVISIONS 15
3.2.1 Phytoplankton bloom 15
3.2.2 RITA Index 18
3.2.3 Cluster Analysis 21
3.3 LABRADOR SEA TRANSECT 23
3.3.1 Phytoplankton bloom 23
3.3.2 SST warming 25
3.3.3 Relationship between the environmental variability and *C. finmarchicus* abundance 27
3.4 NAFO SUBAREA 1 29
3.4.1 SST and Chlorophyll cycles 29
3.4.2 Relationship among ecological indices and *Pandalus borealis* 31
4. DISCUSSION 33
4.1 REGIONAL VARIATION IN THE RITA AMONG NAFO DIVISIONS 33
4.2 RELATIONSHIPS BETWEEN ZOOPLANKTON ABUNDANCE AND ENVIRONMENTAL VARIABLES ON THE L-3 LABRADOR SEA TRANSECT 35
4.3 RELATIONSHIPS BETWEEN THE ABUNDANCE OF SHRIMP AND ENVIRONMENTAL VARIABLES IN NAFO SUBAREA 1 35
ACKNOWLEDGMENTS 35

REFERENCES CITED....36
APPENDICES....51
APPENDIX 1....51
APPENDIX 2....60
APPENDIX 3....74
APPENDIX 4....86

LIST OF TABLES

Table 1.	Phytoplankton bloom indices derived from SeaWiFS in the NAFO Division 0A, between 1998 and 2010.	39
Table 2.	Phytoplankton bloom indices derived from SeaWiFS in the NAFO Division 0B, between 1998 and 2010.	39
Table 3.	Phytoplankton bloom indices derived from SeaWiFS in the NAFO Division 1A, between 1998 and 2010.	40
Table 4.	Phytoplankton bloom indices derived from SeaWiFS in the NAFO Division 1B, between 1998 and 2010.	40
Table 5.	Phytoplankton bloom indices derived from SeaWiFS in the NAFO Division 1C, between 1998 and 2010.	40
Table 6.	Phytoplankton bloom indices derived from SeaWiFS in the NAFO Division 1D, between 1998 and 2010.	41
Table 7.	Phytoplankton bloom indices derived from SeaWiFS in the NAFO Division 1E, between 1998 and 2010.	41
Table 8.	Phytoplankton bloom indices derived from SeaWiFS in the NAFO Division 1F, between 1998 and 2010.	41
Table 9.	Phytoplankton bloom indices derived from SeaWiFS in the NAFO Division 2G, between 1998 and 2010.	42
Table 10.	Phytoplankton bloom indices derived from SeaWiFS in the NAFO Division 2H, between 1998 and 2010.	42
Table 11.	Phytoplankton bloom indices derived from SeaWiFS in the NAFO Division 2J, between 1998 and 2010.	42
Table 12.	Phytoplankton bloom indices derived from SeaWiFS in the NAFO Division 3K, between 1998 and 2010.	43
Table 13.	Phytoplankton bloom indices derived from SeaWiFS in the NAFO Division 3L, between 1998 and 2010.	43
Table 14.	Phytoplankton bloom indices derived from SeaWiFS in the NAFO Division 3M, between 1998 and 2010.	43
Table 15.	Phytoplankton bloom indices derived from SeaWiFS in the NAFO Division 3N, between 1998 and 2010.	44
Table 16.	Phytoplankton bloom indices derived from SeaWiFS in the NAFO Division 3O, between 1998 and 2010.	44

Table 17.	Phytoplankton bloom indices derived from SeaWiFS in the NAFO Division 3Pn, between 1998 and 2010.	44
Table 18.	Phytoplankton bloom indices derived from SeaWiFS in the NAFO Division 3Ps, between 1998 and 2010.	45
Table 19.	Phytoplankton bloom indices derived from SeaWiFS in the NAFO Division 4R, between 1998 and 2010.	45
Table 20.	Phytoplankton bloom indices derived from SeaWiFS in the NAFO Division 4S, between 1998 and 2010.	45
Table 21.	Phytoplankton bloom indices derived from SeaWiFS in the NAFO Division 4T, between 1998 and 2010.	46
Table 22.	Phytoplankton bloom indices derived from SeaWiFS in the NAFO Division 4Vn, between 1998 and 2010.	46
Table 23.	Phytoplankton bloom indices derived from SeaWiFS in the NAFO Division 4Vs, between 1998 and 2010.	46
Table 24.	Phytoplankton bloom indices derived from SeaWiFS in the NAFO Division 4W, between 1998 and 2010.	47
Table 25.	Phytoplankton bloom indices derived from SeaWiFS in the NAFO Division 4X, between 1998 and 2010.	47
Table 26.	Phytoplankton bloom indices derived from SeaWiFS in the NAFO Division 5Y, between 1998 and 2010.	47
Table 27.	Phytoplankton bloom indices derived from SeaWiFS in the NAFO Division 5Ze, between 1998 and 2010.	48
Table 28.	Phytoplankton bloom indices derived from SeaWiFS in the NAFO Division 5Zw, between 1998 and 2010.	48
Table 29.	Sea Surface Temperatures (°C) and times (day of year – DOY) at both, initiation and inflexion point of the seasonal warming at the five regions and the eleven years of data.	49
Table 30.	PCA loadings of the phytoplankton bloom and warming sea surface temperature indices, for the pooled five regions in the Labrador Sea (W, WC, C, EC and E), between 2003 and 2013.	50
Table 31.	PCA loadings of the phytoplankton bloom and warming sea surface temperature indices, for the pooled five regions in Western Greenland (1A, 1B, 1C 1D and 1E), between 1998 and 2010.	50

LIST OF FIGURES

Figure 1.	The study area is located in the North West Atlantic, from 39° to 82° N, and 42° to 95°W.	3
Figure 2.	NAFO Convention Area, showing Subareas 0 to 5 that include the twenty-eight divisions (1A until 5Ze) used in this study.	4
Figure 3.	Labrador Sea Transect: Line 3 of the Atlantic Zone off Shelf Monitoring Program. The *Calanus finmarchicus* sampling stations are located in the centre of each of the 28 rectangles (red). The assemblage in five regions: Western Western-Central, Central, Eastern-Central and Eastern are shown in green.	5
Figure 4.	Approximated correspondence between NAFO Divisions 1A to 1E (left) and *Pandalus borealis* density distribution in West Greenland (right, adapted from Figure 1 in Burmeister *et al* 2013).	7
Figure 5.	Identification of biological indices derived from chlorophyll_a concentration during the phytoplankton bloom. The table (left) shows the day of year (DOY), the average of chlorophyll a concentration (Log (mg m^{-3})), the fitted values, and the first difference. Coloured bars show the bloom characteristics in terms of pigment concentration and time of occurrence: initiation (green), increasing inflexion point (orange), maximum (red), decreasing inflexion point (light blue), and end (dark blue). The top graph shows chlorophyll_a concentration during the blooming period, and the lower graph shows the first order difference.	11
Figure 6.	Hovmöller diagram of the Gaussian fitted climatology of Chlorophyl_a, for the period between 2003 and 2013. The ordinate are weekly Chl_a (Log_{10} (mg m^{-3}), while the abscissa are stations (top) and longitudes (bottom), along Line 3 of AZMP Off Shelf. Vertical lines indicate the stations grouped to define the regions: Western (W), Western-Central (WC), Central (C), Eastern-Central (EC), and Eastern (E).	12
Figure 7.	Identification of warming indices derived from the sea surface temperature (SST) along an extended annual cycle. The table (left) shows the day of year (DOY), the SST (°C), the fitted values, and the first difference. Colours show the characteristics in SST and time of their occurrence: initiation (green), increasing inflexion point (orange), maximum (red), decreasing inflexion point (light blue), and end (dark blue). The top graph is for the SST during the annual cycle, and the lower graph is for the first order difference during the same time period.	13
Figure 8.	Comparison of in situ and satellite-derived chlorophyll_a measurements (Log (mg m^{-3})): left) matching locations (red symbols), centre) SeaWiFS regression and right) MODIS regression. Green lines represent SMA fits and dashed the one to one lines.	14

Figure 9.	Chlorophyll a concentration (Log_{10} (mg m^{-3})) average for each of the 28 NAFO divisions. Open symbols are 13-years mean (1998 to 2010), and the solid line is the regression from the five-parameter logistic equation. Note, the time axes are not of equal duration.	16
Figure 10.	Average for all NAFO division of anomalies annual variability between 1998 and 2010 of: a) Chlorophyll_a concentration at initiation of the bloom (mg m_3), b) Chl_a at the maximum (mg m^{-3}), c) Time at maximum (day of year). A trend line computed using a moving average of 3 years is also shown.	18
Figure 11.	Average of the RITA index (d^{-1}) for all NAFO division of anomalies year variability between 1998 and 2010. The trend line computed using a moving average of 3 years is also shown.	19
Figure 12.	Average of RITA index (d^{-1}) sorted from highest to lowest index values.	19
Figure 13.	Climatology (1998-2010) of RITA Index for all NAFO divisions.	20
Figure 14.	Cluster analysis of NAFO divisions using medoid partitioning algorithms (PAM) applied on RITA anomalies. a) Silhouette width showing five clusters with two negative values (3K and 4Vs), b) Map of the study area showing the spatial distribution of the five clusters, and two regions inferred as transitional environments (orange polygons).	22
Figure 15.	Abundance of *Calanus finmarchicus* copepodites C1 + C2 (Log_{10}(N m^{-2}) by region and year.	23
Figure 16.	Averages (2003 until 2013) of Chlorophyll_a (Log (mg m^{-3})) and abundance of *Calanus f.* copepodites (1+2) (Log_{10}(N m^{-2})) for the five regions (W, WC, C, EC, and E). Pigment concentrations (open circles), Gaussian fit (solid line) and copepods date of sampling and abundance (red line) are shown.	24
Figure 17.	Hovmöller diagram of the climatology of Sea Surface Temperature for the period between 2003 and 2013. The ordinate are weekly SST (°C), while the abscissas are stations (top) and longitudes (bottom), along Line 3 of AZOMP. Vertical lines indicate the stations grouped in the regions definition: Western (W), Western-Central (WC), Central (C), Eastern-Central (EC), and Eastern (E).	25
Figure 18.	Regional averages (2003 until 2013) of Sea Surface Temperature (°C) and abundance of *Calanus f.* copepodites (1+2) (Log_{10}(N m^{-2})). SST (open circles), Gaussian fit (solid line) and copepods date of sampling and abundance (red line) are shown.	26
Figure 19.	a) Non-parametrical (Loess) regression on the abundance of *Calanus*	27

	(copepodites 1+2) and the first two PCA components of the environmental variables, phytoplankton bloom characteristics (CHL), and water warming rate at the sampling date (SST). Empty symbols represent copepods abundance, solid line is the regression, and dashes are the 1 to 1 line. b) Residuals of the Loess regression.	
Figure 20.	Mean carapace length (mm) at age two of *Pandalus borealis* in West Greenland (compiled from Burmeister *et al* 2013, Tables 9 a and b).	29
Figure 21.	Satellite-derived Sea Surface Temperature (°C) annual averages (from 1991 until 2012) for NAFO divisions 1A, 1B, 1C, 1D, 1E, and 1F.	30
Figure 22.	Hovmöller diagram of Sea Surface Temperature (°C) annual cycles (Gaussian fit) for NAFO divisions 1A, 1B, 1C, 1D, 1E and 1F, from 1991 until 2012.	30
Figure 23.	Satellite-derived climatology of SST (red solid line) and phytoplankton bloom (green solid line) for NAFO divisions 1A, 1B, 1C, 1D, and 1E. Red dashed line relates the warming inflexion points and the green dashed line comes near to the maxima of phytoplankton concentrations.	31
Figure 24.	a) Non-parametrical (Loess) regression on the abundance of 2-years old *Pandalus borealis* (lagged 2 years) and the PCA components of the environmental variables. Empty symbols represent shrimp abundance, solid line is the regression and dashes are the 1 to 1 line. b) Residuals of the Loess model regression.	33
Figure APX1-1.	Annual variability of anomalies of Chlorophyll_a at initiation of the bloom (mg m^{-3}), by NAFO division between 1998 and 2010. A trend line computed using a moving average of 3 years is also shown.	52
Figure APX1-2.	Annual variability of anomalies of Chlorophyll_a at maximum of the bloom (mg m^{-3}), by NAFO division between 1998 and 2010. A trend line computed using a moving average of 3 years is also shown.	54
Figure APX1-3.	Annual variability of anomalies of time at maximum of the bloom (day of year), by NAFO division between 1998 and 2010. A trend line computed using a moving average of 3 years is also shown	56
Figure APX1-4.	Annual variability of anomalies of the RITA-index (d^{-1}), by NAFO division between 1998 and 2010. A trend line computed using a moving average of 3 years is also shown.	58
Figure APX2-1.	Anomaly of the RITA index by NAFO divisions in 1998.	61
Figure APX2-2.	Anomaly of the RITA index by NAFO divisions in 1999.	62
Figure APX2-3.	Anomaly of the RITA index by NAFO divisions in 2000.	63

Figure APX2-4.	Anomaly of the RITA index by NAFO divisions in 2001.	64
Figure APX2-5.	Anomaly of the RITA index by NAFO divisions in 2002.	65
Figure APX2-6.	Anomaly of the RITA index by NAFO divisions in 2003.	66
Figure APX2-7.	Anomaly of the RITA index by NAFO divisions in 2004.	67
Figure APX2-8.	Anomaly of the RITA index by NAFO divisions in 2005.	68
Figure APX2-9.	Anomaly of the RITA index by NAFO divisions in 2006.	69
Figure APX2-10.	Anomaly of the RITA index by NAFO divisions in 2007.	70
Figure APX2-11.	Anomaly of the RITA index by NAFO divisions in 2008.	71
Figure APX2-12.	Anomaly of the RITA index by NAFO divisions in 2009.	72
Figure APX2-13.	Anomaly of the RITA index by NAFO divisions in 2010.	73
Figure APX3-1.	Chlorophyll_a (Log_{10}(mg m^{-3})) and abundance of copepodites 1 and 2 (Log_{10}(N m^{-2})) for the Western region from 2003 until 2013. Pigment concentrations (open circles), Gaussian fitted (solid line) and copepods date of sampling and abundance (red line) are shown.	75
Figure APX3-2.	Chlorophyll_a (Log_{10}(mg m^{-3})) and abundance of copepodites 1 and 2 (Log_{10}(N m^{-2})) for the Western-Central region from 2003 until 2013. Pigment concentrations (open circles), Gaussian fitted (solid line) and copepods date of sampling and abundance (red line) are shown.	76
Figure APX3-3.	Chlorophyll_a (Log_{10}(mg m^{-3})) and abundance of copepodites 1 and 2 (Log_{10}(N m^{-2})) for the Central region from 2003 until 2013. Pigment concentrations (open circles), Gaussian fitted (solid line) and copepods date of sampling and abundance (red line) are shown.	77
Figure APX3-4.	Chlorophyll_a (Log_{10}(mg m^{-3})) and abundance of copepodites 1 and 2 (Log_{10}(N m^{-2})) for the Eastern-Central region from 2003 until 2013. Pigment concentrations (open circles), Gaussian fitted (solid line) and copepods date of sampling and abundance (red line) are shown.	78
Figure APX3-5.	Chlorophyll_a (Log_{10}(mg m^{-3})) and abundance of copepodites 1 and 2 (Log_{10}(N m^{-2})) for the Eastern region from 2003 until 2013. Pigment concentrations (open circles), Gaussian fitted (solid line) and copepods date of sampling and abundance (red line) are shown.	79
Figure APX3-6.	Sea Surface Temperature (°C) and abundance of copepodites 1 and 2 (Log_{10}(N m^{-2})) for the Western region from 2003 until 2013. SST (open circles), Gaussian fitted (solid line) and copepods date of sampling and abundance (red line) are shown.	80

Figure APX3-7.	Sea Surface Temperature (°C) and abundance of copepodites 1 and 2 ($Log_{10}(N\ m^{-2})$) for the Western-Central region from 2003 until 2013. SST (open circles), Gaussian fitted (solid line) and copepods date of sampling and abundance (red line) are shown.	81
Figure APX3-8.	Sea Surface Temperature (°C) and abundance of copepodites 1 and 2 ($Log_{10}(N\ m^{-2})$) for the Central region from 2003 until 2013. SST (open circles), Gaussian fitted (solid line) and copepods date of sampling and abundance (red line) are shown.	82
Figure APX3-9.	Sea Surface Temperature (°C) and abundance of copepodites 1 and 2 ($Log_{10}(N\ m^{-2})$) for the Eastern-Central region from 2003 until 2013. SST (open circles), Gaussian fitted (solid line) and copepods date of sampling and abundance (red line) are shown.	83
Figure APX3-10.	Sea Surface Temperature (°C) and abundance of copepodites 1 and 2 ($Log_{10}(N\ m^{-2})$) for the Eastern region from 2003 until 2013. SST (open circles), Gaussian fitted (solid line) and copepods date of sampling and abundance (red line) are shown.	84
Figure APX3-11.	Relative importance of Principal Components of the satellite-derived phytoplankton bloom characteristics (blue line) and warming Sea Surface Temperature (red line) for the pooled five regions in Labrador Sea (W, WC, C, EC and E), and eleven years (2003 until 2013).	85
Figure APX3-12.	f-values for the fitted values (left) and the corresponding residuals (right) for the Loess regression on *Calanus* (copepodites 1+2) abundance in the Labrador Sea.	85
Figure APX4-1.	Relative importance of Principal Components of the satellite-derived phytoplankton bloom characteristics (blue line) and warming Sea Surface Temperature (red line), for the pooled five regions in Western Greenland (1A, 1B, 1C, 1D and 1E), and thirteen years (1998 until 2010).	87
Figure APX4-2.	f-values for the fitted values (left) and the corresponding residuals (right) for the Loess regression on *Pandalus borealis* (age 2) abundance in Western Greenland.	87

ABSTRACT

This document proposes a science-based metric (Remote-Sensing Index of Trophic Availability - RITA) and other environmental indices suitable for reporting on the State of the Oceans, especially in the thematic areas of primary and secondary productivity and climate change. The RITA index is computed from phytoplankton bloom characteristics which are sensitive to variations in a changing climate. Time series of the index (1998-2013) indicate trends that are inherently important to the ecosystem. Results presented in tables and colour-coded maps for NAFO regions indicate whether the index has increased, decreased, or stayed the same when compared to the long-term average. A Partitioning Around Medoid clustering method applied to thirty-eight NAFO divisions (subareas 0 to 5) identified five common and two transitional divisions. The spatial and temporal variability of phytoplankton bloom characteristics and water warming indices derived from satellite complete the set of indicators. A five-parameter Gaussian regression method was used to discern important asymmetries on either side of the time series maximum, leading to suggestions of potential mechanisms for these changes are discussed. The number of indices was reduced via multivariate orthogonal analyses (Principal Component Analysis) and the first two components were used as inputs for a non-parametric model (Loess). The Loess model was applied to study the variability of abundance in zooplankton (*Calanus finmarchicus*, copepodites 1 + 2) and northern shrimp (*Pandalus borealis* at age 2) in the Labrador Sea and Davis Strait, respectively. The ensemble of ecological indices constitutes a valuable way to explore the functional links between environmental variability and the lower trophic levels in oceanic food chains.

RÉSUMÉ

Le présent document propose une mesure scientifique (indice de disponibilité du réseau trophique pour la télédétection) et d'autres indices environnementaux pouvant servir à produire des rapports sur l'état des océans, surtout dans les domaines thématiques de la productivité primaire et secondaire et du changement climatique. L'indice est calculé à partir des caractéristiques de la prolifération du phytoplancton qui sont sensibles aux variations dans un climat en évolution. La série chronologique de l'indice (1998 à 2013) indique les tendances qui sont d'une importance fondamentale pour l'écosystème. Les résultats présentés sous forme de tableaux et de cartes à code de couleur pour les régions de l'Organisation des pêches de l'Atlantique Nord-Ouest (OPANO) indiquent si l'indice a augmenté, a diminué ou est resté le même, lorsque comparé à la moyenne à long terme. Une méthode de partitionnement autour d'un regroupement de médoïdes appliquée à 38 divisions de l'OPANO (sous-secteurs 0 à 5) a relevé cinq divisions communes et deux divisions transitoires. La variabilité spatiale et temporelle des caractéristiques de la prolifération du phytoplancton et les indices de réchauffement de l'eau calculés à partir des données satellitaires complètent l'ensemble d'indicateurs. Une méthode de régression gaussienne à cinq paramètres a été utilisée pour distinguer d'importantes asymétries de chaque côté des maximums de la série chronologique; il a donc été proposé que les mécanismes potentiels de ces changements fassent l'objet de discussions. Le nombre d'indicateurs a été réduit grâce à des analyses orthogonales multivariées (analyse en composantes principales) et les deux premières composantes ont été utilisées comme données d'entrée pour un modèle non paramétrique (modèle Loess). Le modèle Loess a été appliqué pour étudier la variabilité de l'abondance du zooplancton (*Calanus finmarchicus*, copépodites 1 + 2) et de la crevette nordique (*Pandalus borealis* à l'âge 2) dans la mer du Labrador et le détroit de Davis, respectivement. L'ensemble des indices écologiques constitue un excellent moyen d'étudier les liens fonctionnels entre la variabilité environnementale et les niveaux trophiques inférieurs dans les chaînes alimentaires océaniques.

1. INTRODUCTION

1.1 PURPOSE AND OBJECTIVE

The purpose of this study is to support the departmental strategic outcome of Sustainable Aquatic Ecosystems (SAE) using remote sensing data and analyses of Canada's oceans. This document reports ecological indices that provide vital information on the conservation priority of aquatic ecosystem productivity, leading to a balanced or healthy trophic structure, as envisioned in DFO management and protection of oceans.

An ecosystem-based approach to fisheries and ecosystem management should include information on phytoplankton, which are at the base of marine food webs. The purpose of this document is to provide phytoplankton indices that consider potential responses to environmental forcing and effects on higher trophic levels. The data used for computing the indices are obtained from remote sensing, a tool that gives daily information on the ocean's surface colour and temperature over a large spatial scale, and that is the only method that achieves the desired result of region-wide assessment. By analysis of these data and development of these indices past responses of phytoplankton to environmental forcing can be examined and future responses to a warmer, fresher, stormier or more acidic ocean can be anticipated. These responses could significantly influence recruitment in Canadian fisheries and in addition the indices may also help delineate and monitor Ecologically and Biologically Significant Areas (EBSA), Areas of Interest (AOI), Marine Protected Areas (MPA) and aquaculture sites in support of Oceans and Coastal Management, and could be incorporated as indicators of primary production in integrated ecosystem reports of the state of the ocean.

The idea of a "quantitative plankton index" for fisheries applications in DFO was first proposed 20 years ago by Harrison and Sameoto (1996). Candidates for the index were all based on two premises: that the spring bloom is a key event in the annual phytoplankton cycle, and that certain conditions are necessary to maximize the exploitable fraction of primary production. The proof-of-concept was developed largely from data obtained by vessels-of-opportunity deployments of the Continuous Plankton Recorder. At that time, the only source of remotely sensed ocean colour data (from which phytoplankton abundance can be estimated) was NASA's Coastal Zone Color Scanner (CZCS) for the years 1979-1986. Unfortunately, after the demise of CZCS there was an almost 12-year gap in the collection of remotely-sensed ocean colour data, and it was during this period that the collapse of the cod fishery on the Canada's east coast occurred. Since 1997 there has been a steady stream of remotely sensed ocean colour data from various sensors (e.g. Sea-Viewing Wide Field-of-View Sensor (SeaWiFS), Moderate Resolution Imaging Spectroradiometer (MODIS_Aqua), and Medium-Spectral Resolution Imaging Spectrometer (MERIS), that capture the strength and variability of the spring phytoplankton bloom in Canada's Atlantic Zone. The Harrison-Sameoto candidate indices are based on the latitude-related spring phytoplankton bloom, an annual feature that occurs when the winter winds relax and there is enough sunlight for phytoplankton to flourish in the nutrient-rich surface waters. The bloom lasts until the nutrients in the photic zone (the upper layer of the water where there is enough sunlight for photosynthesis to occur) have been exhausted.

The reported indices in the present document are of particular relevance to the fisheries since recruitment for several fisheries (e.g. haddock, shrimp) is related to the timing of the spring phytoplankton bloom (Platt *et al.* 2003; Fuentes-Yaco *et al.* 2007; Koeller *et al.* 2009), with an earlier bloom being advantageous to larval fish survival. Both the timing and the magnitude of the bloom over large spatial regions can be determined from remotely sensed ocean colour data, so that it provides a particularly appropriate source of information from which to develop phytoplankton indices that can be matched to scale with fish recruitment, ecosystem functioning

and characterization, contributing to the development of networks of marine protected areas (DFO, 2012). Oceans and Coastal Management collaborate in the potential use of these products in State of the Oceans Reporting in the thematic areas of Primary & Secondary Productivity, Trophic Structure, Offshore Ecosystems, and Climate Change. In particular, a better description of the phenology of phytoplankton blooms has implications for the development of the St. Ann's Bank AOI/MPA and the Gully MPA monitoring program.

The primary objectives of this study are to develop and test a suite of metrics based on remotely sensed estimates of phytoplankton abundance, and to explore spatial and temporal descriptors that synthesize important elements of the annual phytoplankton cycle. The late winter/early spring rate of warming of sea surface temperature is an environmental index that is also assessed in the context of the phytoplankton indices.

1.2 STUDY AREA

The geographical extent under study is located in the North West Atlantic. The area includes semi-enclosed seas (Baffin Bay, Gulf of St. Lawrence, Gulf of Maine), shallow shelf regions (Labrador Shelf, The Grand Banks of Newfoundland, Flemish Cap, Scotian Shelf) and deep water regions (Labrador Sea, Sohm Abyssal Plain) (Figure 1).

A brief description of the regions which contain many common and contrasting features follows. In the north, Tang *et al.* (2004) describe Baffin Bay as a Mediterranean sea, connected through restrictive straits to the Arctic Ocean and the Labrador Sea/Atlantic Ocean. Baffin Bay is a marginal ice zone with almost complete clearance of ice in late summer, and it is on the pathway of the fresh and cold Arctic water to the Labrador Sea, where deep convection occurs and contributes to the thermohaline circulation of the North Atlantic. The deep convection zone in the Labrador Sea is a region that meets the description of an Ecologically or Biologically Significant Area according to criteria designations of the United Nations Convention on Biological Diversity (UNEP/CBD/COP/DEC/XII/22, 17 October 2014). The sea off West Greenland has a varied topography that significantly influences the area's physical and biological characteristics (UNEP, 2004). Between 69°N and 60°N, is a shelf area with a number of shallower banks with depths as shallow as 30 m, but deep channels down to more than 500 m intersect the shelf in several places and divide the shelf bank systems. A sea ridge at 66°N with a maximum depth of 600 m connects Greenland and Canada and forms the Davis Strait between two deep basins of Baffin Bay to the north and the Labrador Sea to the south.

The northeastern coast of North America borders on the North Atlantic Ocean with a continental shelf, extending for approximately 5000 km between 60°N and 40°N. The shelf width and depth are typically 100-200 km and 100-200 m, but there are significant regional variations, particularly associated with coastline indentations by gulfs and submarine banks and basins. The North Atlantic subpolar gyre and its multibranch western boundary current, the Labrador Current, strongly influence the shelf-slope waters. The Labrador Shelf is relatively long, straight and rugged and extends from Hudson Strait to the Strait of Belle Isle. There it adjoins the Newfoundland Shelf, which extends around the seaward coast of Newfoundland to Cabot Strait and Laurentian Channel, and includes the broad Grand Bank and the offshore Flemish Cap. To the west of Newfoundland lies the Gulf of St. Lawrence, a nearly enclosed shallow sea which receives the freshwater discharge of the St. Lawrence River system and whose principal connection to the open shelf is through Cabot Strait. The open shelf continues along the south of Nova Scotia, as the Scotian Shelf, which at its southwestern limit adjoins the Gulf of Maine, a tidally energetic semi-enclosed shallow sea encompassing the Bay of Fundy and Georges Bank. Beyond the Scotian Shelf the deep western boundary current (DWBC) carries water from the Labrador Sea to the southwest at depth, while farther offshore the Gulf Stream carries water to the northeast that is warm and occupies a layer between the surface and several hundred metres depth (Loder *et al.* 1998).

Hydro-dynamically, the Northwest Atlantic region is a complex and interconnected system. The circulation on the continental shelves transports relatively cold, fresh water of Arctic origin, toward the equator, reaching as far south as the Gulf Stream. Most of this current flows onto the Northeast Newfoundland Shelf and continues southward into the Grand Banks region; a small amount is diverted toward the Gulf of St. Lawrence via the Strait of Belle Isle. The Scotian Shelf receives inputs of water from the Gulf of St. Lawrence, the on-shelf Labrador Current and the offshore slope water region. The resulting composition is relatively fresh, with a large seasonal temperature range.

The state of physical, chemical and biological conditions (with particular emphasis on phytoplankton) in the Northwest Atlantic region is monitored on an ongoing basis by DFO (Atlantic Zone Monitoring Program, Atlantic Zone Off Shelf Monitoring Program), and SAHFOS (the Sir Alister Hardy Foundation for Ocean Science) via their Continuous Plankton Recorder survey in the NW Atlantic. Assessments are provided to the United Nations Environment Programme (UNEP 2004) and annually to the Canadian Science Advisory Secretariat (e.g. Colbourne *et al.* 2014, Galbrait *et al.* 2014, Johnson *et al.* 2014), and are supplemented by other technical contributions (Li 2014).

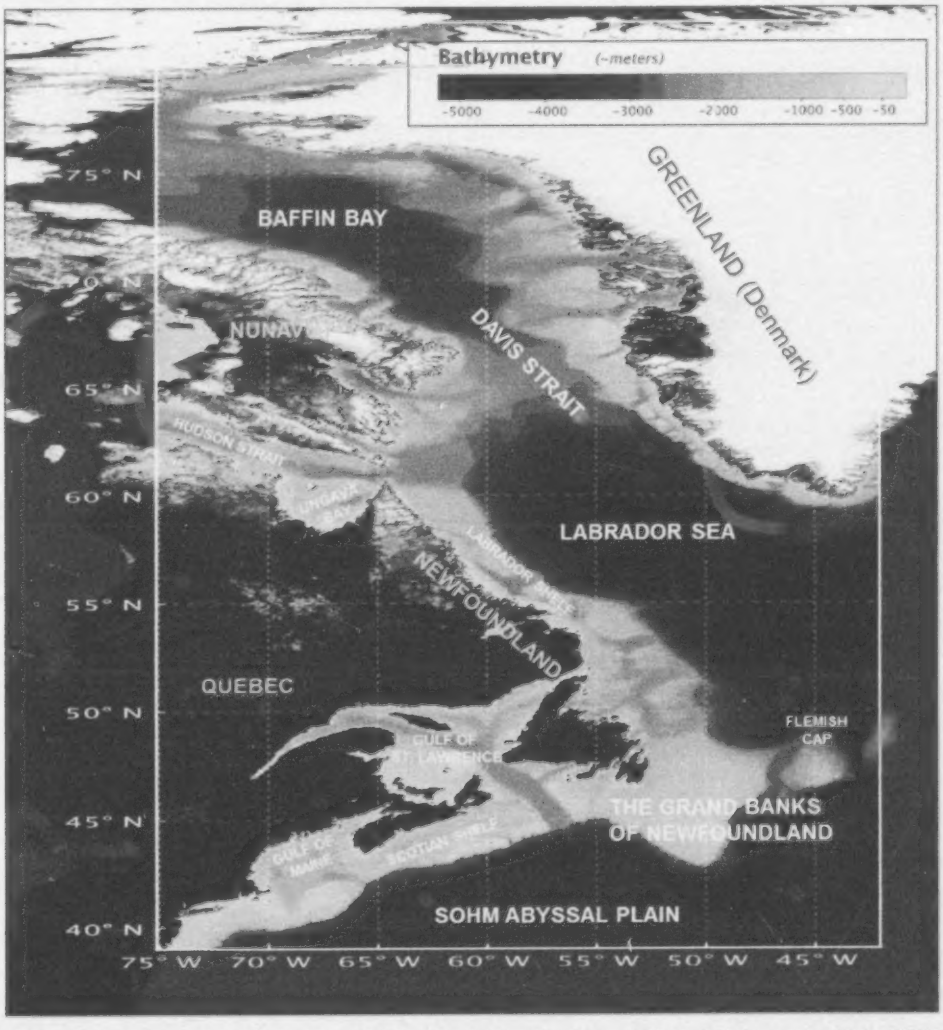

Figure 1. The study area is located in the North West Atlantic, from 39° to 82° N, and 42° to 95°W.

1.2.1 NAFO Convention Area

For the general objectives of this analysis, the study area was subdivided following the Northwest Atlantic Fisheries Organization (NAFO) Convention Area. This partition encompasses a large portion of the Northwest Atlantic Ocean and includes the 200-mile zones of Coastal States' jurisdictions (USA, Canada, St. Pierre et Miquelon and Greenland). The analyses in this work include twenty-eight Divisions from Subareas 0 to 5 (Figure 2). Subareas 6 were not included in the study (http://www.nafo.int/about/frames/area.html).

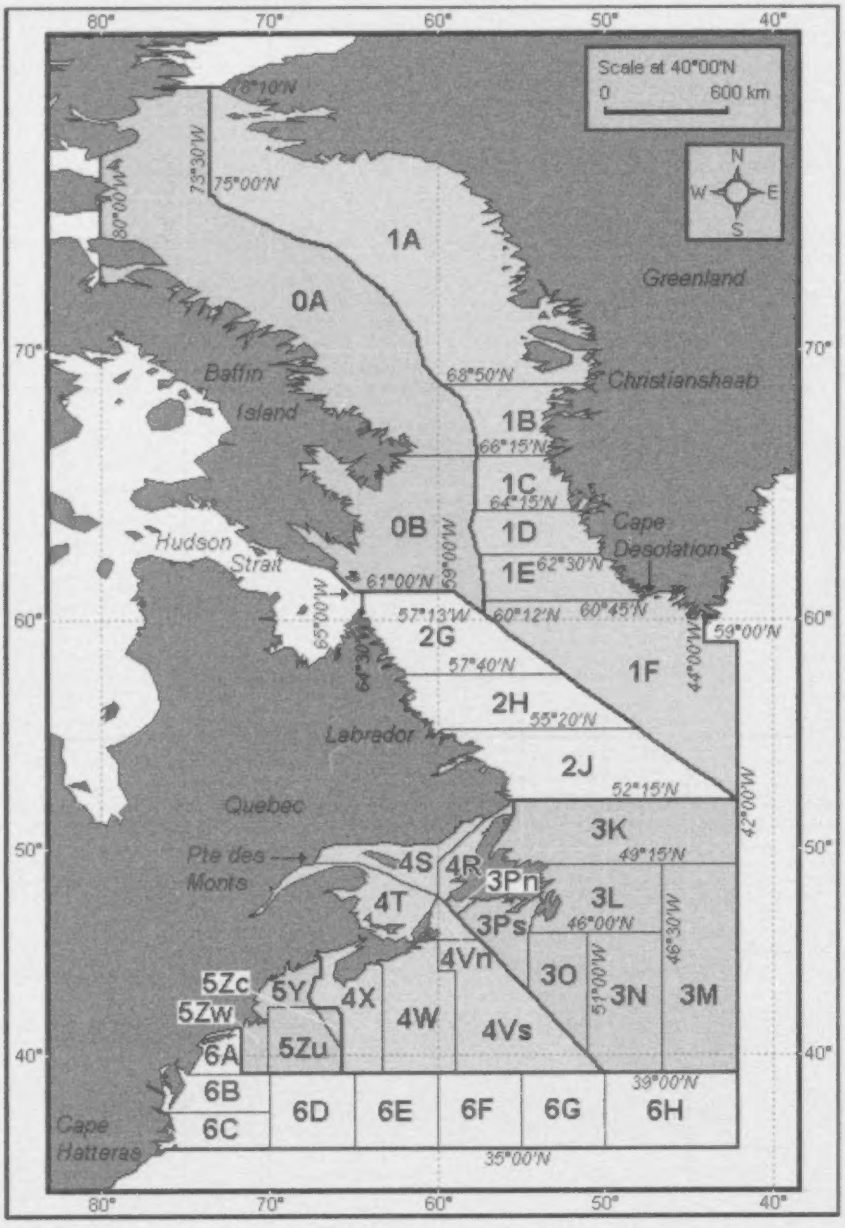

Figure 2. NAFO Convention Area, showing Subareas 0 to 5 that include the twenty-eight divisions (1A until 5Ze) used in this study.

1.2.2 Labrador Sea

An additional spatial set was defined to link abundances of copepodites stages 1 + 2 of *Calanus finmarchicus* and ecological indices along a transect across the Labrador Sea. The area is a 50 km wide band centred on the L-3 line (a.k.a. the AR7W line) of the Atlantic Zone Off-Shelf Monitoring Program (AZOMP). Figure 3 shows the twenty-eight AZOMP sampling stations (Li and Harrison 2014) located in the centre of each rectangle (red) and the five regions of assemblage (green).

A detailed explanation of how the stations for each of the five regions were selected is provided in the methodology section. Copepods sampling, preservation and size distribution analyses used to distinguish the early copepodite stages followed the methodology reported in Mitchel *et al.* (2002) and Head *et al.* (2003).

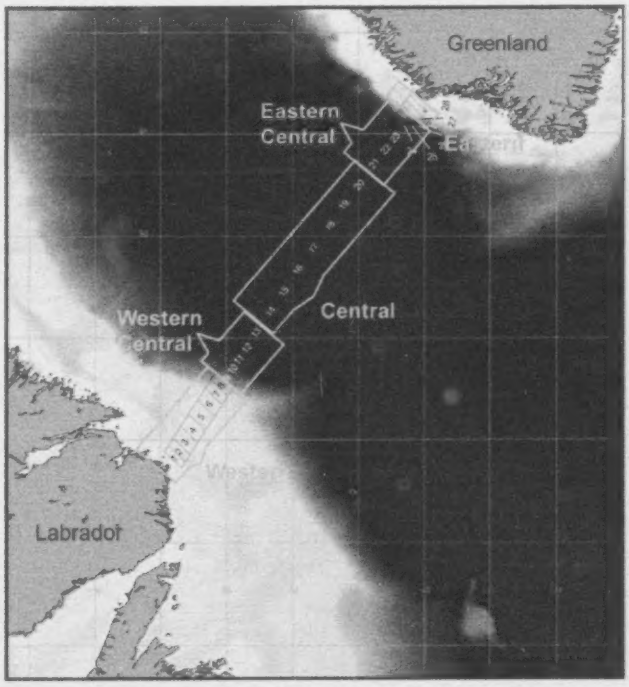

Figure 3. Labrador Sea Transect : Line 3 of the Atlantic Zone off Shelf Monitoring Program. The Calanus finmarchicus sampling stations are located in the centre of each of the 28 rectangles (red). The assemblage in five regions: Western Western-Central, Central, Eastern-Central and Eastern are shown in green.

1.2.3 NAFO Subarea 1

The main goal of studying this region was to test that the biological and physical indices derived from remotely-sensed methods were statistically related to the characteristics of a particular fishery resource species, the Northern shrimp *Pandalus borealis*. It is the most important commercial export in Western Greenland, with annual catches of around 100 000 tonnes that contribute more than 1 billion Dkr to the Greenland economy (UNEP, 2004).

A brief synthesis on West Greendland *Pandalus borealis* biology is taken from Jørgensen and Hammeken Arboe (2013), and references therein. The species distribution is on the continental shelf from 60°N to 77°30'N, with the fishery historically taking place from Cape Farewell to

Upernavik (73°N). Organisms are found at depths between 50 m and 1000 m, with the highest densities between 150 m and 500 m. The preferred habitat is muddy bottom and the temperature optimum for Northern shrimp is between 2°C and 4°C.

Northern shrimp usually migrate up to the water column at night to depths a few meters from the surface, where they feed, returning to the bottom during the day. Shrimp are omnivores, i.e. they live on many different types of food, such as worms, dead organic material, algae and zooplankton, and they are themselves food for large fish such as cod and Greenland halibut. It is important to mention that the concentrations of both zooplankton and phytoplankton in the habitat at the time of larval swarming are important to the larvae survival (Stickney and Perkins 1981). *P. borealis* is a protandric hermaphrodite (i.e. individuals change sex during their life spans). In West Greenland waters, the juveniles mature as males when they are about 3 years old, and function as males for 2-3 years, and then undergo a transition to females at an age of 5 to 6 years, living for another 8 years.

Mating and spawning occur in July - September, and the egg-bearing period lasts 8 to 10 months, depending on the bottom temperature: the larvae hatch in April - June of the following year. When hatching time approaches, the females migrate to depths of < 150 m and the newly hatched larvae are deposited in the upper part of the water column, where they live during spring and summer, passing through six planktonic stages over three to four months. In their final larval stage, the larvae settle on the bottom as immature shrimps. Hatching is believed to take place along the entire coast of West Greenland, but because of the northbound West Greenland current, which dominates the West Greenland shelf, larvae drift from hatching areas (spawning grounds) to settling areas, which can be up to 500 km apart. The banks north of 64°N and the Disko Bay are believed to be important nursery areas for larvae and juvenile shrimps.

Pandalus borealis has been routinely surveyed in NAFO Subarea 1 by the Greenland Institute of National Resources (Burmeister *et al.*, 2013). Figure 4 shows the spatial correspondence between the shrimp spatial distribution and NAFO divisions. In this study we only used shrimp data from Burmeister *et al.* (2013)'s areas U1 to U3; C0, W1 to W4; W5 and W6, and W7 to W9. These regions were matched with NAFO's divisions 1A to 1E, note that NAFO divisions 1D and 1E were used for the shrimp area W5 and W6.

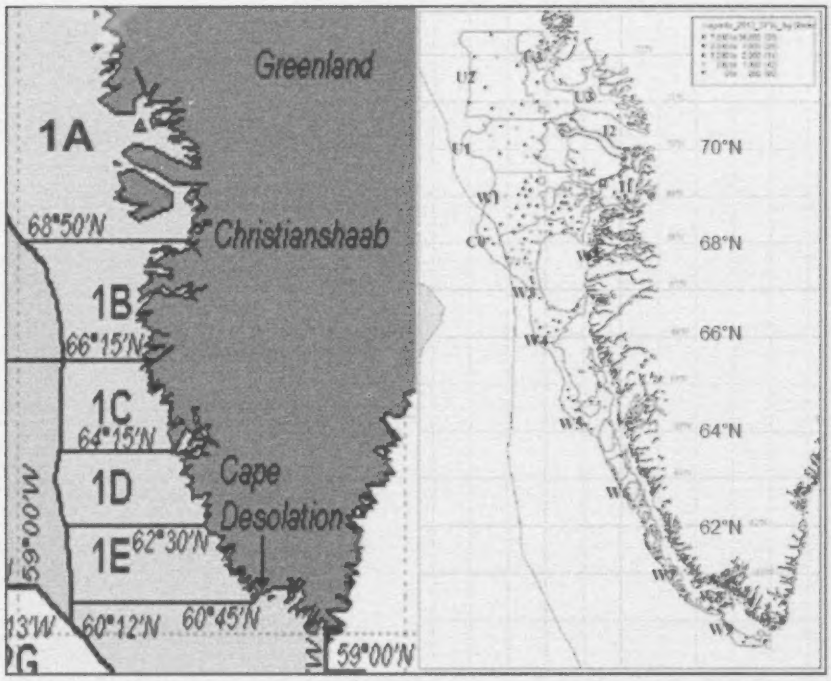

Figure 4 Approximated correspondence between NAFO Divisions 1A to 1E (left) and Pandalus borealis density distribution in West Greenland (right, adapted from Figure 1 in Burmeister et al 2013).

2. METHODS

2.1 SATELLITE-DERIVED DATA

Level-1 daily data of 4 km resolution Sea-Viewing Wide Field-of-View Sensor (SeaWIFS) were downloaded for the period between 1997 and 2010. A second set of data was acquired from the Moderate Resolution Imaging Spectroradiometer (MODIS_Aqua) images, which are received at 1 km^2 resolution, but were later remapped at 1.5 km for the period from 2003 until 2013. Both SeaWiFS and MODIS data were obtained from NASA's Ocean Color anonymous ftp site. NASA uses real-time attitude/ephemeris files which are required for precise geolocation, and the most recent near real-time (not climatological) MET/OZONE files for atmospheric processing. Details about these processing steps can be found at these websites[1]. The Level-2 data from both sensors were processed using SeaDAS (version 6.4) to obtain chlorophyll concentrations. Further description of the algorithms can be found at this address[2].

The resulting MODIS files have a nominal resolution of 1 km^2 and do not need to be geographically navigated because the geolocation values are estimated to be within 100 m of the actual locations. The processing masks applied in Level 1 to Level 2 processing were: high solar zenith angle, high satellite zenith angle and stray light. Finally, cloud albedo was set at

---

[1] http://oceancolor.gsfc.nasa.gov/DOCS/SW_proc.html and
http://oceancolor.gsfc.nasa.gov/DOCS/MODISA_processing.html

[2] http://oceancolor.gsfc.nasa.gov/REPROCESSING/R2009/ocv6/

0.015, which is different from NASA's default value (0.027). Information used in this research is from the 2012 reprocessing by the NASA's Ocean Biology Processing Group.

Sea surface temperature (SST) data for the analyses in Labrador Sea (2003 to 2013) were derived from Advanced Very High Resolution Radiometer (AVHRR) of the US National Oceanic and Atmospheric Administration (NOAA) and Metop from European Organisation for the Exploitation of Meteorological Satellites (Eumetsat, 2012) instruments. Both datasets were processed using Terascan software, which is a product of the SeaSpace Corporation (Sea Space, 2013).

SST in NAFO Subarea 1 (Divisions 1A to 1F) was examined in the Remote Sensing Unit /Bedford Institute of Oceanography. Existing archives are from the global ocean AVHRR Pathfinder Version 5.2 (PFV5.2) data, obtained from the US National Oceanographic Data Center and HRLTSST (http://pathfinder.nodc.noaa.gov). This information is the source for High Resolution Long Term Sea Surface Temperature layers (GHRSST, 2011). The PFV5.2 data are an updated version of the Pathfinder Version 5.0 and 5.1 collections described in Casey *et al.* (2010). Further details of the processing steps can be found in Greenlaw *et al.* (2015).

The images were averaged to produce Level-3 weekly composite images and mapped under cylindrical projection. SeaWiFS and GHRSST images retained 4 km spatial resolution but MODIS and AVHRR data were resampled at 1.5 km of spatial resolution as part of RSU/BIO standard processing.

2.1.1 Phytoplankton bloom

Objective identification and analysis of phytoplankton blooms were achieved by fitting a function to the satellite-derived chlorophyll-a data points. This took the form of a five-parameter logistic equation (Fuentes-Yaco *et al.* 2013), modified following Ricketts and Head (1999). This approach enabled the fitted curves to be non-symmetrical on either side of the maxima. Prior to the logistic fit, the data were smoothed using a non-parametric local regression (Loess). The fitted curve $\hat{y}$ is of the form:

$$\hat{y} = \mathcal{P}1 + \frac{\mathcal{P}2}{1 + f_x \cdot e^{\mathcal{P}3(\mathcal{P}4 - x')} + (1 - f_x) \cdot e^{\mathcal{P}5(\mathcal{P}4 - x')}} \tag{1}$$

where $\mathcal{P}1$ is the value at maximum chlorophyll-a concentration, $\mathcal{P}2$ is the range of chlorophyll-a values fitted, $\mathcal{P}3$ and $\mathcal{P}5$ describe the curvature parameters, and $\mathcal{P}4$ gives the inflexion point. The parameters were derived using R software (R Core Team, 2012). The logistic weighting function f_x is given by:

$$f_x = \frac{1}{1 + e^{-C_f(\mathcal{P}4 - x')}} \tag{2}$$

and the mean curvature of f is given by:

$$C_f = \frac{2 \cdot \mathcal{P}3 \cdot \mathcal{P}5}{|\mathcal{P}3 + \mathcal{P}5|} \tag{3}$$

2.2 ECOLOGICAL INDICES COMPUTATION

An objective characterization of a phytoplankton bloom was made through simple indices, based on significant locus of the fitted curve and its first order difference (Figure 5). The indices are: i) the bloom initiation (Chl_{ini} - demarcated as the beginning of exponential growth – green line), ii) the increasing inflexion point ($IfPt_{inc}$ - where the curve changes sign from positive to negative – yellow line), iii) the maximum pigment concentration (Chl_{max} - the maximum value of the fitted Gaussian curve – red line); iv) the timing of this maximum concentration (DOY_{max}), v) the decreasing inflexion point ($IfPt_{dec}$ - where the curve changes of sign from negative to positive – light blue line), vi) the termination of the bloom (Chl_{end} - the end of exponential decay – dark blue line), and vii) the duration of the bloom (*Durat* - the number of days elapsed between bloom initiation and termination). Several of these indices have been used in previous studies: Platt *et al.* (2003) related the timing of maximum concentration with larval haddock survival, Fuentes-Yaco *et al.* (2007) found significant correlations between bloom intensity and timing *versus* the size of young shrimp *Pandalus borealis*, and Koeller *et al.* (2009) linked shrimp egg hatching times and the timing of the spring phytoplankton bloom at sites throughout the North Atlantic.

The Remote-Sensing Index of Trophic Availability (RITA), was defined as follows:

$$RITA = \frac{log_{10}\mathrm{Chl}_{max} - log_{10}\mathrm{Chl}_{ini}}{DOY_{max}} \tag{4}$$

where Chl_{max} (Log_{10}[mg m^{-3}]) is the maximum chlorophyll-a concentration, Chl_{ini} (Log_{10}[mg m^{-3}]) is the chlorophyll-a concentration at bloom initiation, and DOY_{max} (day of year) is the date on which the chlorophyll-a maximum concentration occurs. Units of RITA are the inverse of days (d^{-1}). The values of all these parameters are obtained by the fitted curve as described above.

RITA is an indicator (but not a measure) of the phytoplankton in spring putatively available for use by members of higher trophic levels. By definition, RITA has a high value when phytoplankton in spring attains a concentration much higher than its winter level, and/or when the maximum concentration is attained earlier in the year. Conversely, RITA has a low value when phytoplankton in spring attain a concentration only little higher than its winter level, and/or when the maximum concentration is attained later in the year. However, information from RITA is ambiguous when high concentrations occur late in the year, or when low concentrations occur early in the year.

The calculation of RITA was repeated for every year to compute the index annual climatology for the 13 years of available SeaWiFS data (1998–2013), and standardized as follows:

$$\frac{\Pi - \mu}{\sigma} \tag{5}$$

where Π is the annual RITA, μ is the 13 years arithmetical mean, and σ represents the standard deviation of the 13 annual indices. This standardization method is used for other ecological indices, and these "standardized anomalies" referred to as "anomalies" in the text.

2.2.1 NAFO divisions

The study area was analyzed for the twenty-eight NAFO divisions[3]. In general coastal waters are optically complex, i.e. chlorophyll-a and other optically active water constituents do not co-vary (Morel and Prieur 1977). The satellite chlorophyll algorithms assume that all optically active water constituents co-vary. However, in these coastal waters, this assumption does not hold and gives rise to erroneous chlorophyll a estimates. Therefore, in the NAFO divisions including coastal waters measurements in regions <50 m deep were omitted from the analyses.

2.2.2 Labrador Sea Transect

Regional climatologies of MODIS-derived chlorophyll_a concentration were computed by averaging the forty-eight weekly composites per year for each of the twenty-eight rectangles along AZOMP transect, for the period between 2003 and 2013. A Hovmöller diagram displays the chlorophyll-a fitted climatology as a function of time and Longitude (station) and provides a good separation of stations in five regions: Western (W), Western-Central (WC), Central (C), Eastern-Central (EC), and Eastern (E) regions, as shown in Figure 6. The selected stations are: 1 to 8 for W region, 9 to 13 for region WC, 14 to 20 grouped in region C, 21 to 26 for region EC, and finally, 27-28 for region E.

RITA indices were computed for each of the five regions and for the period between 2003 and 2013, following the same approach as for the SeaWiFS-derived data.

In addition to phytoplankton bloom indices, sea surface temperature warming indices were also calculated. To do this, the SST annual cycle was analysed following a similar procedure as was applied to the phytoplankton bloom. Figure 7 describes the method.

---

[3] http://www.nafo.int/about/frames/area.html

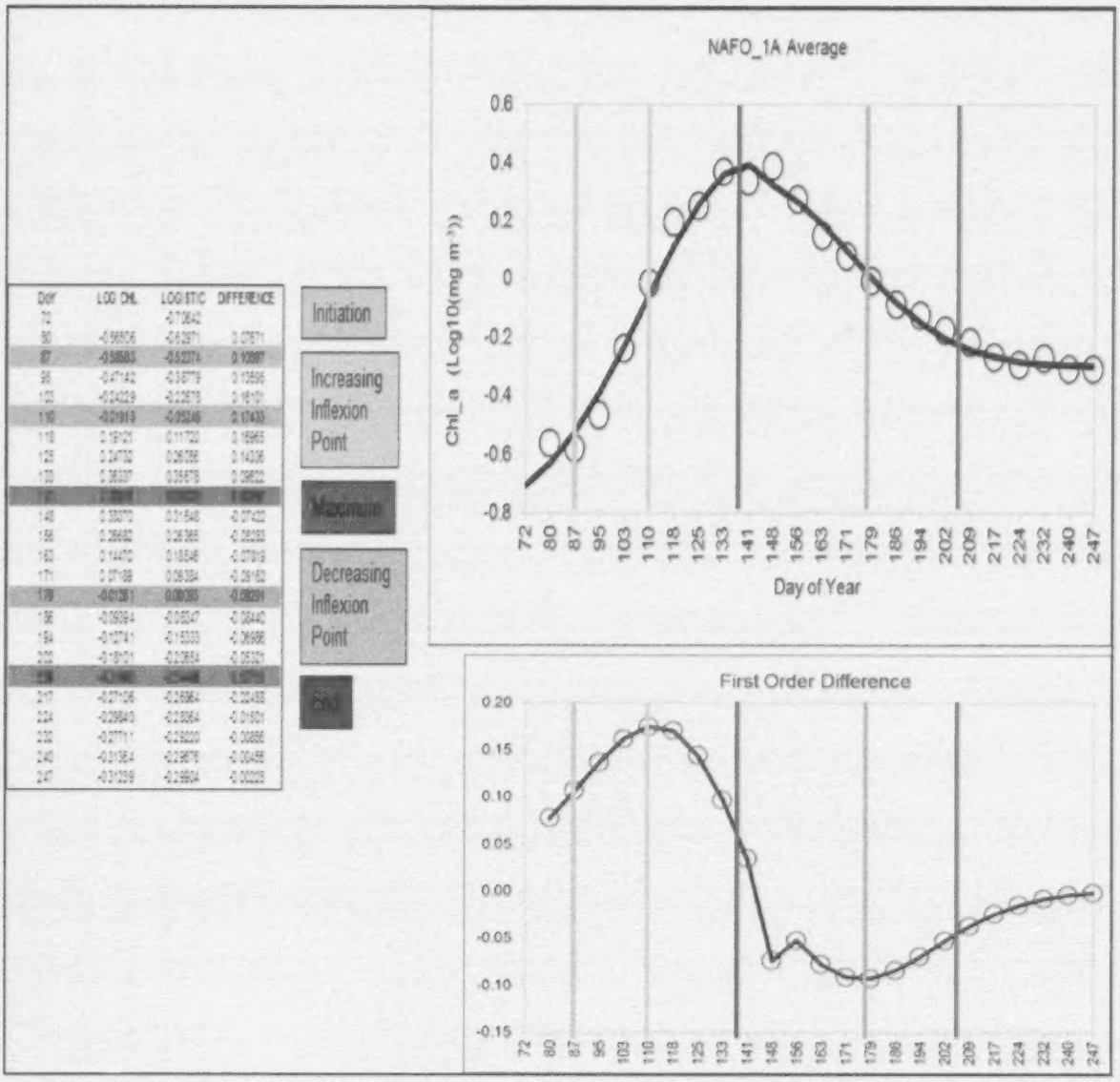

Figure 5. Identification of biological indices derived from chlorophyll_a concentration during the phytoplankton bloom. The table (left) shows the day of year (DOY), the average of chlorophyll a concentration (Log (mg m^{-3})), the fitted values, and the first difference. Coloured bars show the bloom characteristics in terms of pigment concentration and time of occurrence: initiation (green), increasing inflexion point (orange), maximum (red), decreasing inflexion point (light blue), and end (dark blue). The top graph shows chlorophyll_a concentration during the blooming period, and the lower graph shows the first order difference.

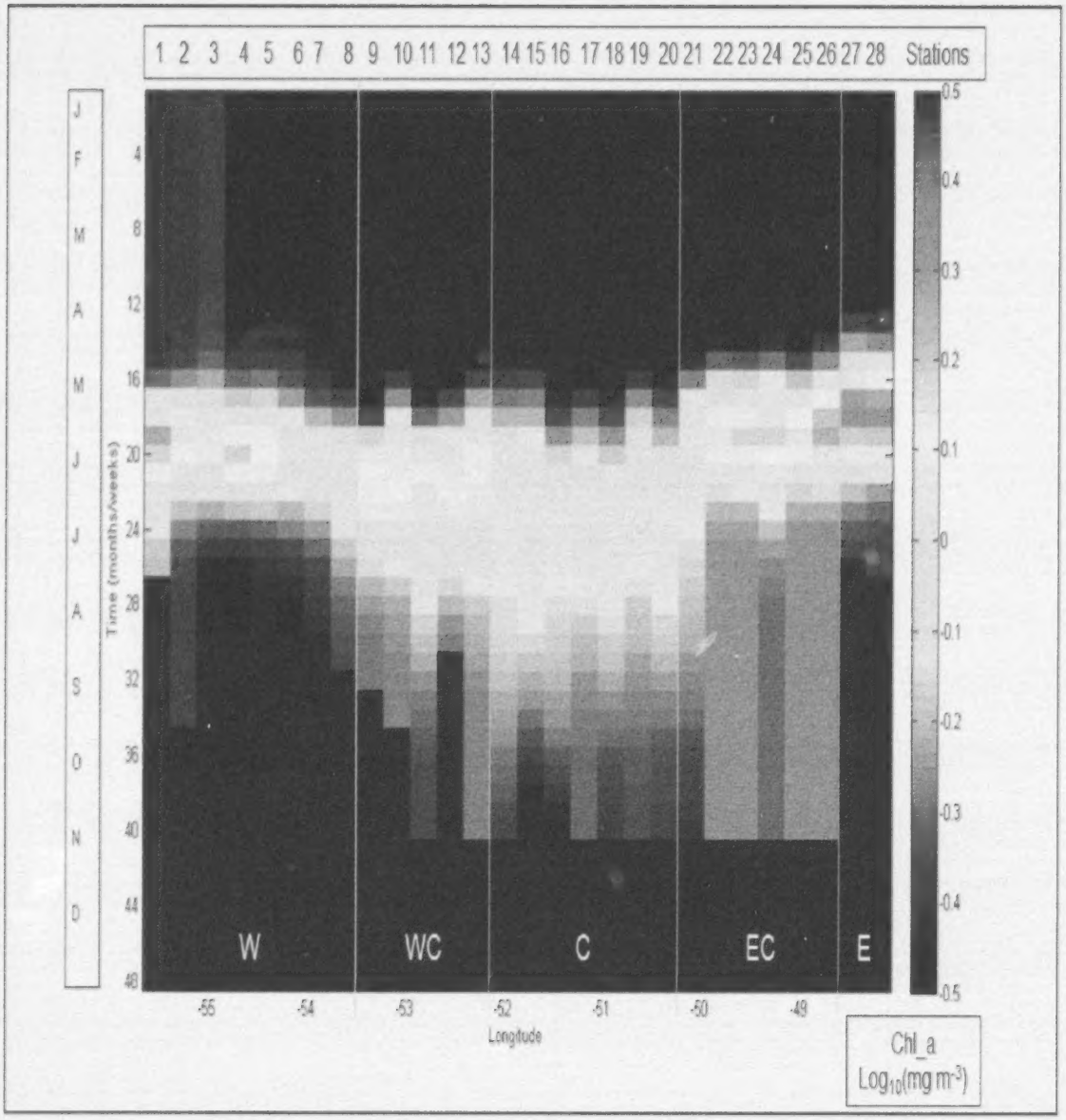

Figure 6. A Hovmöller diagram of the Gaussian fitted climatology of Chlorophyl_a, for the period between 2003 and 2013. The colour coding shows weekly Chl_a concentrations ($Log_{10}(mg\ m^{-3})$), the ordinate shows the time of year in one week block, and the abscissa shows the station numbers (top) and longitudes (bottom), along the L-3 line. Vertical lines indicate how the stations were grouped into regions: Western (W), Western-Central (WC), Central (C), Eastern-Central (EC), and Eastern (E).

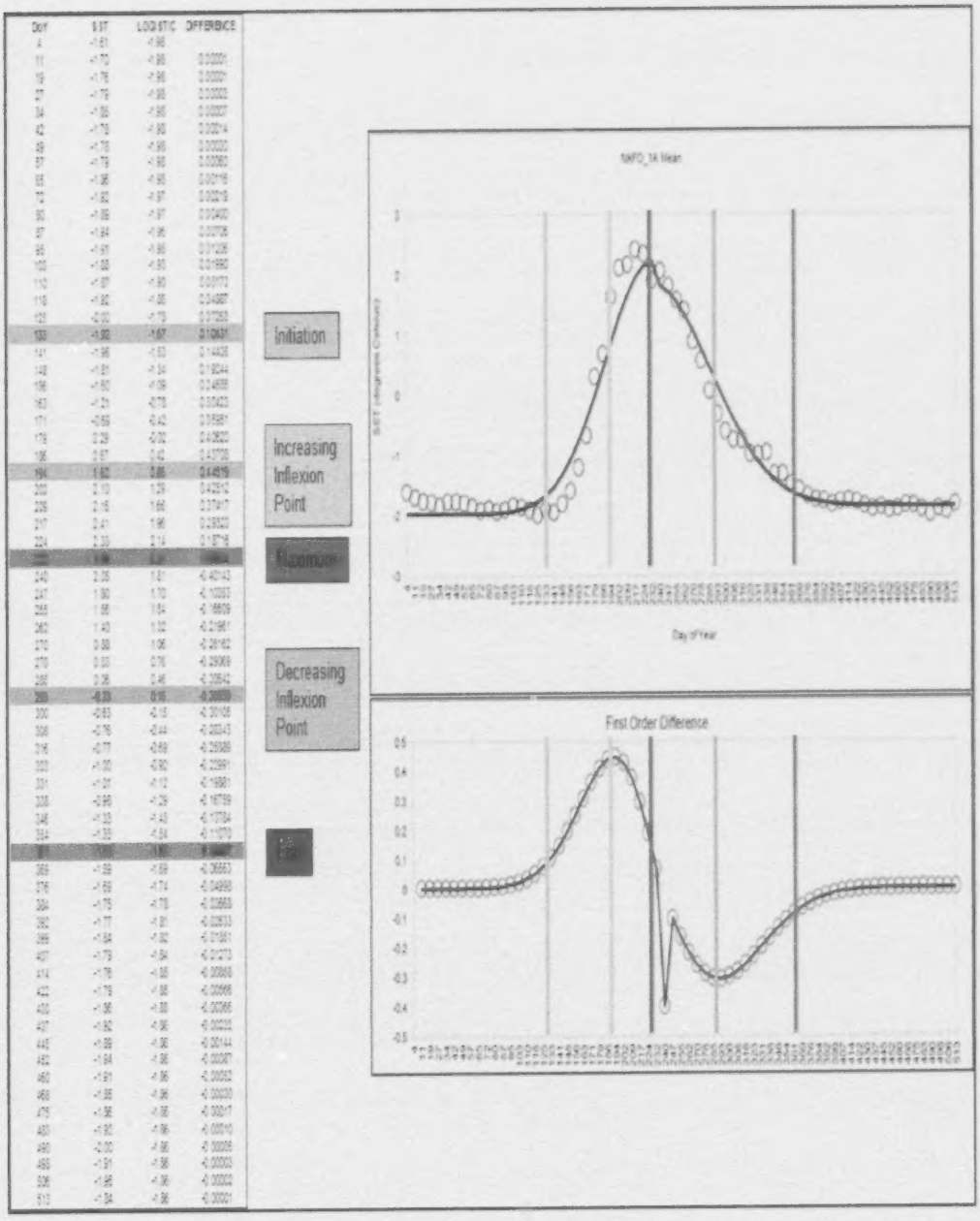

Figure 7. Identification of warming indices derived from the sea surface temperature (SST) along an extended annual cycle. The table (left) shows the day of year (DOY), the SST (°C), the fitted values, and the first difference. Colours show the characteristics in SST and time of their occurrence: initiation (green), increasing inflexion point (orange), maximum (red), decreasing inflexion point (light blue), and end (dark blue). The top graph is for the SST during the annual cycle, and the lower graph is for the first order difference during the same time period.

3. RESULTS

3.1 COMPARISON OF *IN SITU* AND SATELLITE DATA

A simple comparison of *in situ* measurements and the satellite-derived data used in this work allows a broad approximation of the accuracy of satellite estimates of chlorophyll-a concentration in the study area. The estimates for 9 pixels (matrix of 3x3 with at least 50% of valid –i.e. unflagged pixels) were averaged and compared against *in situ* arithmetic means of chlorophyll concentrations obtained from water samples collected in the top ten meters of the water column, measured by fluorometric methods (Mitchell *at el.* 2002, Johnson *at el.* 2014, Pepin *et al.* 2015). The 8-day composites of both SeaWiFS (4km/pixel) and MODIS (1.5 km/pixel) remotely-sensed matrices produced a total of 7059 match-ups with daily sampling during DFO's AZMP and AZOMP missions between 2003 and 2010.

The linear regression procedure for this analysis is a Model II method (Standard Major Axis, SMA), which is typically applied for situations where both variables are random (Legendre, 2015[4]). The regression results for both sensors are as follows. SeaWiFS: n = 3010, r^2 = 0.36, Intercept = 0.18, Slope = 0.89, and Angle (degrees) = 41.77. MODIS: n = 4049, r^2 = 0.25, Intercept = 0.17, Slope = 0.96, and Angle (degrees) = 43.73. Figure 8 shows SMA fitted regression curves. For both sensors the angle is close to the 45 degrees, although the satellite-derived values seem to slightly overestimate chlorophyll a concentrations. It is worth mentioning that the matching locations include coastal and offshore locations, which might contribute to the data dispersion along the regression lines.

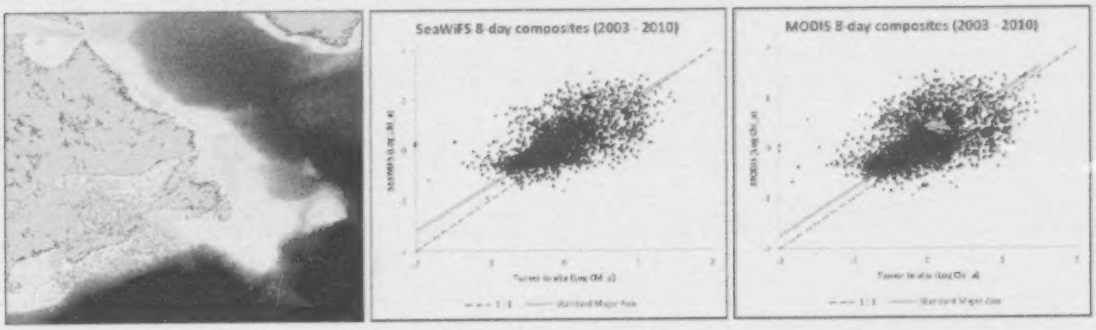

Figure 8.Comparison of in situ and satellite-derived chlorophyll_a measurements (Log_{10}(mg m^{-3}): left) matching locations (red symbols), centre) SeaWiFS regression and right) MODIS regression. Green lines represent SMA fits and dashed the one to one lines.

[4] http://adn.biol.umontreal.ca/~numericalecology/old/model-ii.html

3.2 NAFO DIVISIONS

3.2.1 Phytoplankton bloom

The average annual cycles of SeaWiFS-derived chlorophyll a concentration during the spring/summer bloom for each of the 28 NAFO divisions during 13-years (1998-2010) are shown in Figure 9. The graphs present weekly means (open symbols) and regressions from the five-parameter logistic fit (solid line). The fitting method gives the phytoplankton bloom parameters (magnitude of the bloom and initiation, peak, end timing and duration), and allows the fitted curves to be non-symmetrical on either side of the maxima (Fuentes-Yaco *et al* 2013). It is the first time that the high variability of these blooms has been demonstrated in a synoptic form for the NAFO divisions.

Chlorophyll_a concentrations (Log Chl_a (mg m^{-3})) at the *initiation*, *maximum*, and *end* of the bloom are shown in Tables 1-28 for each of 13 sampling years, along with the dates on which each of these occurred (day of year) and bloom *durations* (days). The corresponding graphs of yearly anomalies (1998 until 2010) with trend lines computed using three-year moving averages are shown in Appendix 1. Fig. APX1-1 shows the anomalies for chlorophyll_a concentrations at the initiation of the bloom for the twenty-eight NAFO divisions, Fig. APX1-2 shows the anomalies for chlorophyll concentrations at the bloom maxima, and Fig. APX1-3 shows the anomalies for the dates at the bloom maxima were reached.

These results indicate notable spatial and temporal variability. For example, 70% of the regions showed a negative temporal trend in pigment concentration at the initiation of the phytoplankton bloom (Figs. APX1-1 and 10a). A smaller percentage of regions (50%) showed a positive trend over time in chlorophyll_a concentration at the maximum of the bloom, especially in the southern NAFO regions (Figs. APX1-2 and 10b). Finally, the timing of the bloom maximum showed a negative trend (i.e it developed sooner than the climatological mean) in 43% of the NAFO regions; a trend which can be seen for the average of all NAFO regions between 2002 and 2010 (Fig. 10c).

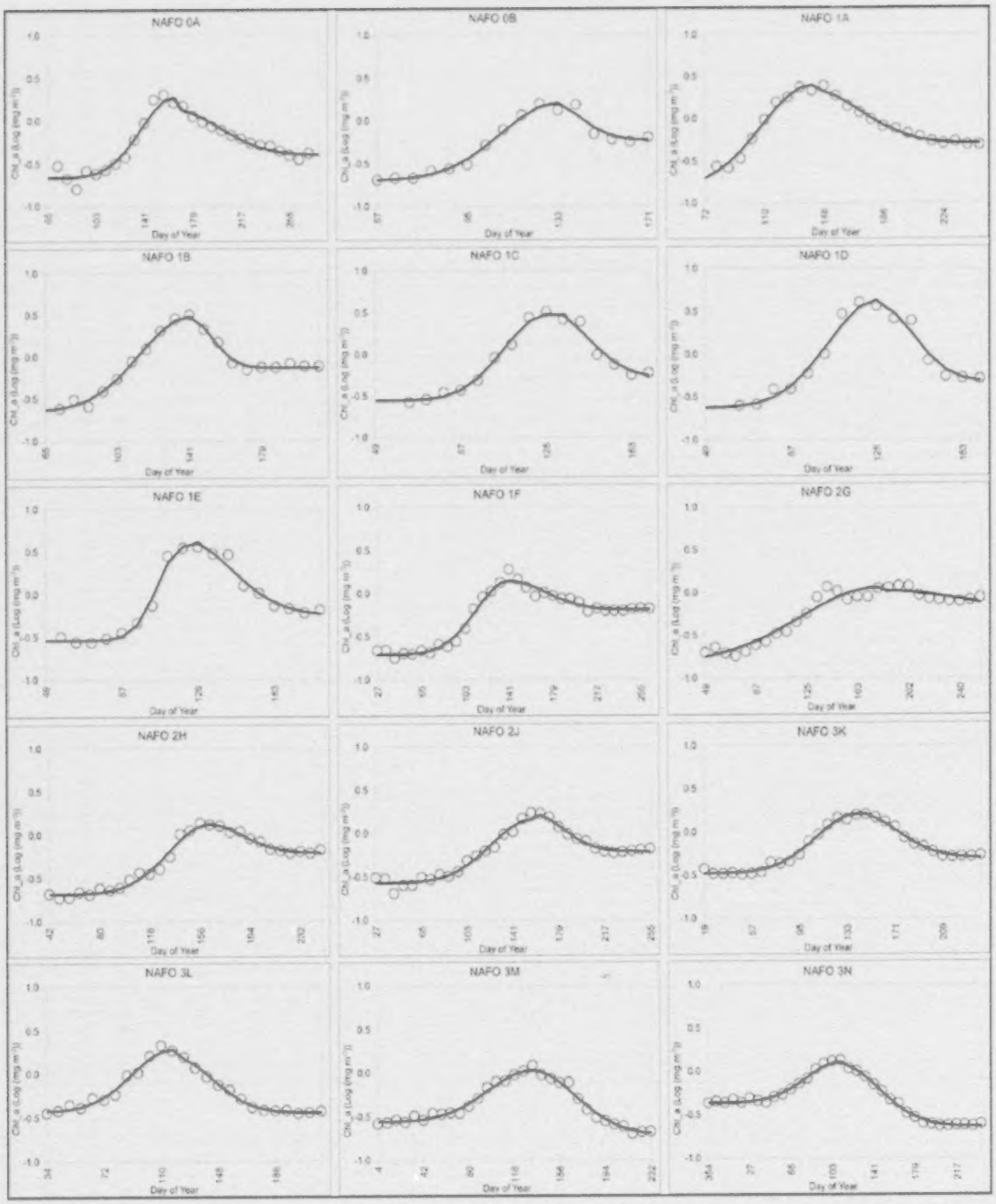

Figure 9. Average annual cycles of chlorophyll a concentration (Log_{10}(mg m^{-3})) for each of the 28 NAFO divisions. Open symbols are 13-years mean (1998 to 2010), and the solid line is the regression from the five-parameter logistic equation. Note that the time axes (x-axes) are not of equal duration.

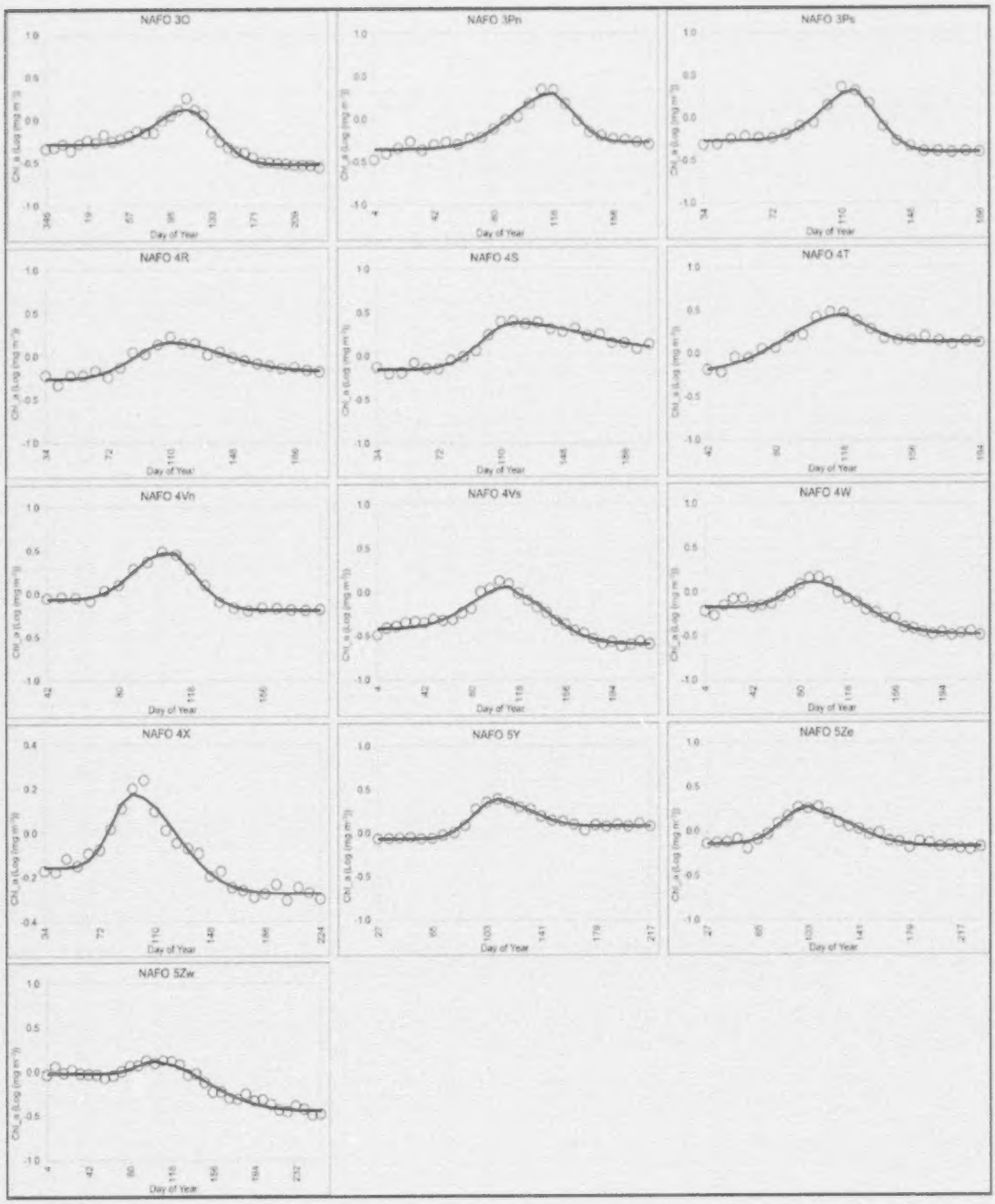

Figure 9. Continued.

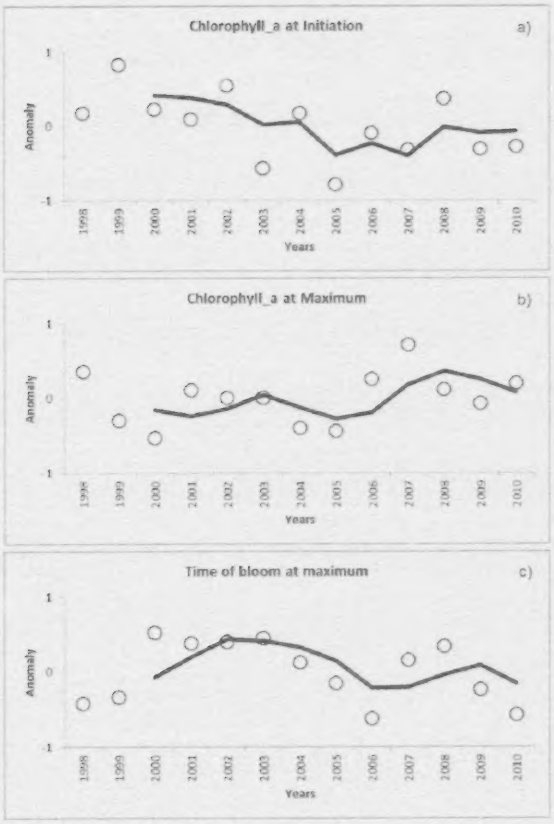

Figure 10. Average for all NAFO division of anomalies annual variability between 1998 and 2010 of: a) Chlorophyll_a concentration at initiation of the bloom (mg m^{-3}), b) Chl_a at the maximum (mg m^{-3}), c) Time at maximum (day of year). Trend lines were calculated using a 3 year moving average.

3.2.2 RITA Index

The RITA index was calculated, for the twenty-eight NAFO divisions, following a brief exploratory analysis of the spatial and temporal variability of the concentration of chlorophyll_a at the initiation and at the maximum value of the phytoplankton bloom as well as the time to reach this maximum point.

RITA values by division and year are shown in the last column of Tables 1 to 28 and RITA anomalies are shown graphically in Figure APX1-4. Almost 60% of the twenty-eight divisions show a positive temporal trend in their 3-year moving averages during the study period. Furthermore, a linear regression using the average anomalies of all NAFO divisions from 1999 to 2010 ($p<0.05$), confirms the increasing tendency, and suggests important ecological fluctuations probably linked to climate change (Fig. 11).

The spatial variability of RITA is illustrated in Figures 12 and 13. Figure 12 presents the sequence of the NAFO subdivisions ranked in order of decreasing annual average values of RITA, while Figure 13 shows regional variations. A latitudinal trend is apparent in both figures with high values of the RITA index in the northern divisions (0 and 1), and low values in the southwestern divisions (4 and 5). Thirteen maps of yearly anomalies of the ecological index are included in Appendix 2. These illustrations show annual discrepancies from the long-term mean for the period between 1998 and 2010, Figures APX-2-1 to 13 illustrate the corresponding years.

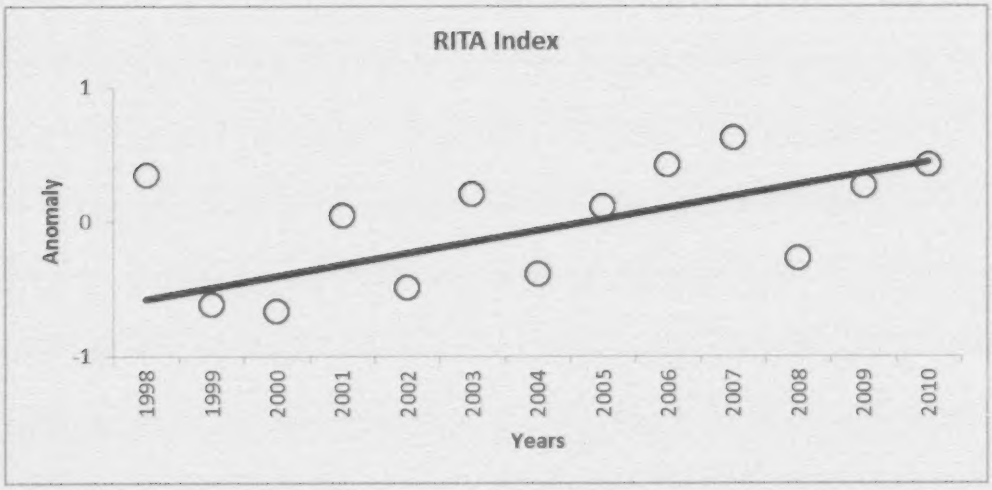

Figure 11. Average of the RITA index (d^{-1}) for all NAFO division of anomalies year variability between 1998 and 2010. A linear regression using only data from 1999 to 2010 is also shown.

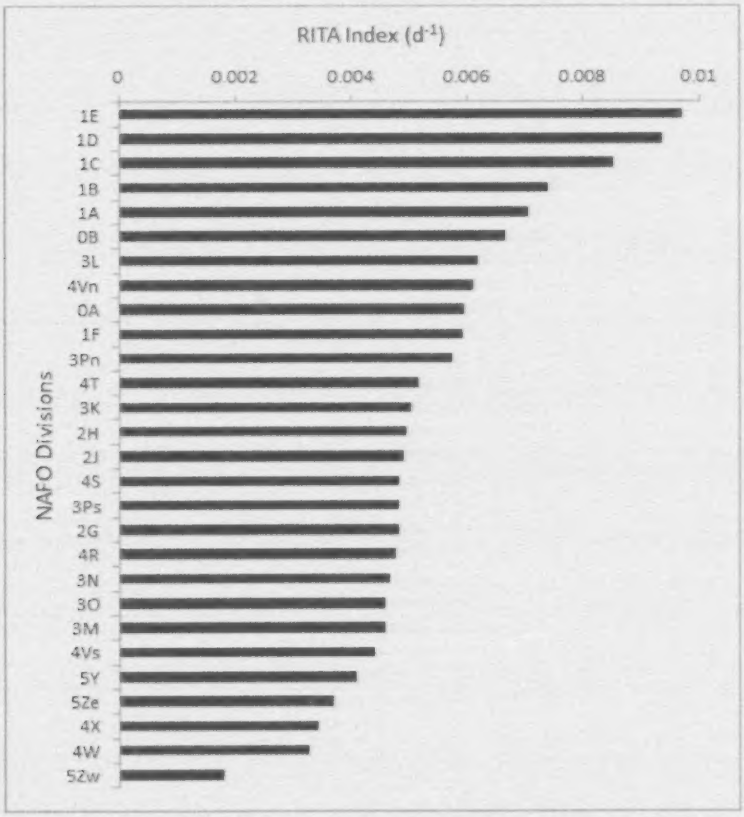

Figure 12. Average of RITA index (d^{-1}) sorted from highest to lowest index values.

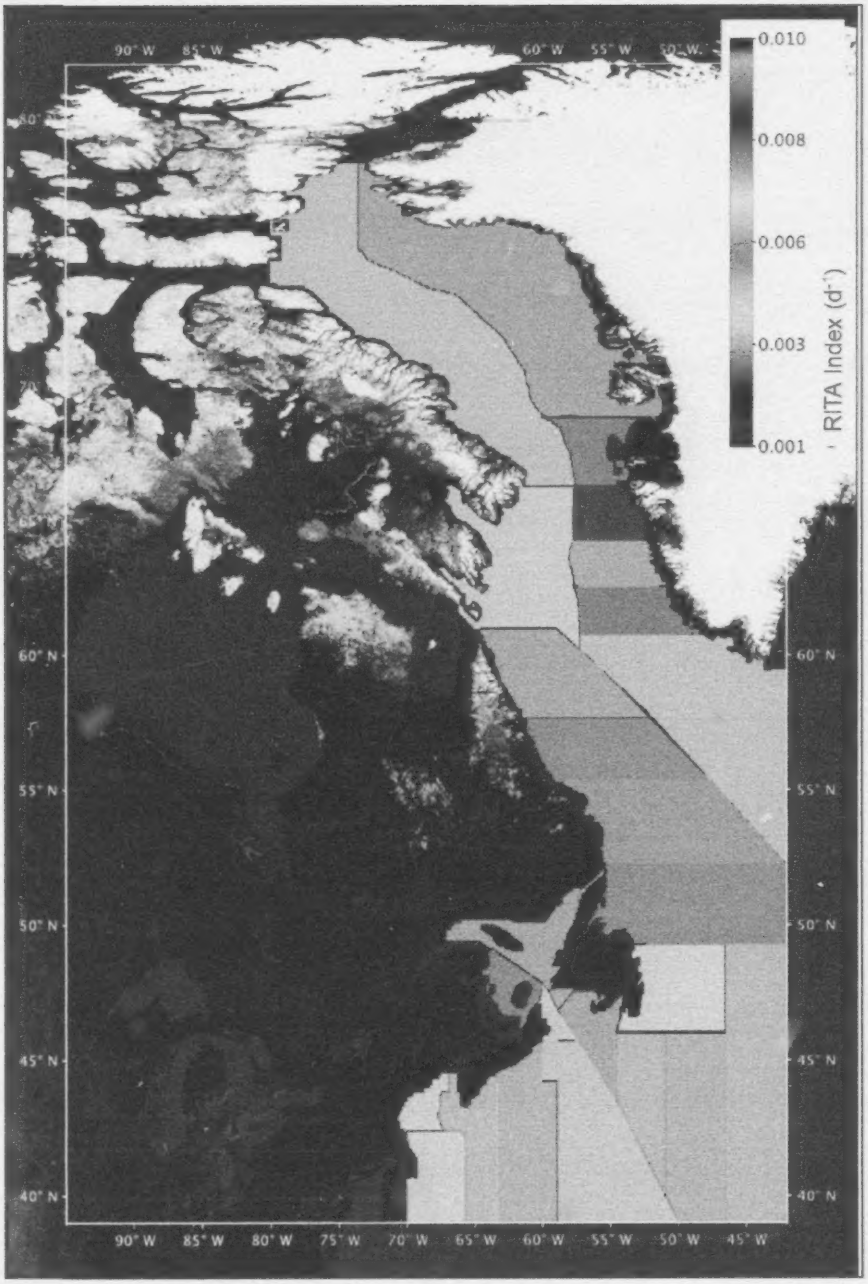

Figure 13. Climatology (1998-2010) of RITA Index (d^{-1}) for all NAFO divisions.

3.2.3 Cluster Analysis

A cluster analysis was performed using the Partinioning Around Medoids "PAM" method (Kaufman and Rousseeuw, 1990; TIBCO, 2010) to compare spatial and temporal changes in the RITA index among regions. The input were 364 RITA anomaly values corresponding to the 28 regions and 13 years. Results shown in Figure 14a, are the silhouette width of five clusters, and in Figure 14b their corresponding geographic distribution.

The regions in Baffin Bay correspond to NAFO's divisions 0A, 1A and 1B (violet colour in Figure 14b) and appear together in Cluster 1. Cluster 2 groups together divisions 0B, 1C, 1D, and 1E corresponding to Labrador Sea (dark blue colour), although divisions 4T (Southern Gulf of St. Lawrence) and 5Y (Gulf of Maine) also appear in this Cluster.

Groups on the Labrador and Newfoundland shelves, corresponding to NAFO divisions 2G, 2H, 2J (dark green colour) with similar silhouettes are associated in Cluster 4.

In contrast, divisions classified in Cluster 3 appear dissimilar; however the spatial and temporal interactions of Chl_{max}, Chl_{init} and DOY_{max} resulted in their groupement. They include Southern Newfoundland (3Pn and 3Ps), Northeastern GSL (4R, 4S and 4Vn), Scotian Shelf (4W and 4X), Georges Bank (5Ze), but also a South Greenland region (1F).

Finally, the Grand Banks of Newfoundland (NAFO divisions 3L, 3M, 3N and 3O), were grouped in Cluster 5 (pale green colour); division 5Zw corresponding to the Western Geogers Bank region was also grouped in this cluster.

The results for NAFO divisions 3K and 4Vs were noteworthy. They had negative silhouete values, which are interpreted as poorly classified by the cluster analysis. They seem to correspond to transitional areas, division 3K links northern cold to warm regimes at 50°N, whereas NAFO division 4Vs might be the most northern penetration of warm water masses associated to the Gulf Stream. Actually, both regions have very dynamic surface current patterns.

In conclusion, RITA is shown here as an index capable of identifying similarities of the underlying phytoplankton bloom characteristics in the twenty-eight NAFO subdivisions (Subareas 0 to 5).

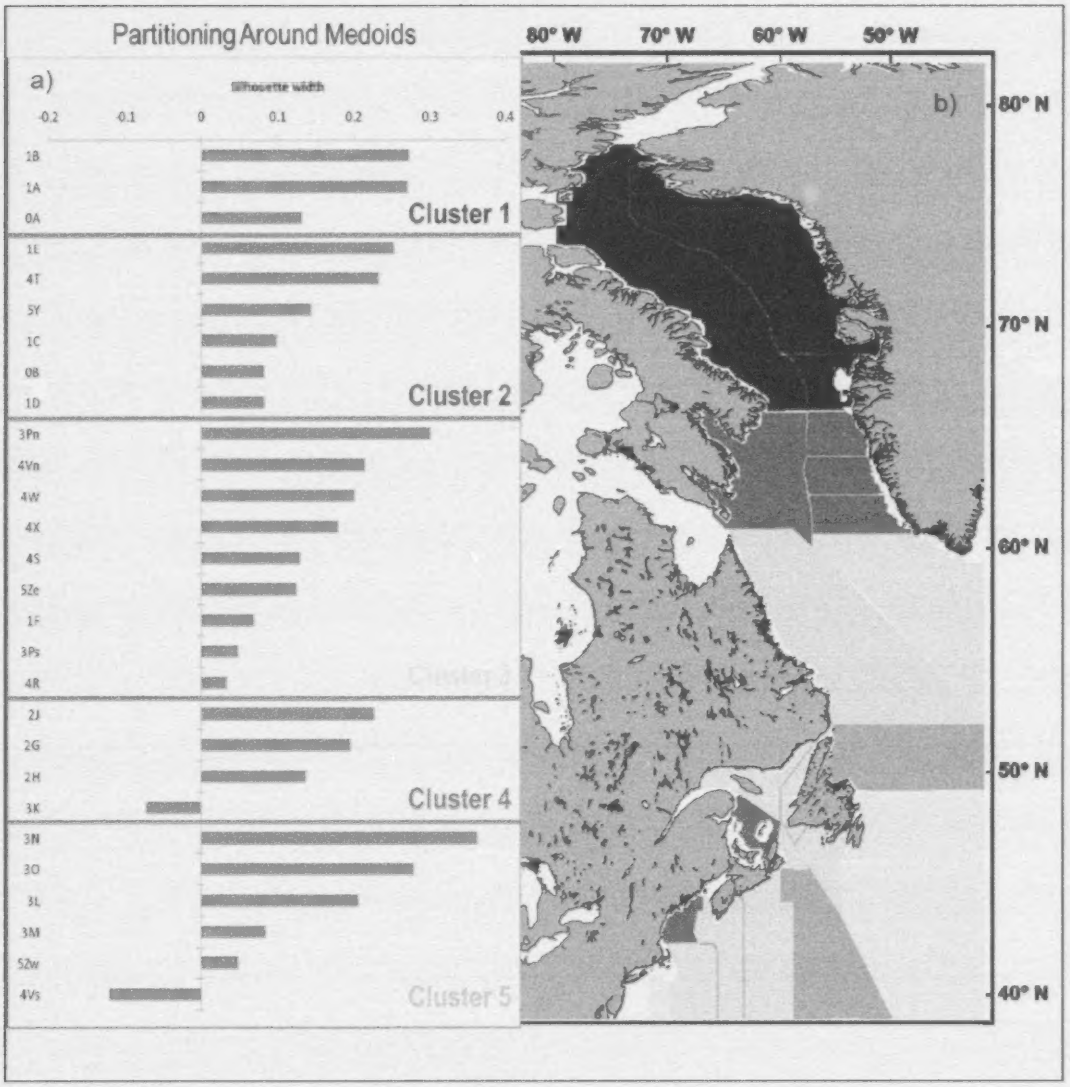

Figure 14. Cluster analysis of NAFO divisions using medoid partitioning algorithms (PAM) applied on RITA anomalies. a) Silhouette width showing five clusters with two negative values (3K and 4Vs), b) Map of the study area showing the spatial distribution of the five clusters, and two regions inferred as transitional environments (orange polygons).

3.3 LABRADOR SEA TRANSECT

A detailed analysis of the phytoplankton bloom in the Labrador Sea along the AZOMP L-3 line (Figure 3) was carried out to see if the abundances of the youngest stage copepodites of *Calanus finmarchicus*, (*i.e.* C1 and C2) (Figure 15) are related to the phytoplankton bloom and/or warming SST indices.

Zooplankton samples are collected at fixed stations on annual missions to monitor community abundance and composition. The organisms are routinely collected with a 202 pm mesh ring net towed vertically between 100 m and the surface. Samples are preserved in 2% formalin and *C. finmarchicus* (and two other *Calanus* species) are identified and enumerated to species and stage in sub-samples containing >200 inidividuals.

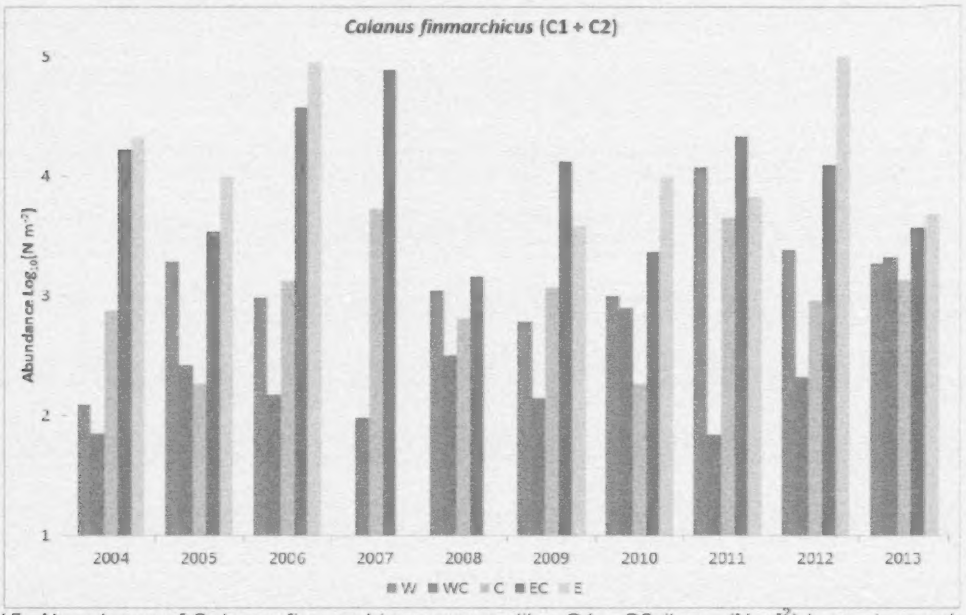

Figure 15. Abundance of Calanus finmarchicus copepodites C1 + C2 ($Log_{10}(N\ m^{-2})$) by region and year.

3.3.1 Phytoplankton bloom

Chlorophyll concentrations were averaged for 8-day periods for each of 28 rectangular areas, centered on the 28 stations of the L-3 line, in five regions (W, WC, C, EC, E), for the period between 2003 and 2013 (Figure 3). A modified Gaussian curve was fitted to the chlorophyll_a climatology and biological indices, as shown in Fig. 5.

The Gaussian fits for the climatologies in the five regions are shown in Fig. 16. The abundances of *C. finmarchicus* copepodites C1 + C2 ($Log_{10}(N\ m^{-2})$) and the corresponding average sampling dates are shown as red lines, with the units on the right-hand vertical axes. Similar information for the individual regions (W, WC, C, EC, and E) by year (2003 until 2013) is shown in Appendix 3 (Figs. APX3-1 to 3-5). Asymmetries in the climatological (Fig. 16) and annual phytoplankton bloom dynamics are evident, with higher chlorophyll a concentrations at the end than at beginning of the bloom in fifty-two from fifty-five regions and years, the exception is Eastern region in 2003, 2007 and 2010 (Fig. APX-3-5). This is the first time that this pattern has been noted for the Labrador Sea. However, it is important to point out that in Figure 16 there are no data for January, February, November and December – thus explaining why there appears a step-change from the end of year to the beginning of the year.

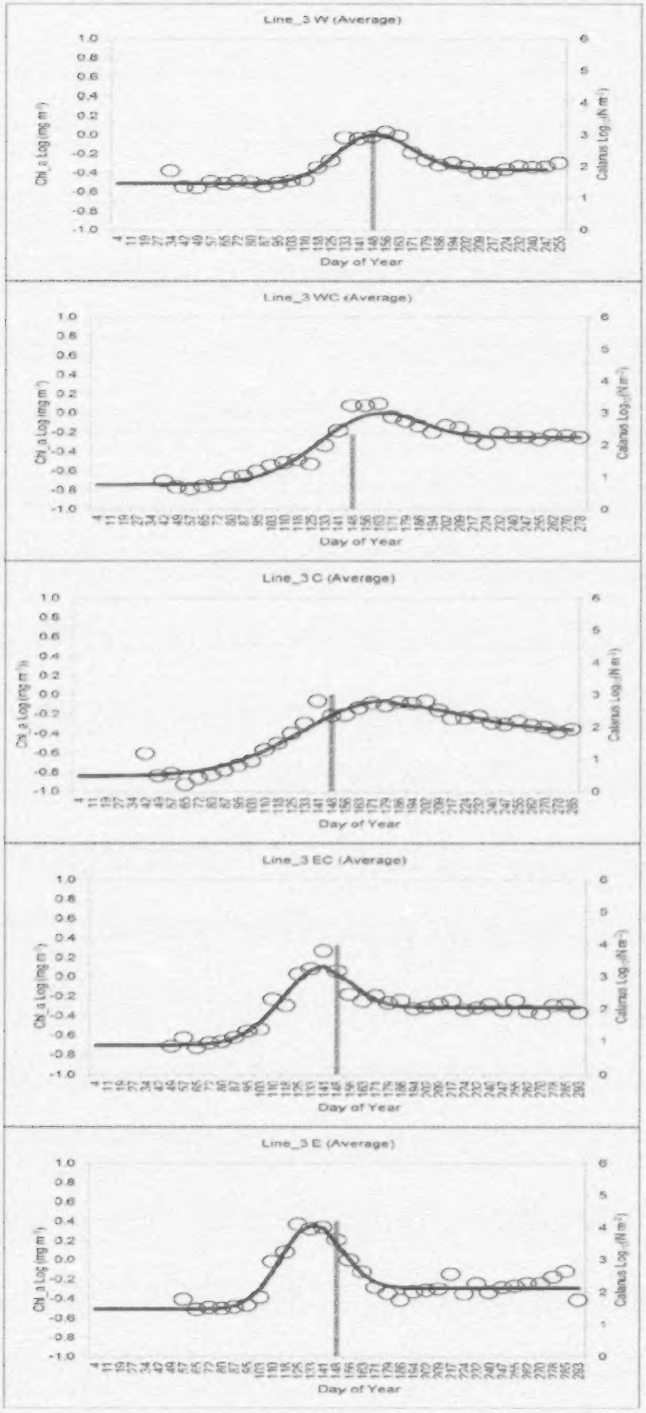

Figure 16. Average (2003 to 2013) of Chlorophyll_a (Log(mg m^{-3}) and abundances of C. finmarchicus C1 + C2 copepodites (1+2) (Log_{10}(N m^{-2}) for the five regions (W, WC, C, EC, and E) along the L-3 line across the Labrador Sea . Average 8-day chlorophyll a concentrations (open circles), Gaussian fits (solid line) and average dates of sampling and abundances of the copepods (red line) are shown.

3.3.2 SST warming

Water temperature influences development rate in copepods, so that inter-annual differences in temperature, as well as chlorophyll concentration, will influence the abundance of C1+C2 *C. finmarchicus* copepodites found on a particular date in a particular year. Thus, the seasonal cycle of sea surface temperature was analyzed using 8-day composites of AVHRR-derived data between 2003 and 2013. A Hovmöller diagram of the SST climatology for the twenty-eight rectangular areas along Line 3 stations is shown in Figure 17.

Figure 18 shows the SST averages (°C) with the Gaussian fits, in addition to the abundances of C1 + C2 *C. finmarchicus* copepodites ($Log_{10}(Num\ m^{-2})$) and the corresponding date of sampling, for the five regions. Appendix 3, (Figures APX-3-6 until 10) illustrates similar information but for the individual regions (W, WC, C, EC, and E) and period of study (2003 until 2013).

As expected, the Western regions reach higher maxima SST's than the Eastern regions. Interannual temperature values and the associated times at initiation and times of copepod sampling were extracted from the Gaussian fitted lines and incorporated in Table 28.

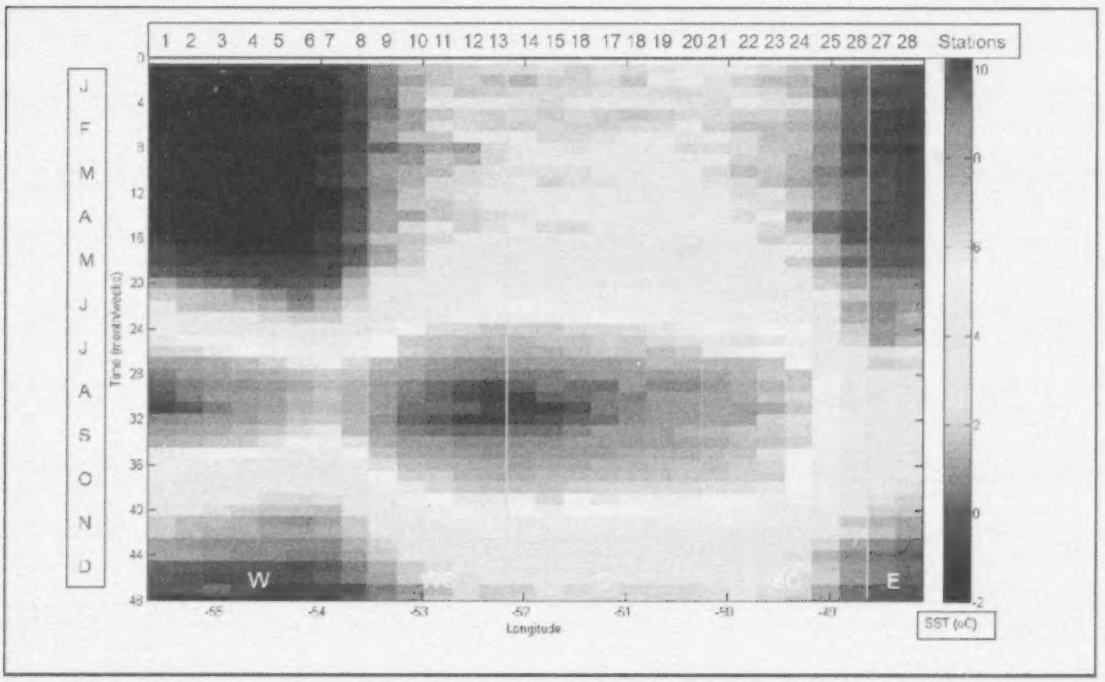

Figure 17. Hovmöller diagram of the climatology of Sea Surface Temperature for the period between 2003 and 2013. The colour shows average weekly SSTs (°C), the y-axis show the date (months or day of year) and the x-axis shows the station numbers (top) and longitudes (bottom), along the L-3 line. Vertical lines indicate the stations' regional groupings : Western (W), Western-Central (WC), Central (C), Eastern-Central (EC), and Eastern (E).

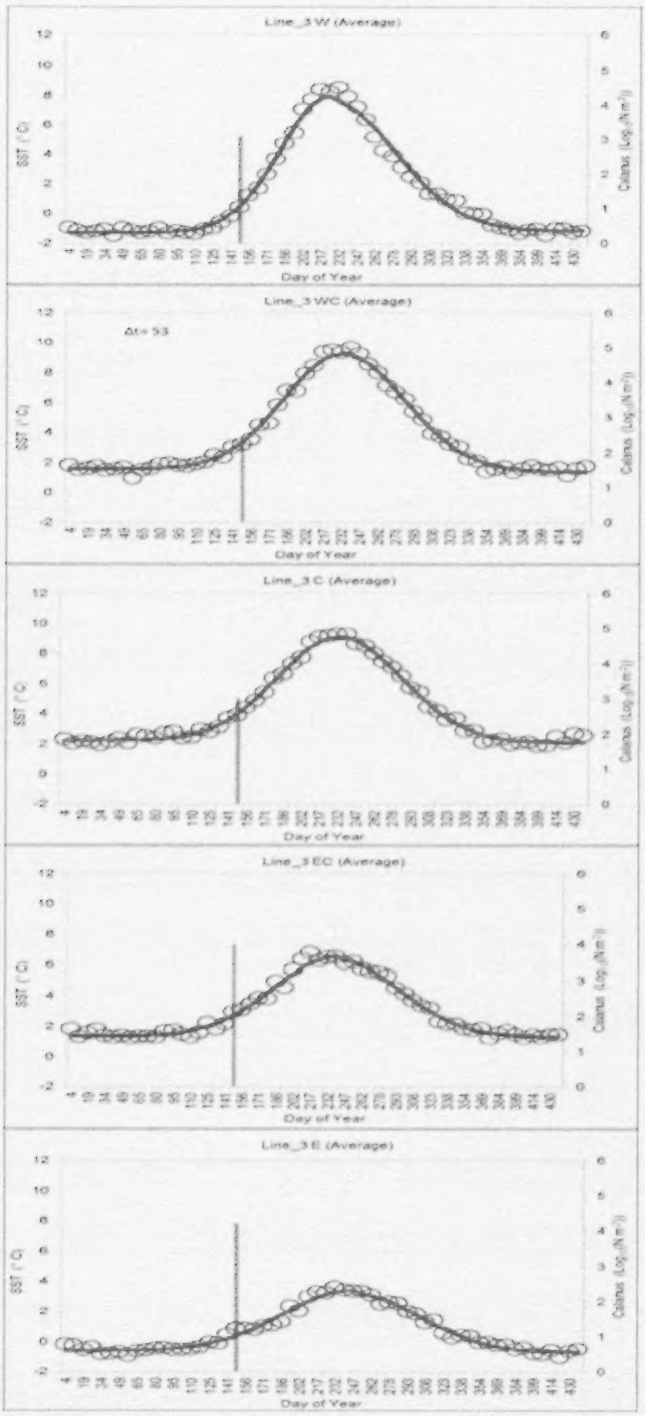

Figure 18. Regional averages (2003-2013) of Sea Surface Temperature (°C) and abundance of C. finmarchicus C1 + C2 copepodites ($Log_{10}(N\ m^{-2})$). SSTs (open circles), Gaussian fits (solid line) and copepodite sampling dates and abundances (red line) are shown.

3.3.3 Relationships between the environmental variability and C. finmarchicus abundance

The satellite-derived characteristics of the environmental variables used in this study (phytoplankton bloom and SST warming) were reduced by multivariate orthogonal transformations, using Principal Component Analysis (Cleveland *et al* 1993, TIBCO, 2010). PCA was independently applied to each of the variables: the characteristics of phytoplankton bloom Chl_{ini}, Chl_{max}, Chl_{end}, and the associated times (see Figure 5), and warming SST (water surface temperature and time at initiation and at sampling dates – see Figure 7), pooling the eleven years of data and five regions.

As Jollife (2002) states, "the central idea of PCA is to reduce the dimensionality of a data set consisting of a large number of interrelated variables, while retaining as much as possible of the variation present in the data set". In this study we analyzed the first component because it has the largest variance among all the standardized linear combinations of the PCA analysis. The second component was also included because of it had the largest variance among the linear combinations of the environmental variables uncorrelated with the first component.

The results of PCA analyses applied to the environmental data anomalies are shown in tables and annexes, as follows. Figure APX-3-11, shows the components relative importance pertaining to the phytoplankton bloom characteristics and the warming surface water. The first two components of the phytoplankton characteristics explain 56% of the variance, and the first two components of SST warming explain 80% of the variance. Table 3- shows the PCA loadings for both environmental indices.

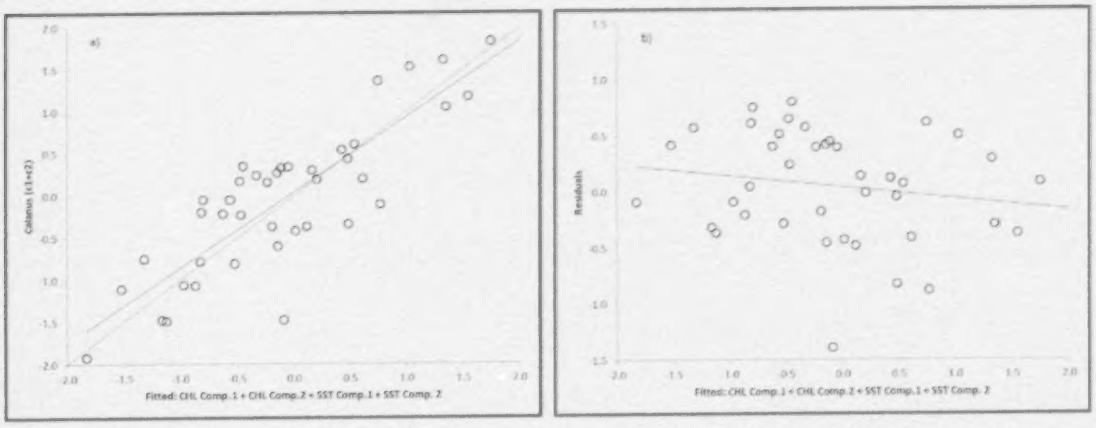

Figure 19.a) Non-parametrical (Loess) regression for the abundance of C. finmarchicus (C1 + C2 copepodites) and the first two PCA components of the environmental variables, phytoplankton bloom characteristics (CHL), and water warming rate on the sampling date (SST). Open symbols represent copepodite abundance, the solid line is the regression, and the dashed line is the 1:1 line. b) Residuals of the Loess regression.

A non-parametric multivariate local regression (Loess) model (TIBCO, 2010) was applied to relate the *C. finmarchicus C1 + C2* abundance to the principal components of the environmental variables previously described. The Loess model allows a large amount of flexibility because it does not require an *a priori* specification of the relationship between the dependent (copepods) and the independent (environmental) variables.

The first two principal components of each environmental variable used in the Loess model explained most of the original variation. Figure 19a shows the Loess regression with a Multiple R-squared of 0.74. The residuals presented in Figure 19b specified a median of 0.072, with -1.392 and 0.800 as minimum and maximum, respectively. F-values (ratio of the mean square of

the regression to the estimated variance) for the fitted values and the corresponding residuals are shown in Figure APX-3-12 a and b, respectively.

In conclusion, the results of this non-parametric regression model suggest strong interactions between physical (SST warming) and biological (phytoplankton bloom) characteristics, and showed that they explained most of the variations in the abundance of *C. finmarchicus* C1 + C2 copepodites among regions and years.

3.4 NAFO SUBAREA 1

In this section the relationship between the abundance of age-two Northern shrimp (*Pandalus borealis*) and biological and physical indices derived from satellite imagery are examined in Davis Strait, Northern Labrador Sea.

Mean carapace lengths (mm) for *P. borealis* in West Greenland were compiled from Burmeister *et al.* (2013, Tables 9 a and b). The data were grouped to match the phytoplankton and SST indices in NAFO divisions 1A to 1E for the 1993-2013 period. Figure 20 shows the changes of mean carapace length of northern shrimp at age two over time for five groups of substrata along West Greenland, between 1993 and 2013. There were no data for substrata W5 and W6 in 2010 and 2013, and no data for W7 to W9 in 1994, and between 2007 and 2013. In general, shrimp are longer in substrata W7 to W9 and shorter in areas U1 to U3. In addition there is marked temporal variability in substrata C0 and W1- W6.

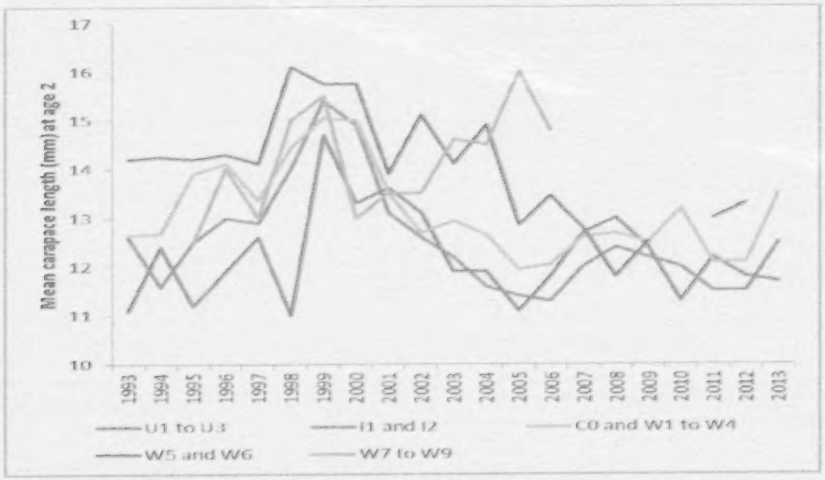

Figure 20 Mean carapace length (mm) at age two of Pandalus borealis in West Greenland (compiled from Burmeister et al 2013, Tables 9 a and b).

3.4.1 SST and Chlorophyll cycles

The yearly averages of SST between 1991 and 2012 for NAFO Subarea 1: Divisions 1A, 1B, 1C, 1D, 1E and 1F are shown in Figure 21. Mean values in division 1A are below 0°C, while there are warmer temperatures in the more southerly areas, *e.g.* Division 1F is above 2 °C. Hovmöller diagrams of SST by NAFO divisions show spatial and temporal variations, with a latitudinal gradient from cold (north) to warm (south) (Figure 22). The warm season is shorter in the north than in the south, and there is a positive trend in SST over time in all NAFO divisions for the twenty-two years of observations.

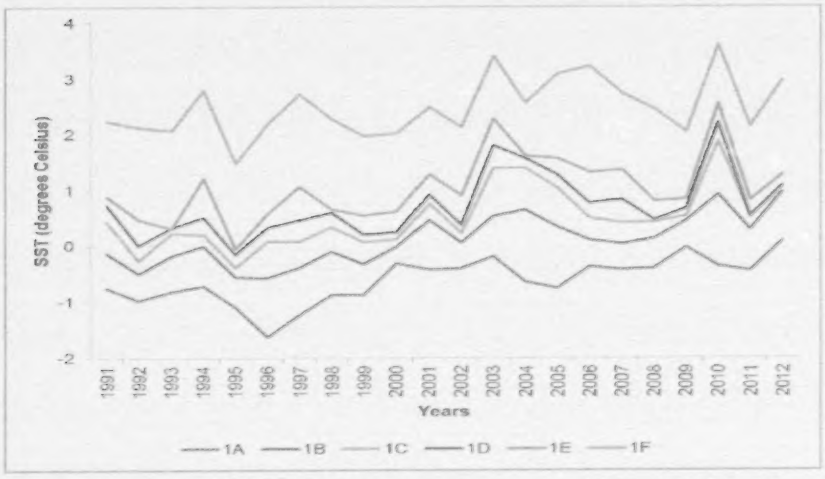

Figure 21 Annual average satellite-derived Sea Surface Temperatures (°C, 1991-2012) for NAFO divisions 1A, 1B, 1C, 1D, 1E, and 1F.

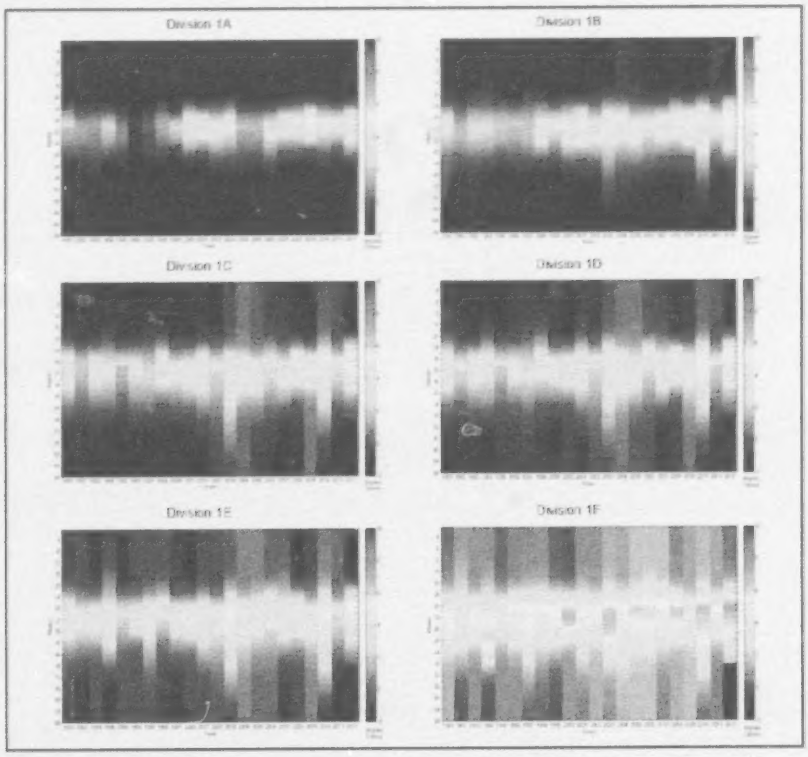

Figure 22 Hovmöller diagrams of Sea Surface Temperature (°C) for NAFO divisions 1A, 1B, 1C, 1D, 1E and 1F, from 1991 until 2012.

3.4.2 Relationships among ecological indices and Pandalus borealis

Environmental variability in shrimp fishing areas in the Western Greenland appear closely related to the seasonal warming and phytoplankton bloom characteristics. There is clearly a latitudinal progression in these environmental factors (Figure 23).

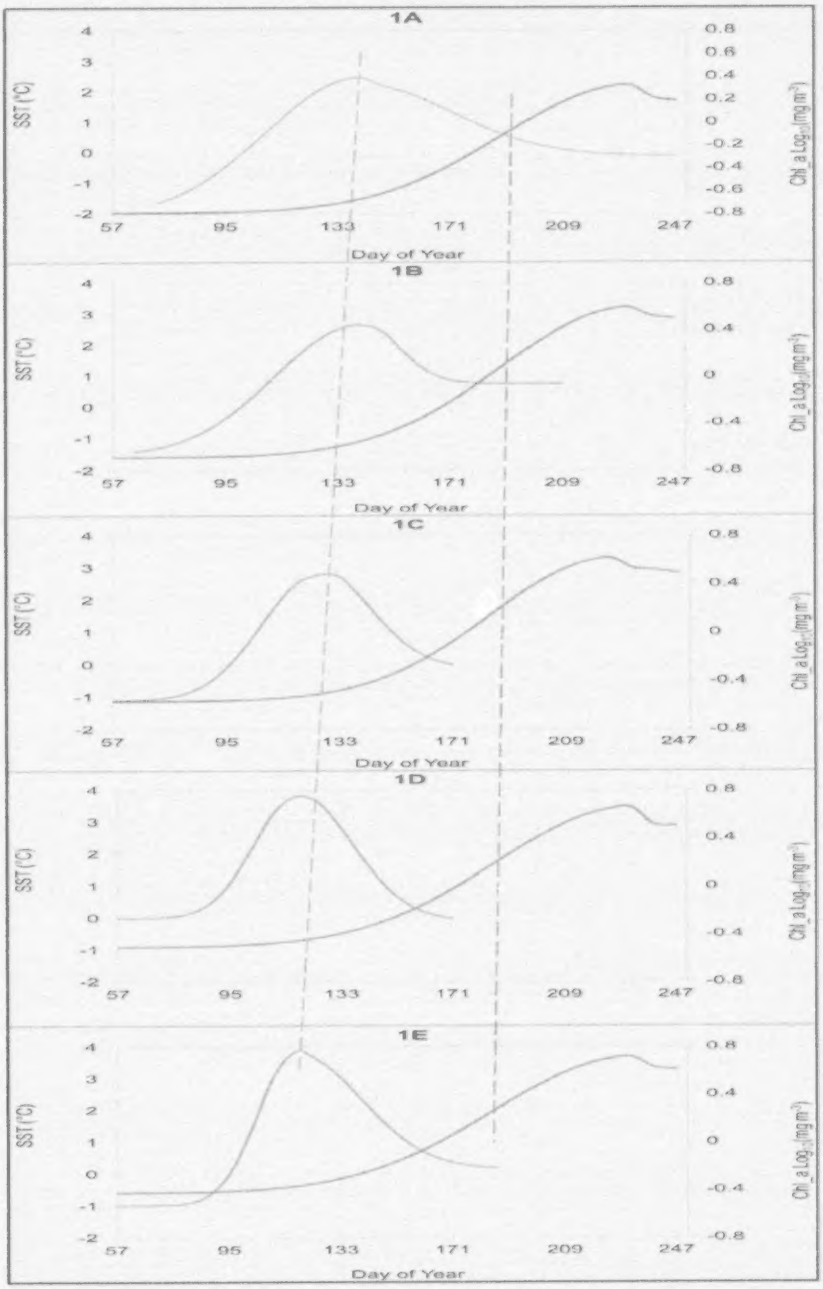

Figure 23 Satellite-derived climatology of SST (red solid line) and phytoplankton bloom (green solid line) for NAFO divisions 1A, 1B, 1C, 1D, and 1E. Red dashed line relates the warming inflexion points and the green dashed line is close to the maxima of phytoplankton concentrations.

In addition to there being colder temperatures in the northern (1A) than in southern divisions (1E), the time to reach the increasing inflexion point is later in these regions (Fig. 23). A similar change is seen in the timing of phytoplankton blooming (green hatched line). The bloom shape is also different in each of these divisions, broad in the north (1A) and narrow in the south (1E), with important asymmetries in all divisions.

Using a similar approach to that used for the assessment of copepod abundance, PCA and Loess regressions were applied to investigate the relationship between northern shrimp abundance and environmental variability. After calculation of the environmental anomalies, the data were used as input in PCA to reduce information contained in the plankton indices (concentration and timing of Chlorophyll at initiation, maximum and end). The warming SST was characterized by the satellite-derived temperatures (°C) at the initiation and at the SST inflexion point associated with spring warming, and the associated timings.

Table 31 shows the PCA loadings of the phytoplankton bloom and SST indices for the pooled five NAFO divisions in Western Greenland (1A, 1B, 1C, 1D and 1E), and thirteen years (1998-2010). Their relative importance is shown in Figure APX-4-1, where the first two components of the phytoplankton bloom characteristics explained 56% of the variance and the first two components of SST warming explained up to 83%.

The first two PCA components of the physical (SST warming) and the second component of biological (Chl bloom) properties were used as independent variables in a Loess model to explain the abundance of 2-years *Pandalus borealis* in four of Burmeister *et al* (2013) shrimp density distribution regions (U1 to U3; C0, W1 to W4; W5+W6, and W7 to W9). Shrimp data in the regression were abundance anomalies lagged by 2 years to match the corresponding environmental data times. The time-lag is an intrinsic period related to shrimp hatching, and is associated to the shrimp larvae success and environmental variables (Allen 1959, Koeller 2000, Ouellet *et al.* 2011). Shrimp mating and spawning occur in July - September, the egg-bearing period lasts 8 to 10 months, depending on the bottom temperature. The larvae hatch in April - June the following year (Shumway et al. 1985, Bergström 2000, Horsted 1978). When the hatching time approaches, the female migrates to relatively shallow water (< 150 meters). The newly hatched larvae live in the upper part of the water column. During spring and summer, the larvae pases through six planktonic stages in three to four months. In the last larval stages, the larvae settle at the bottom as immature shrimps (Shumway et al. 1985, Bergström 2000, Storm & Pedersen 2003). Hatching is believed to take place along the entire coast of West Greenland (Storm & Pedersen 2003). Due to the northbound West Greenland current which dominates the West Greenland shelf (Ribergaard et al. 2004), larval drift from hatching areas (spawning grounds) to settling areas can cover distances of up to 500 km (Storm & Pedersen 2003). The banks north of 64°N and the Disko Bay are believed to be important nursery areas for larvae and juvenile shrimps (Storm & Pedersen 2003, Ribergaard et al. 2004, Wieland 2005).

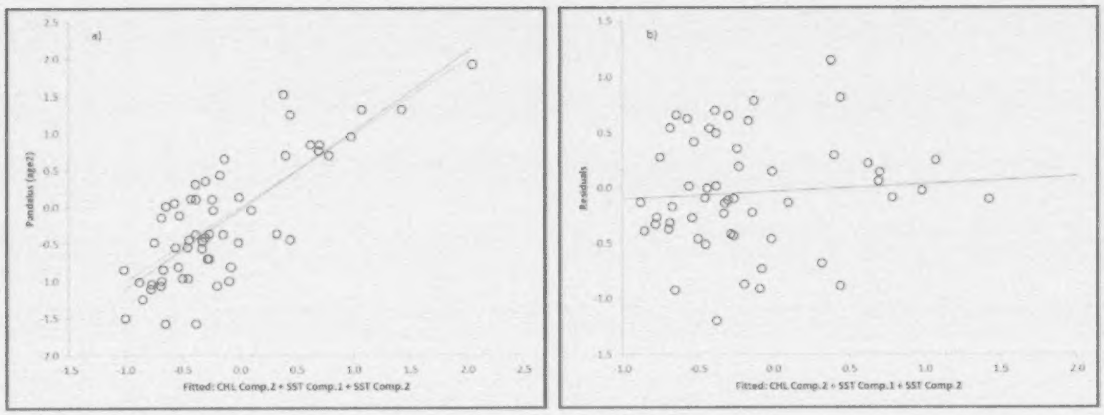

Figure 24.a) Non-parametrical (Loess) regression on the abundance of 2-year old Pandalus borealis (lagged 2 years) and the PCA components of the environmental variables. Open symbols represent shrimp abundance, the solid line is the regression and dashed line is the 1:1 line. b) Residuals of the Loess model regression.

The biological second component was selected as an explanatory variable after testing different combinations of the physical and biological PCA components. Other study have also found that using the 2nd PCA component in non-parametric models explained more of the variance, when looking at the effect of environmental variability on fish body condition and recruitment success (Plourde *et al* 2015).

The Loess regression had a Multiple R-squared of 0.64 (Fig. 24a). The residuals had a median of -0.097, with values of -1.197 and 1.147 as minimum and maximum, respectively (Fig. 24b). F-values for the fitted values and the corresponding residuals are presented in Figure APX-4-2.

4. DISCUSSION

4.1 REGIONAL VARIATION IN THE RITA AMONG NAFO DIVISIONS

The information that underlies the RITA (Remote-sensing Index of Trophic Availability) index for all NAFO divisions is chlorophyll a climatology. The spring phytoplankton bloom displayed in graphic representations show distinct asymmetries on either side of the maxima. It is worthy of mention that the pelagic ecosystem in the Northwest Atlantic Ocean has a pronounced seasonality, with two chlorophyll blooms, which vary with latitude. In southern regions there are generally blooms in spring and autumn, while in northern regions there is generally only one "spring/summer" bloom (Platt *et al* 2009).

The northern NAFO divisions, but also part of the Gulf of St. Lawrence, display relatively low chlorophyll a concentrations at the beginning of the bloom but after reaching their maxima they continue to have high concentrations thereafter. It has been suggested that high nutrient concentrations and adequate light (photosynthetically active radiation,PAR) may help to sustain the elevated pigment values. In general, the southern divisions show the opposite pattern: relatively high chlorophyll a concentrations at the beginning of the bloom and low values at the end. These regions also have phytoplankton blooms in autumn (not examined in this work). The fall bloom may be caused by the increased vertical mixing and breakdown of stratification

allowing the influx of nutrients from depth into the upper layers. It has also been suggested, however, that zooplankton grazing may be affected by increased vertical mixing, such that the abundance of microzooplankton grazers is diluted, and promoting phytoplankton growth (Findlay et al 2006).

The phytoplankton bloom characteristics used in the calculation of the RITA index showed clear spatial and temporal variability. The average of all NAFO regions showed Chlorophyll a concentrations at the initiation of the phytoplankton bloom with a negative trend over time. Conversely, a positive trend is seen in the maximum chlorophyll intensity of the bloom. It is interesting to notice that the maximum values developed sooner that the climatology in almost 50% of the 13 years of study, in specific: 1998, 1999, 2005, 2006, 2009 and 2010.

The combination of phytoplankton bloom characteristics incorporated in the RITA index is a new metric suitable for reporting on the State of the Oceans, especially in the context of primary productivity and climate change. Our analysis reveals a weak but positive increase in the annual average value of RITA from 1999 to 2010. It is possible that this positive trend is still occurring, due to ongoing climatic trends (e.g. global warming). As well, there is a latitudinal trend, with high index values in the north, in particular in Western Greenland, and low values in the southwest, such as Western Georges Bank. Nevertheless, interannual changes in the RITA for individual regions are complex, as shown by the maps of the anomalies (Figs. APX-2-1 to APX-2-13).

An appropriate interpretation of spatial and temporal changes in the RITA starts by finding similarities in the index among NAFO divisions. The five groups appearing from PAM (Medoid Partitioning Algorithms) cluster analyses identify strong and short blooms in northern areas, even more where Baffin Bay and Labrador Sea are classified as different entities. Ambiguous PAM grouping of the Southern GSL and Gulf of Maine suggest that individual components of RITA, such as the bloom timings, which are quite variable in these regions, are less important than the similarities in maximum absolute chlorophyll a concentration, which keep them in the same cluster. The Labrador and Newfoundland shelves share similar combinations of bloom characteristics, which are different from those of the ensemble of NAFO divisions. This may be because there is a common driver (Labrador Current), which provides similar conditions to the entire shelf. The opposite circumstances seem to occur in Cluster 3 where rather disparate geographical divisions were grouped (Southern Greenland, Northeastern GSL, South Newfoundland, Scotian Shelf, and Georges Bank). On the other hand, some associations are consistent; for example, it is well known that the current along the shelf of in Southern Newfoundland turns north through Cabot Strait toward the Northeastern GSL. As well, the Scotian Shelf regions share similar characteristics because they are connected by circulation (Loder *et al* 1998). Division 3K is an interesting region, since it separates, northern and southern groups of divisions. This dynamic area, with frequent eddies, is also known as the Slope Water Jet region (Fratantoni and Pickart 2007). It combines properties of the warm Gulf Stream and cold Labrador Current, and is a transitional zone. Division 1F is a large area, which shares characteristics with members of different groups, confounding the clustering process. The Grand Banks of Newfoundland are separated from more northerly regions by a second transitional zone, NAFO division 3K. This area includes North Atlantic current meanders, providing a combination of mostly cold Labrador Current and warm Gulf Stream water masses. Division 5Zw is a small region that could not be properly classified.

Overall, the RITA provides a way of classifying NAFO divisions in Subareas 0 to 5, according to their phytoplankton bloom characteristics. Detailed analyses with appropriate fisheries data sets are needed to identify functional links.

4.2 RELATIONSHIPS BETWEEN ZOOPLANKTON ABUNDANCE AND ENVIRONMENTAL VARIABLES ON THE L-3 LABRADOR SEA TRANSECT

The abundance of *Calanus finmarchicus* (C1 + C2) are linked to biological (phytoplankton bloom) and physical (warming SST) indices in the Labrador Sea. The analyses involved using data from twenty-eight rectangular areas and zooplankton sampling stations, which could be classified as belonging to one of five regions (W, WC, C, EC, and E) along the L-3 line of the AZOMP. The use of remote-sensing allowed for the explanation of inter-annual differences in *C. finmarchicus* C1 + C2 abundance, based on inter-annual differences in phytoplankton bloom dynamics and late winter/spring warming in the Labrador Sea over 13 years of sampling.

The first two PCA loadings for the phytoplankton blooms identified low chlorophyll a concentrations associated with late bloom timings, while the first two PCA loadings for the SST warming retrieved high temperatures both at bloom initiation and during the zooplankton sampling, in combination with early bloom initiation and/or late zooplankton sampling timings.

The PCA analysis showed that early blooms in warm years were associated with higher C1+C2 abundances, for zooplankton sampling collected on similar dates, but if the latter were later, SSTs were higher and C1+C2 abundances were higher, regardless of the timing of the spring bloom.

4.3 RELATIONSHIPS BETWEEN THE ABUNDANCE OF SHRIMP AND ENVIRONMENTAL VARIABLES IN NAFO SUBAREA 1

We extended the method of PCA for reduction of remotely-sensed physical and environmental variables followed by their use as input for a Loess model to the study of age-two Northern shrimp *Pandalus borealis* abundance in the eastern Labrador Sea. Using SST warming inflexion points and the second biological PCA component as an independent variables, enhanced the results for the Loess regressions. The PCA loadings associated with late spring warming and late bloom initiation and maxima occurred at NAFO Subarea 1 in years that had high abundances for age-two shrimp two years later.

As a final point, it appears that the warming SSTs and also the spring rates of warming are important in the NAFO subareas. The increasing trends in SST are expected to continue and their effects should be incorporated in any future ecological studies relating to primary and secondary producers. The clustering of NAFO divisions described here provides information about which areas share similar bloom characteristics and physical forcings. Thus, it may be possible to apply results of detailed ecological studies in one region to others, leading to a greater understanding of the likely effects of environmental (i.e. climate) change over a region much larger than the original study area.

ACKNOWLEDGMENTS

The authors thank the Strategic Program For Ecosystem-Based Research and Advice (SPERA) for financing this project. We also express our thanks to DFO Maritime Sciences sector management, the AZMP committees and the Canadian Coast Guard for their support and facilitate the field work. We especially thank to our colleagues Devred (Emmanuel), Horne (Edward), Breeze (Heather), and Hanke (Alex) for their contribution in the scientific design of this project. We thank Li Zhai and Edward Horne for their review of this report.

REFERENCES CITED

Allen, J.A. 1959. On the biology of *Pandalus borealis* Krøyer, with reference to a population off the Northumberland coast. J. Mar. Biol. Assoc. U.K., 38:189-220.

Burmeister, A., Kingsley, M.C.S. and Siegstad, H. 2013. The West Greenland trawl survey for Pandalus borealis, 2013, with reference to earlier results. NAFO SCR Doc. 13/056, NAFO/ICES WG PANDALUS ASSESSMENT GROUP.

Casey, K.S., T.B. Brandon, P. Cornillon, and R. Evans (2010). "The Past, Present and Future of the AVHRR Pathfinder SST Program", in Oceanography from Space: Revisited, eds. V. Barale, J.F.R. Gower, and L. Alberotanza, Springer. DOI: 10.1007/978-90-481-8681-5_16.

Cleveland, W.S., Grosse, E., Shyu, W.M. (1993). Local regression models. In: Chambers, J.M., Hastie, T.J. (Eds.), Statistical models in S. Chapman and Hall, London.

Colbourne, E., Holden, J., Craig, J., Senciall, D., Bailey, W., Stead, P., and Fitzpatrick, C. 2014. Physical oceanographic conditions on the Newfoundland and Labrador Shelf during 2013. DFO Can. Sci. Advis. Sec. Res. Doc. 2014/094. v + 38 p.

Eumetsat (2013). Retrieved 10 31, 2013, from METOP: http://www.eumetsat.int/website/home/Satellites/CurrentSatellites/Metop/index.html

DFO (2012). Marine Protected Area Network Planning in the Scotian Shelf Bioregion: Objectives, Data, and Methods 2012/064. In, *DFO Canadian Science Advisory Secretariat.*

Findlay,H.S., Yool, A., Nodale M., and Pitchford, J.W. 2006. Modelling of autumn plankton bloom dynamics. Journal of Plankton Research. 28(2): 209–220.

Fratantoni, P.S., and Pickart, R.S. 2007. The western North Atlantic shelfbreak current system in summer. *Journal of Physical Oceanography*, 37: 2509-2533.

Fuentes-Yaco, C., Koeller, P.A., Sathyendranath, S., & Platt, T. (2007). Shrimp (Pandalus borealis) growth and timing of the spring phytoplankton bloom on the Newfoundland–Labrador Shelf. *Fisheries Oceanography, 16*, 116-129.

Fuentes-Yaco, C., A. Hanke, C. Caverhill, G. White and W. Li. 2013. Phytoplankton blooms in the Gulf of St. Lawrence: a remote sensing approach. Atlantic Canada Coastal and Estuarine Science Society (ACCESS) Conference, Lawrencetown, Nova Scotia, Canada, May 9th to 11th.

Greenlaw, M.E., Fuentes-Yaco, C., McCurdy, Q.M., Page, F., and White, G.N. III. 2015. A geodatabase of oceanographic datasets for habitat mapping and species distribution modeling on the Scotian Shelf. Can. Tech. Rep. Fish. Aquat. Sci. *In revision.*

Harrison, W.G., & Sameoto, D.D. (1996). Incorporating ecosystem information into the Fisheries Assessment: Can we develop a quantitative "plankton index"? In: Canadian Science Advisory Secretariat, Department of Fisheries and Oceans.

Head, E. J. H., Harris, L. R. and Yashayaev, I. 2003. Distributions of Calanus spp. and other mesozooplankton in the Labrador Sea in relation to hydrography in spring and early summer (1995–2000). Prog. Oceanogr., 59: 1–30.

Johnson, C., Li, W., Head, E., Casault, B., and Spry, J. 2014. Optical, chemical, and biological oceanographic conditions on the Scotian Shelf and in the eastern Gulf of Maine in 2013. DFO Can. Sci. Advis. Sec. Res. Doc. 2014/104 v + 49 p.

Jollife, I.T. (2002) Principal Component Analysis, 2nd ed. Springer-Verlag New York Inc., 487 p.

Jørgensen, O.A. and Hammeken Arboe N. 2013. Distribution of the commercial fishery for Greenland halibut and Northern shrimp in Baffin Bay. Technical Report no. 91. Greenland Institute of Natural resources.

Kaufman, L. and Rousseeuw, P.J. (1990). Finding Groups in Data: An Introduction to Cluster Analysis. New York: John Wiley & Sons, Inc.

Koeller, P. 2000. Relative importance of abiotic and biotic factors to the management of the Northern shrimp (*Pandalus borealis*) fishery on the Scotian Shelf. J. Northw. Atl. Fish. Sci. 27: 21-33.

Koeller, P., Fuentes-Yaco, C., Platt, T., Sathyendranath, S., Richards, A., Ouellet, P., Orr, D., Skúladóttir, U., Wieland, K., Savard, L., & Aschan, M. (2009). Basin-Scale Coherence in Phenology of Shrimps and Phytoplankton in the North Atlantic Ocean. *Science, 324*, 791-793.

Li, W.K.W. 2014. The state of phytoplankton and bacterioplankton on the Scotian Shelf and Slope: Atlantic Zone Monitoring Program 1997-2013. Can. Tech. Rep. Hydrogr. Ocean. Sci. 303: xx + 140 p.

Loder, W.J., Petrie, B., and Gawarkiewicz, G. 1998. The coastal ocean off northeastern north America: a large-scale view coastal segment (1,W). *In*: Robinson, A.R. and Brink, K.H. (Eds.), The Sea, Vol. 11, Chapter 5, p. 105-133.

Mitchell, M.R., G. Harrison, K. Pauley, A. Gagné, G. Maillet, and P. Strain. 2002. Atlantic Zonal Monitoring Program Sampling Protocol. Can. Tech. Rep. Hydrogr. Ocean Sci. 223: iv + 23 pp.

Ouellet, P. Fuentes-Yaco, C., Savard, L., Platt, T., Sathyendranath, S., Koeller, P., Orr, D., and Siegstad, H. 2011. Ocean surface characteristics influence recruitment variability of populations of northern shrimp (*Pandalus borealis*) in the Northwest Atlantic. ICES Journal of Marine Science, 68(4):737–744.

Pepin, P., Maillet, G., Fraser, S., Shears, T. and Redmond G. 2015. Optical, chemical, and biological oceanographic conditions on the Newfoundland and Labrador Shelf during 2013. DFO Can. Sci. Advis. Sec. Res. Doc. 2015/027. v + 37p.

Platt, T., Fuentes-Yaco, C., & Frank, K.T. (2003). Marine ecology: Spring algal bloom and larval fish survival. *Nature, 423*, 398-399.

Platt, T., Sathyendranath, S., Forget, M.-H.l.n., White Iii, G.N., Caverhill, C., Bouman, H., Devred, E., & Son, S. (2008). Operational estimation of primary production at large geographical scales. *Remote Sensing of Environment, 112*, 3437-3448.

Platt, T., Sathyendranath, S., White, G.N., Fuentes-Yaco, C., Zhai, L., Devred. E., Tang, C. 2009. Diagnostic properties of phytoplankton time series from remote sensing. *Estuaries and Coasts*, DOI 10.1007/s12237-009-9161-0.

Plourde, S., Gregoire, F., Lehoux C., Galbraith, P.S., Castonguay, M., and Ringuette, M. 2015. Effect of environmental variability on body condition and recruitment success of Atlantic Mackerel (Scomber scombrus L.) in the Gulf of St. Lawrence. Fish. Oceanogr. 24:4, 347–363.

R Core Team. 2012. R: A language and environment for statistical computing. R Foundation for Statistical Computing, Vienna, Austria. ISBN 3-900051-07-0, URL http://www.R-project.org/.

Ricketts, J.H. and G.A. Head. 1999. A five-parameter logistic equation for investigating asymmetry of curvature in baroreflex studies. *Am J Physiol Regul Integr Comp Physiol* 277:R441-R454.

Sea Space. (2013). Retrieved 10 31, 2013, from Sea Space home page: http://www.seaspace.com/.

Stickney, A.P. and Perkins, H.C. 1981. Observations on the food of the larvae of the northern shrimp, Pandalus borealis Kröyer (Decapoda, Caridea). *Crustaceana* 40:36–49.

TIBCO. 2010. Spotfire S+® 8.2 Guide to Statistics Volumes 1 and 2, TIBCO Software Inc., 557 p.

Tang, C.L., Ross, C.K., Yao, T., Petrie, B. , Detracey, B.M., and Dunlap, E. 2004. The circulation, water masses and sea-ice of Baffin Bay. Progress in Oceanography, 63, 183-228.

UNEP, 2004. Pedersen, S.A., Madsen, J. and M. Dyhr-Nielsen, Arctic Greenland, East Greenland Shelf, West Greenland Shelf, GIWA Regional assessment 1b, 15, 16. University of Kalmar, Kalmar, Sweden.

Wu, Y., Tang, C. Hannah, C. 2012. The circulation of eastern Canadian seas. Progress in Oceanography, 106, 28–48.

TABLES

Table 1. Phytoplankton bloom indices derived from SeaWiFS in the NAFO Division 0A, between 1998 and 2010.

	Initiation	Maximum	End	Initiation	Maximum	End	Duration	Index
Year	Log10 Chl_a (mg/m^3)			Day of Year			days	(d^-1)
1998	-0.53	0.42	-0.24	110.26	163.49	224.32	114.06	0.006
1999	-0.45	0.44	-0.14	133.07	163.49	231.93	98.85	0.005
2000	-0.51	0.48	-0.31	125.47	163.49	224.32	98.85	0.006
2001	-1.01	0.42	-0.37	102.66	155.89	224.32	121.67	0.009
2002	-0.66	0.30	0.30	102.66	155.89	224.32	121.67	0.006
2003	-0.55	0.10	-0.32	102.66	163.49	247.14	144.48	0.004
2004	-0.66	0.18	-0.35	95.05	140.68	231.93	136.87	0.006
2005	-0.64	0.17	-0.52	110.26	155.89	247.14	136.88	0.005
2006	-0.69	0.23	-0.43	102.66	148.28	247.14	144.48	0.006
2007	-0.60	0.49	-0.41	117.86	155.89	239.53	121.67	0.007
2008	-0.62	0.13	-0.44	95.05	155.89	262.34	167.29	0.005
2009	-0.62	0.34	-0.40	102.66	163.49	262.34	159.69	0.006
2010	-0.79	0.11	-0.29	117.86	163.49	209.11	91.25	0.006

Table 2. Phytoplankton bloom indices derived from SeaWiFS in the NAFO Division 0B, between 1998 and 2010.

	Initiation	Maximum	End	Initiation	Maximum	End	Duration	Index
Year	Log10 Chl_a (mg/m^3)			Day of Year			days	(d^-1)
1998	-0.51	0.61	-0.09	102.66	117.86	155.89	53.23	0.010
1999	-0.47	0.36	-0.23	79.84	133.07	148.28	68.44	0.006
2000	-0.60	0.01	-0.28	79.84	125.47	155.89	76.04	0.005
2001	-0.75	0.43	-0.20	79.84	125.47	148.28	68.44	0.009
2002	-0.50	0.04	-0.14	95.05	117.86	133.07	38.02	0.005
2003	-0.65	0.31	-0.20	87.45	140.68	155.89	68.44	0.007
2004	-0.60	0.22	-0.30	95.05	133.07	155.89	60.83	0.006
2005	-0.58	0.16	-0.01	110.26	133.07	163.49	53.23	0.006
2006	-0.73	0.20	-0.15	72.24	133.07	155.89	83.65	0.007
2007	-0.47	0.36	-0.23	79.84	133.07	148.28	68.44	0.006
2008	-0.56	0.28	-0.16	79.84	140.68	155.89	76.04	0.006
2009	-0.60	0.18	-0.10	72.24	133.07	148.28	76.04	0.006
2010	-0.72	0.29	-0.15	79.84	117.86	155.89	76.04	0.009

Table 3. Phytoplankton bloom indices derived from SeaWiFS in the NAFO Division 1A, between 1998 and 2010.

	Initiation	Maximum	End	Initiation	Maximum	End	Duration	Index
Year	Log10 Chl_a (mg/m^3)			Day of Year			days	(d^-1)
1998	-0.67	0.42	-0.14	87.45	125.47	209.11	121.67	0.009
1999	-0.62	0.31	-0.12	95.05	163.49	216.72	121.67	0.006
2000	-0.75	0.37	-0.28	79.84	140.68	209.11	129.27	0.008
2001	-0.69	0.35	-0.27	79.84	148.28	216.72	136.88	0.007
2002	-0.63	0.49	-0.22	87.45	140.68	201.51	114.06	0.008
2003	-0.46	0.28	-0.10	87.45	148.28	178.70	91.25	0.005
2004	-0.52	0.46	-0.14	87.45	125.47	186.30	98.85	0.008
2005	-0.44	0.56	-0.31	95.05	133.07	201.51	106.46	0.008
2006	-0.55	0.42	-0.26	87.45	140.68	209.11	121.67	0.007
2007	-0.53	0.52	-0.27	95.05	140.68	216.72	121.67	0.007
2008	-0.38	0.34	-0.28	95.05	140.68	209.11	114.06	0.005
2009	-0.56	0.41	-0.16	87.45	140.68	193.91	106.46	0.007
2010	-0.50	0.52	-0.21	87.45	133.07	186.30	98.85	0.008

Table 4. Phytoplankton bloom indices derived from SeaWiFS in the NAFO Division 1B, between 1998 and 2010.

	Initiation	Maximum	End	Initiation	Maximum	End	Duration	Index
Year	Log10 Chl_a (mg/m^3)			Day of Year			days	(d^-1)
1998	-0.54	0.62	-0.16	95.05	125.47	155.89	60.83	0.009
1999	-0.46	0.64	-0.19	87.45	133.07	163.49	76.04	0.008
2000	-0.42	0.58	-0.09	87.45	140.68	163.49	76.04	0.007
2001	-0.49	0.82	-0.18	72.24	110.26	155.89	83.65	0.012
2002	-0.20	0.59	0.00	95.05	117.86	163.49	68.44	0.007
2003	-0.35	0.75	-0.15	102.66	117.86	155.89	53.23	0.009
2004	-0.50	0.72	-0.27	95.05	125.47	155.89	60.83	0.010
2005	-0.58	0.44	-0.01	95.05	133.07	148.28	53.23	0.008
2006	-0.60	0.40	-0.35	87.45	117.86	155.89	68.44	0.008
2007	-0.32	1.02	-0.30	110.26	133.07	163.49	53.23	0.010
2008	-0.29	0.80	-0.41	102.66	133.07	155.89	53.23	0.008
2009	-0.09	0.48	-0.21	87.45	110.26	163.49	76.04	0.005
2010	-0.44	0.60	-0.10	87.45	117.86	148.28	60.83	0.009

Table 5. Phytoplankton bloom indices derived from SeaWiFS in the NAFO Division 1C, between 1998 and 2010.

	ınitiation	Maximum	End	Initiation	Maximum	End	Duration	Index
Year	Log10 Chl_a (mg/m^3)			Day of Year			days	(d^-1)
1998	-0.54	0.62	-0.16	95.05	125.47	155.89	60.83	0.009
1999	-0.46	0.64	-0.19	87.45	133.07	163.49	76.04	0.008
2000	-0.42	0.58	-0.09	87.45	140.68	163.49	76.04	0.007
2001	-0.49	0.82	-0.18	72.24	110.26	155.89	83.65	0.012
2002	-0.20	0.59	0.00	95.05	117.86	163.49	68.44	0.007
2003	-0.35	0.75	-0.15	102.66	117.86	155.89	53.23	0.009
2004	-0.50	0.72	-0.27	95.05	125.47	155.89	60.83	0.010
2005	-0.58	0.44	-0.01	95.05	133.07	148.28	53.23	0.008
2006	-0.60	0.40	-0.35	87.45	117.86	155.89	68.44	0.008
2007	-0.32	1.02	-0.30	110.26	133.07	163.49	53.23	0.010
2008	-0.29	0.80	-0.41	102.66	133.07	155.89	53.23	0.008
2009	-0.09	0.48	-0.21	87.45	110.26	163.49	76.04	0.005
2010	-0.44	0.60	-0.10	87.45	117.86	148.28	60.83	0.009

Table 6. Phytoplankton bloom indices derived from SeaWiFS in the NAFO Division 1D, between 1998 and 2010.

	Initiation	Maximum	End	Initiation	Maximum	End	Duration	Index
Year	Log10 Chl_a (mg/m^3)			Day of Year			days	(d^-1)
1998	-0.50	0.74	-0.43	87.45	117.86	163.49	76.04	0.011
1999	-0.41	0.58	-0.37	79.84	125.47	163.49	83.65	0.008
2000	-0.60	0.56	-0.17	64.64	133.07	155.89	91.25	0.009
2001	-0.43	0.82	-0.26	79.84	117.86	155.89	76.04	0.011
2002	-0.33	0.86	-0.04	95.05	117.86	155.89	60.83	0.010
2003	-0.37	0.86	-0.27	95.05	117.86	155.89	60.83	0.010
2004	-0.50	0.56	-0.39	95.05	125.47	155.89	60.83	0.008
2005	-0.72	0.46	-0.14	87.45	117.86	140.68	53.23	0.010
2006	-0.51	0.52	-0.36	87.45	117.86	155.89	68.44	0.009
2007	-0.44	0.80	-0.30	95.05	125.47	163.49	68.44	0.010
2008	-0.14	0.91	-0.15	117.86	133.07	163.49	45.63	0.008
2009	-0.61	0.72	-0.10	64.64	125.47	155.89	91.25	0.011
2010	-0.15	0.75	-0.15	87.45	117.86	155.89	68.44	0.008

Table 7. Phytoplankton bloom indices derived from SeaWiFS in the NAFO Division 1E, between 1998 and 2010.

	Initiation	Maximum	End	Initiation	Maximum	End	Duration	Index
Year	Log10 Chl_a (mg/m^3)			Day of Year			days	(d^-1)
1998	-0.56	0.77	-0.39	79.84	125.47	178.70	98.85	0.011
1999	-0.36	0.55	-0.18	87.45	117.86	178.70	91.25	0.008
2000	-0.48	0.59	-0.02	87.45	133.07	155.89	68.44	0.008
2001	-0.52	0.81	-0.24	87.45	110.26	171.09	83.65	0.012
2002	-0.38	0.82	-0.02	87.45	125.47	155.89	68.44	0.010
2003	-0.45	0.81	-0.24	95.05	117.86	171.09	76.04	0.011
2004	-0.56	0.61	-0.11	87.45	125.47	155.89	68.44	0.009
2005	-0.58	0.70	-0.24	95.05	117.86	133.07	38.02	0.011
2006	-0.53	0.62	-0.14	87.45	133.07	155.89	68.44	0.009
2007	-0.43	0.99	-0.03	95.05	125.47	163.49	68.44	0.011
2008	-0.38	0.70	0.16	102.66	140.68	171.09	68.44	0.008
2009	-0.58	0.58	-0.40	72.24	125.47	178.70	106.46	0.009
2010	-0.45	0.76	-0.11	87.45	117.86	163.49	76.04	0.010

Table 8. Phytoplankton bloom indices derived from SeaWiFS in the NAFO Division 1F, between 1998 and 2010.

	Initiation	Maximum	End	Initiation	Maximum	End	Duration	Index
Year	Log10 Chl_a (mg/m^3)			Day of Year			days	(d^-1)
1998	-0.60	0.43	-0.12	79.84	140.68	178.70	98.85	0.007
1999	-0.64	0.21	-0.20	57.03	155.89	186.30	129.27	0.005
2000	-0.67	0.13	-0.20	64.64	140.68	209.11	144.48	0.006
2001	-0.63	0.23	-0.16	79.84	148.28	193.91	114.06	0.006
2002	-0.58	0.05	-0.29	72.24	155.89	231.93	159.69	0.004
2003	-0.77	0.23	-0.26	64.64	140.68	239.53	174.90	0.007
2004	-0.66	0.00	-0.14	57.03	163.49	239.53	182.50	0.004
2005	-0.82	0.10	-0.14	64.64	148.28	239.53	174.90	0.006
2006	-0.65	0.36	-0.09	87.45	133.07	171.09	83.65	0.008
2007	-0.84	0.21	-0.11	57.03	133.07	209.11	152.08	0.008
2008	-0.58	0.29	-0.15	102.66	148.28	193.91	91.25	0.006
2009	-0.67	0.18	-0.22	79.84	163.49	201.51	121.67	0.005
2010	-0.70	0.03	-0.04	64.64	155.89	178.70	114.06	0.005

Table 9. Phytoplankton bloom indices derived from SeaWiFS in the NAFO Division 2G, between 1998 and 2010.

	Initiation	Maximum	End	Initiation	Maximum	End	Duration	Index
Year	Log10 Chl_a (mg/m^3)			Day of Year			days	(d^-1)
1998	-0.64	0.11	-0.04	79.84	140.68	171.09	91.25	0.005
1999	-0.67	0.20	-0.06	64.64	133.07	148.28	83.65	0.007
2000	-0.71	0.04	-0.08	72.24	193.91	216.72	144.48	0.004
2001	-0.67	0.06	-0.14	72.24	171.09	239.53	167.29	0.004
2002	-0.64	0.14	-0.02	79.84	201.51	224.32	144.48	0.004
2003	-0.76	-0.03	-0.06	72.24	171.09	216.72	144.48	0.004
2004	-0.61	0.05	-0.09	72.24	193.91	239.53	167.29	0.003
2005	-0.83	0.20	-0.10	72.24	193.91	239.53	167.29	0.005
2006	-0.76	0.18	-0.06	72.24	171.09	209.11	136.87	0.005
2007	-0.66	0.11	-0.01	87.45	193.91	216.72	129.27	0.004
2008	-0.66	0.32	-0.10	72.24	148.28	209.11	136.87	0.007
2009	-0.68	-0.01	-0.10	79.84	148.28	209.11	129.27	0.005
2010	-0.84	0.14	0.06	72.24	193.91	209.11	136.87	0.005

Table 10. Phytoplankton bloom indices derived from SeaWiFS in the NAFO Division 2H, between 1998 and 2010.

	Initiation	Maximum	End	Initiation	Maximum	End	Duration	Index
Year	Log10 Chl_a (mg/m^3)			Day of Year			days	(d^-1)
1998	-0.57	0.24	-0.13	110.26	155.89	193.91	83.65	0.005
1999	-0.59	-0.02	-0.22	72.24	163.49	216.72	144.48	0.003
2000	-0.66	0.09	-0.20	87.45	178.70	209.11	121.67	0.004
2001	-0.54	0.13	-0.11	64.64	178.70	231.93	167.29	0.004
2002	-0.58	0.20	-0.15	117.86	178.70	209.11	91.25	0.004
2003	-0.85	0.06	-0.22	87.45	163.49	216.72	129.27	0.006
2004	-0.56	0.13	-0.19	110.26	171.09	216.72	106.46	0.004
2005	-0.73	0.19	-0.11	87.45	155.89	224.32	136.88	0.006
2006	-0.68	0.17	-0.22	64.64	155.89	231.93	167.29	0.005
2007	-0.65	0.22	-0.12	117.86	171.09	201.51	83.65	0.005
2008	-0.63	0.42	-0.24	102.66	140.68	209.11	106.46	0.007
2009	-0.74	0.12	-0.26	79.84	163.49	209.11	129.27	0.005
2010	-0.59	0.17	-0.06	87.45	163.49	193.91	106.46	0.005

Table 11. Phytoplankton bloom indices derived from SeaWiFS in the NAFO Division 2J, between 1998 and 2010.

	Initiation	Maximum	End	Initiation	Maximum	End	Duration	Index
Year	Log10 Chl_a (mg/m^3)			Day of Year			days	(d^-1)
1998	-0.53	0.30	-0.21	87.45	155.89	201.51	114.06	0.005
1999	-0.51	0.26	-0.20	72.24	163.49	201.51	129.27	0.005
2000	-0.48	0.20	-0.16	79.84	148.28	216.72	136.87	0.005
2001	-0.47	0.25	-0.06	95.05	171.09	216.72	121.67	0.004
2002	-0.48	0.21	-0.17	110.26	171.09	209.11	98.85	0.004
2003	-0.56	0.24	-0.20	110.26	163.49	201.51	91.25	0.005
2004	-0.48	0.12	-0.12	64.64	155.89	216.72	152.08	0.004
2005	-0.63	0.26	-0.23	49.43	155.89	201.51	152.08	0.006
2006	-0.62	0.23	-0.27	64.64	133.07	231.93	167.29	0.006
2007	-0.70	0.15	-0.08	57.03	178.70	209.11	152.08	0.005
2008	-0.53	0.30	-0.29	87.45	148.28	224.32	136.87	0.006
2009	-0.66	0.23	-0.15	64.64	163.49	201.51	136.87	0.005
2010	-0.33	0.32	-0.09	110.26	148.28	193.91	83.65	0.004

Table 12. Phytoplankton bloom indices derived from SeaWiFS in the NAFO Division 3K, between 1998 and 2010.

	Initiation	Maximum	End	Initiation	Maximum	End	Duration	Index
Year	Log10 Chl_a (mg/m^3)			Day of Year			days	(d^-1)
1998	-0.39	0.25	-0.33	64.64	155.89	201.51	136.87	0.004
1999	-0.51	0.27	-0.21	41.82	140.68	201.51	159.69	0.005
2000	-0.39	0.27	-0.31	57.03	148.28	231.93	174.90	0.004
2001	-0.45	0.10	-0.13	64.64	155.89	201.51	136.87	0.004
2002	-0.36	0.25	-0.37	79.84	155.89	224.32	144.48	0.004
2003	-0.48	0.17	-0.15	102.66	155.89	178.70	76.04	0.004
2004	-0.43	0.22	-0.28	49.43	140.68	224.32	174.90	0.005
2005	-0.57	0.31	-0.37	49.43	125.47	216.72	167.29	0.007
2006	-0.44	0.39	-0.35	64.64	117.86	209.11	144.48	0.007
2007	-0.56	0.43	-0.14	72.24	140.68	193.91	121.67	0.007
2008	-0.43	0.13	-0.28	72.24	155.89	201.51	129.27	0.004
2009	-0.42	0.21	-0.25	87.45	148.28	209.11	121.67	0.004
2010	-0.54	0.28	-0.23	49.43	133.07	186.30	136.87	0.006

Table 13. Phytoplankton bloom indices derived from SeaWiFS in the NAFO Division 3L, between 1998 and 2010.

	Initiation	Maximum	End	Initiation	Maximum	End	Duration	Index
Year	Log10 Chl_a (mg/m^3)			Day of Year			days	(d^-1)
1998	-0.25	0.31	-0.51	72.24	117.86	186.30	114.06	0.005
1999	-0.35	0.46	-0.37	57.03	102.66	155.89	98.85	0.008
2000	-0.27	0.34	-0.39	64.64	117.86	186.30	121.67	0.005
2001	-0.39	0.12	-0.40	64.64	140.68	193.91	129.27	0.004
2002	-0.32	0.34	-0.43	72.24	133.07	186.30	114.06	0.005
2003	-0.44	0.05	-0.40	72.24	140.68	193.91	121.67	0.003
2004	-0.31	0.29	-0.42	57.03	117.86	178.70	121.67	0.005
2005	-0.47	0.31	-0.38	57.03	110.26	155.89	98.85	0.007
2006	-0.39	0.35	-0.43	64.64	110.26	155.89	91.25	0.007
2007	-0.41	0.53	-0.42	79.84	117.86	163.49	83.65	0.008
2008	-0.38	0.27	-0.42	57.03	133.07	171.09	114.06	0.005
2009	-0.57	0.51	-0.41	57.03	102.66	171.09	114.06	0.011
2010	-0.50	0.33	-0.28	41.82	102.66	178.70	136.88	0.008

Table 14. Phytoplankton bloom indices derived from SeaWiFS in the NAFO Division 3M, between 1998 and 2010.

	Initiation	Maximum	End	Initiation	Maximum	End	Duration	Index
Year	Log10 Chl_a (mg/m^3)			Day of Year			days	(d^-1)
1998	-0.49	-0.07	-0.72	34.22	125.47	216.72	182.50	0.003
1999	-0.45	0.02	-0.81	41.82	102.66	216.72	174.90	0.005
2000	-0.45	0.10	-0.69	49.43	140.68	224.32	174.90	0.004
2001	-0.51	0.04	-0.51	64.64	140.68	209.11	144.48	0.004
2002	-0.39	0.02	-0.79	64.64	148.28	209.11	144.48	0.003
2003	-0.59	0.06	-0.63	79.84	148.28	224.32	144.48	0.004
2004	-0.48	0.13	-0.67	49.43	133.07	224.32	174.90	0.005
2005	-0.62	0.22	-0.70	26.61	125.47	216.72	190.10	0.007
2006	-0.45	0.12	-0.72	64.64	117.86	209.11	144.48	0.005
2007	-0.72	-0.16	-0.49	34.22	125.47	216.72	182.50	0.004
2008	-0.49	0.12	-0.48	64.64	133.07	171.09	106.46	0.005
2009	-0.76	0.04	-0.74	19.01	125.47	216.72	197.71	0.006
2010	-0.63	0.06	-0.70	26.61	133.07	224.32	197.71	0.005

Table 15. Phytoplankton bloom indices derived from SeaWiFS in the NAFO Division 3N, between 1998 and 2010.

	Initiation	Maximum	End	Initiation	Maximum	End	Duration	Index
Year	Log10 Chl_a (mg/m^3)			Day of Year			days	(d^-1)
1998	-0.31	0.05	-0.63	57.03	102.66	186.30	129.27	0.003
1999	-0.16	0.22	-0.55	41.82	95.05	155.89	114.06	0.004
2000	-0.26	0.09	-0.55	41.82	110.26	171.09	129.27	0.003
2001	-0.27	0.02	-0.54	49.43	133.07	193.91	144.48	0.002
2002	-0.17	0.26	-0.59	72.24	117.86	171.09	98.85	0.004
2003	-0.27	0.12	-0.59	72.24	125.47	201.51	129.27	0.003
2004	-0.26	0.09	-0.55	49.43	110.26	201.51	152.08	0.003
2005	-0.39	0.18	-0.55	49.43	110.26	186.30	136.88	0.005
2006	-0.26	0.11	-0.61	72.24	95.05	171.09	98.85	0.004
2007	-0.51	0.07	-0.60	41.82	117.86	193.91	152.08	0.005
2008	-0.37	0.21	-0.55	34.22	117.86	178.70	144.48	0.005
2009	-0.58	0.28	-0.52	26.61	79.84	178.70	152.08	0.011
2010	-0.57	0.22	-0.49	26.61	95.05	201.51	174.90	0.008

Table 16. Phytoplankton bloom indices derived from SeaWiFS in the NAFO Division 3O, between 1998 and 2010.

	Initiation	Maximum	End	Initiation	Maximum	End	Duration	Index
Year	Log10 Chl_a (mg/m^3)			Day of Year			days	(d^-1)
1998	-0.23	0.32	-0.50	64.64	110.26	171.09	106.46	0.005
1999	-0.09	0.12	-0.49	26.61	110.26	148.28	121.67	0.002
2000	-0.19	0.07	-0.42	49.43	102.66	155.89	106.46	0.002
2001	-0.25	0.09	-0.45	64.64	110.26	171.09	106.46	0.003
2002	-0.16	0.40	-0.50	72.24	117.86	155.89	83.65	0.005
2003	-0.13	0.29	-0.44	95.05	125.47	163.49	68.44	0.003
2004	-0.09	0.23	-0.42	95.05	117.86	178.70	83.65	0.003
2005	-0.37	0.12	-0.45	64.64	102.66	163.49	98.85	0.005
2006	-0.31	0.27	-0.55	64.64	102.66	155.89	91.25	0.006
2007	-0.35	0.26	-0.54	64.64	117.86	178.70	114.06	0.005
2008	-0.35	0.04	-0.48	11.41	110.26	186.30	174.90	0.003
2009	-0.57	0.21	-0.53	11.41	79.84	186.30	174.90	0.010
2010	-0.49	0.17	-0.32	11.41	87.45	163.49	152.08	0.008

Table 17. Phytoplankton bloom indices derived from SeaWiFS in the NAFO Division 3Pn, between 1998 and 2010.

	Initiation	Maximum	End	Initiation	Maximum	End	Duration	Index
Year	Log10 Chl_a (mg/m^3)			Day of Year			days	(d^-1)
1998	-0.25	0.64	-0.27	57.03	110.26	155.89	98.85	0.008
1999	-0.19	0.35	-0.26	41.82	117.86	148.28	106.46	0.005
2000	-0.37	0.05	-0.13	26.61	102.66	155.89	129.27	0.004
2001	-0.23	0.12	-0.24	95.05	125.47	155.89	60.83	0.003
2002	-0.21	0.27	-0.22	79.84	125.47	163.49	83.65	0.004
2003	-0.41	0.51	-0.26	79.84	117.86	148.28	68.44	0.008
2004	-0.19	0.39	-0.21	95.05	117.86	148.28	53.23	0.005
2005	-0.24	0.09	-0.34	79.84	102.66	140.68	60.83	0.003
2006	-0.30	0.67	-0.27	57.03	110.26	133.07	76.04	0.009
2007	-0.47	0.59	-0.35	72.24	117.86	148.28	76.04	0.009
2008	-0.31	0.27	-0.26	57.03	125.47	163.49	106.46	0.005
2009	-0.31	0.39	-0.22	57.03	110.26	148.28	91.25	0.006
2010	-0.50	0.20	-0.09	26.61	110.26	155.89	129.27	0.006

Table 18. Phytoplankton bloom indices derived from SeaWiFS in the NAFO Division 3Ps, between 1998 and 2010.

	Initiation	Maximum	End	Initiation	Maximum	End	Duration	Index
Year	Log10 Chl_a (mg/m^3)			Day of Year			days	(d^-1)
1998	-0.19	0.67	-0.42	79.84	117.86	148.28	68.44	0.007
1999	-0.14	0.23	-0.42	64.64	117.86	148.28	83.65	0.003
2000	-0.19	0.14	-0.34	79.84	110.26	155.89	76.04	0.003
2001	-0.25	0.45	-0.40	87.45	117.86	155.89	68.44	0.006
2002	-0.12	0.22	-0.37	87.45	125.47	163.49	76.04	0.003
2003	-0.32	0.47	-0.44	87.45	117.86	155.89	68.44	0.007
2004	-0.23	0.29	-0.35	87.45	117.86	155.89	68.44	0.004
2005	-0.23	0.22	-0.37	79.84	110.26	140.68	60.83	0.004
2006	-0.25	0.72	-0.40	79.84	110.26	140.68	60.83	0.009
2007	-0.42	0.42	-0.44	72.24	117.86	148.28	76.04	0.007
2008	-0.23	0.17	-0.37	72.24	125.47	163.49	91.25	0.003
2009	-0.20	0.33	-0.35	79.84	117.86	148.28	68.44	0.004
2010	0.01	0.22	-0.28	72.24	110.26	148.28	76.04	0.002

Table 19. Phytoplankton bloom indices derived from SeaWiFS in the NAFO Division 4R, between 1998 and 2010.

	Initiation	Maximum	End	Initiation	Maximum	End	Duration	Index
Year	Log10 Chl_a (mg/m^3)			Day of Year			days	(d^-1)
1998	-0.16	0.50	-0.16	72.24	102.66	140.68	68.44	0.006
1999	-0.11	0.24	-0.15	64.64	95.05	171.09	106.46	0.004
2000	-0.14	0.29	-0.02	87.45	133.07	110.26	22.81	0.003
2001	-0.20	0.27	-0.17	79.84	117.86	163.49	83.65	0.004
2002	-0.19	0.17	-0.15	102.66	140.68	178.70	76.04	0.003
2003	-0.27	0.27	0.02	102.66	133.07	155.89	53.23	0.004
2004	-0.17	0.24	-0.01	72.24	110.26	133.07	60.83	0.004
2005	-0.34	0.17	-0.16	79.84	110.26	171.09	91.25	0.005
2006	-0.16	0.50	-0.16	72.24	102.66	140.68	68.44	0.006
2007	-0.37	0.43	-0.11	79.84	117.86	160.49	83.65	0.007
2008	-0.19	0.21	-0.15	95.05	133.07	155.89	60.83	0.003
2009	-0.38	0.24	-0.24	49.43	110.26	193.91	144.48	0.006
2010	-0.21	0.54	-0.06	57.03	95.05	125.47	68.44	0.008

Table 20. Phytoplankton bloom indices derived from SeaWiFS in the NAFO Division 4S, between 1998 and 2010.

	Initiation	Maximum	End	Initiation	Maximum	End	Duration	Index
Year	Log10 Chl_a (mg/m^3)			Day of Year			days	(d^-1)
1998	-0.04	0.58	0.15	72.24	110.26	171.09	98.85	0.006
1999	-0.01	0.48	0.13	87.45	140.68	186.30	98.85	0.003
2000	-0.12	0.41	0.20	95.05	140.68	193.91	98.85	0.004
2001	-0.09	0.56	0.18	87.45	117.86	155.89	68.44	0.006
2002	-0.11	0.45	0.18	79.84	133.07	178.70	98.85	0.004
2003	-0.23	0.45	0.08	72.24	140.68	193.91	121.67	0.005
2004	-0.10	0.43	0.10	72.24	133.07	193.91	121.67	0.004
2005	-0.16	0.40	0.29	72.24	171.09	201.51	129.27	0.003
2006	-0.12	0.60	0.20	79.84	117.86	148.28	68.44	0.006
2007	-0.10	0.57	0.11	87.45	125.47	155.89	68.44	0.005
2008	-0.12	0.50	0.24	72.24	117.86	163.49	91.25	0.005
2009	-0.13	0.42	0.13	72.24	117.86	178.70	106.46	0.005
2010	-0.10	0.59	0.14	57.03	102.66	148.28	91.25	0.007

Table 21. Phytoplankton bloom indices derived from SeaWiFS in the NAFO Division 4T, between 1998 and 2010.

	Initiation	Maximum	End	Initiation	Maximum	End	Duration	Index
Year	Log10 Chl_a (mg/m^3)			Day of Year			days	(d^-1)
1998	-0.04	0.61	0.08	57.03	110.26	140.68	83.65	0.006
1999	-0.05	0.38	0.15	57.03	95.05	178.70	121.67	0.005
2000	0.02	0.38	0.19	64.64	133.07	163.49	98.85	0.003
2001	-0.08	0.67	0.11	79.84	125.47	148.28	68.44	0.006
2002	-0.04	0.61	0.08	57.03	110.26	140.68	83.65	0.006
2003	-0.33	0.53	0.09	57.03	117.86	140.68	83.65	0.007
2004	-0.19	0.37	0.28	57.03	110.26	171.09	114.06	0.005
2005	-0.41	0.35	0.14	57.03	117.86	133.07	76.04	0.006
2006	0.10	0.58	0.15	87.45	117.86	140.68	53.23	0.004
2007	-0.09	0.70	0.22	64.64	117.86	148.28	83.65	0.007
2008	0.14	0.49	0.11	102.66	117.86	140.68	38.02	0.003
2009	-0.18	0.44	0.19	57.03	117.86	140.68	83.65	0.005
2010	0.06	0.49	0.07	57.03	95.05	148.28	91.25	0.005

Table 22. Phytoplankton bloom indices derived from SeaWiFS in the NAFO Division 4Vn, between 1998 and 2010.

	Initiation	Maximum	End	Initiation	Maximum	End	Duration	Index
Year	Log10 Chl_a (mg/m^3)			Day of Year			days	(d^-1)
1998	-0.08	0.76	-0.19	64.64	95.05	148.28	83.65	0.009
1999	0.13	0.57	-0.22	64.64	87.45	148.28	83.65	0.005
2000	0.06	0.68	-0.14	79.84	102.66	125.47	45.63	0.006
2001	-0.01	0.35	-0.26	95.05	117.86	148.28	53.23	0.003
2002	-0.10	0.72	-0.14	64.64	110.26	140.68	76.04	0.007
2003	-0.24	0.72	-0.17	79.84	110.26	133.07	53.23	0.009
2004	-0.13	0.31	-0.18	87.45	117.86	148.28	60.83	0.004
2005	0.03	0.27	-0.19	72.24	102.66	133.07	60.83	0.002
2006	0.11	0.76	-0.17	72.24	102.66	133.07	60.83	0.006
2007	-0.03	0.92	-0.11	79.84	110.26	140.68	60.83	0.009
2008	-0.04	0.35	-0.10	64.64	95.05	148.28	83.65	0.004
2009	-0.07	0.54	-0.14	79.84	110.26	140.68	60.83	0.006
2010	0.04	0.81	0.06	64.64	79.84	102.66	38.02	0.010

Table 23. Phytoplankton bloom indices derived from SeaWiFS in the NAFO Division 4Vs, between 1998 and 2010.

	Initiation	Maximum	End	Initiation	Maximum	End	Duration	Index
Year	Log10 Chl_a (mg/m^3)			Day of Year			days	(d^-1)
1998	-0.33	0.24	-0.51	64.64	110.26	163.49	98.85	0.005
1999	-0.09	0.06	-0.65	57.03	87.45	171.09	114.06	0.002
2000	-0.31	0.04	-0.52	57.03	110.26	171.09	114.06	0.003
2001	-0.31	0.06	-0.49	64.64	110.26	178.70	114.06	0.003
2002	-0.28	0.09	-0.63	57.03	110.26	178.70	121.67	0.003
2003	-0.41	0.14	-0.58	64.64	110.26	186.30	121.67	0.005
2004	-0.36	0.03	-0.59	64.64	110.26	193.91	129.27	0.003
2005	-0.59	-0.09	-0.56	19.01	102.66	193.91	174.90	0.005
2006	-0.33	0.11	-0.55	41.82	110.26	163.49	121.67	0.004
2007	-0.44	0.21	-0.55	57.03	110.26	178.70	121.67	0.006
2008	-0.35	0.20	-0.55	57.03	102.66	186.30	129.27	0.005
2009	-0.52	-0.06	-0.66	19.01	110.26	201.51	182.50	0.004
2010	-0.67	0.10	-0.35	19.01	95.05	193.91	174.90	0.008

Table 24. Phytoplankton bloom indices derived from SeaWiFS in the NAFO Division 4W, between 1998 and 2010.

Year	Initiation	Maximum	End	Initiation	Maximum	End	Duration	Index
	Log10 Chl_a (mg/m^3)			Day of Year			days	(d^-1)
1998	-0.16	0.11	-0.41	64.64	87.45	155.89	91.25	0.003
1999	-0.01	0.15	-0.51	34.22	57.03	171.09	136.88	0.003
2000	-0.09	0.10	-0.41	72.24	102.66	171.09	98.85	0.002
2001	-0.12	0.13	-0.37	26.61	110.26	155.89	129.27	0.002
2002	-0.14	0.12	-0.46	49.43	87.45	171.09	121.67	0.003
2003	-0.22	0.18	-0.47	49.43	95.05	163.49	114.06	0.004
2004	-0.15	0.08	-0.46	41.82	95.05	171.09	129.27	0.002
2005	-0.23	0.03	-0.43	49.43	87.45	201.51	152.08	0.003
2006	-0.12	0.20	-0.37	49.43	79.84	178.70	129.27	0.004
2007	-0.20	0.33	-0.33	57.03	95.05	140.68	83.65	0.005
2008	-0.10	0.20	-0.40	57.03	87.45	163.49	106.46	0.003
2009	0.00	0.22	-0.51	57.03	95.05	171.09	114.06	0.002
2010	-0.34	0.06	-0.32	26.61	87.45	193.91	167.29	0.005

Table 25. Phytoplankton bloom indices derived from SeaWiFS in the NAFO Division 4X, between 1998 and 2010.

Year	Initiation	Maximum	End	Initiation	Maximum	End	Duration	Index
	Log10 Chl_a (mg/m^3)			Day of Year			days	(d^-1)
1998	-0.15	0.17	-0.27	49.43	95.05	148.28	98.85	0.003
1999	-0.07	0.20	-0.25	49.43	79.84	140.68	91.25	0.003
2000	-0.08	0.22	-0.19	79.84	110.26	163.49	83.65	0.003
2001	-0.08	0.25	-0.25	72.24	110.26	155.89	83.65	0.003
2002	-0.07	0.07	-0.19	57.03	95.05	171.09	114.06	0.001
2003	-0.18	0.39	-0.21	72.24	102.66	133.07	60.83	0.006
2004	-0.14	0.13	-0.36	64.64	102.66	178.70	114.06	0.003
2005	-0.18	0.05	-0.25	57.03	102.66	171.09	114.06	0.002
2006	-0.22	0.10	-0.18	41.82	95.05	155.89	114.06	0.003
2007	-0.22	0.37	-0.19	57.03	95.05	140.68	83.65	0.006
2008	-0.14	0.21	-0.23	57.03	110.26	178.70	121.67	0.003
2009	-0.05	0.42	-0.20	64.64	102.66	148.28	83.65	0.005
2010	-0.02	0.26	-0.17	79.84	102.66	148.28	68.44	0.003

Table 26. Phytoplankton bloom indices derived from SeaWiFS in the NAFO Division 5Y, between 1998 and 2010.

Year	Initiation	Maximum	End	Initiation	Maximum	End	Duration	Index
	Log10 Chl_a (mg/m^3)			Day of Year			days	(d^-1)
1998	-0.05	0.47	0.02	72.24	110.26	155.89	83.65	0.005
1999	0.09	0.36	0.12	79.84	125.47	148.28	68.44	0.002
2000	0.00	0.32	0.12	72.24	155.89	171.09	98.85	0.002
2001	-0.04	0.52	-0.01	64.64	110.26	155.89	91.25	0.005
2002	-0.06	0.44	0.07	79.84	133.07	201.51	121.67	0.004
2003	-0.11	0.52	0.00	79.84	117.86	178.70	98.85	0.005
2004	-0.07	0.49	-0.03	87.45	117.86	148.28	60.83	0.005
2005	-0.05	0.47	0.02	72.24	110.26	155.89	83.65	0.005
2006	0.00	0.41	0.13	72.24	102.66	133.07	60.83	0.004
2007	-0.04	0.33	0.09	64.64	117.86	178.70	114.06	0.003
2008	-0.05	0.43	0.09	64.64	117.86	171.09	106.46	0.004
2009	0.05	0.53	0.19	79.84	102.66	140.68	60.83	0.005
2010	-0.05	0.47	0.02	72.24	110.26	155.89	83.65	0.005

Table 27. Phytoplankton bloom indices derived from SeaWiFS in the NAFO Division 5Ze, between 1998 and 2010.

	Initiation	Maximum	End	Initiation	Maximum	End	Duration	Index
Year	Log10 Chl_a (mg/m^3)			Day of Year			days	(d^-1)
1998	-0.11	0.11	-0.14	72.24	95.05	133.07	60.83	0.002
1999	-0.10	0.15	-0.13	34.22	110.26	155.89	121.67	0.002
2000	-0.11	0.17	0.02	57.03	87.45	178.70	121.67	0.003
2001	-0.01	0.39	-0.18	72.24	117.86	163.49	91.25	0.003
2002	-0.11	0.20	-0.16	49.43	95.05	193.91	144.48	0.003
2003	-0.19	0.35	-0.18	49.43	102.66	178.70	129.27	0.005
2004	-0.07	0.39	-0.15	72.24	102.66	155.89	83.65	0.004
2005	-0.15	0.21	-0.17	57.03	117.86	163.49	106.46	0.003
2006	-0.18	0.28	-0.11	57.03	102.66	163.49	106.46	0.004
2007	-0.07	0.31	-0.05	64.64	87.45	186.30	121.67	0.004
2008	-0.12	0.32	-0.10	57.03	102.66	178.70	121.67	0.004
2009	-0.15	0.11	-0.14	64.64	95.05	133.07	68.44	0.003
2010	-0.20	0.37	-0.17	64.64	110.26	163.49	98.85	0.005

Table 28. Phytoplankton bloom indices derived from SeaWiFS in the NAFO Division 5Zw, between 1998 and 2010.

	Initiation	Maximum	End	Initiation	Maximum	End	Duration	Index
Year	Log10 Chl_a (mg/m^3)			Day of Year			days	(d^-1)
1998	0.00	0.05	-0.41	64.64	95.05	209.11	144.48	0.001
1999	0.02	0.09	-0.46	87.45	110.26	171.09	83.65	0.001
2000	-0.03	0.21	-0.38	72.24	133.07	224.32	152.08	0.002
2001	-0.01	0.37	-0.40	79.84	110.26	171.09	91.25	0.003
2002	-0.03	0.13	-0.47	49.43	95.05	239.53	190.10	0.002
2003	-0.06	0.19	-0.24	57.03	95.05	171.09	114.06	0.003
2004	-0.03	0.11	-0.38	79.84	117.86	163.49	83.65	0.001
2005	-0.17	0.07	-0.51	19.01	110.26	224.32	205.31	0.002
2006	0.02	0.13	-0.33	64.64	87.45	155.89	91.25	0.001
2007	0.05	0.11	-0.56	72.24	95.05	247.14	174.90	0.001
2008	-0.05	0.09	-0.44	49.43	110.26	216.72	167.29	0.001
2009	-0.02	0.25	-0.33	34.22	72.24	193.91	159.69	0.004
2010	-0.10	0.21	-0.43	72.24	110.26	171.09	98.85	0.003

Table 29. Sea Surface Temperatures (°C) and times (day of year – DOY) at both, initiation and inflexion point of the seasonal warming at the five regions and the eleven years of data.

	Western		Western Central		Central		Eastern Central		Eastern	
Units	(°C)	(DOY)	(°C)	(DOY)	(°C)	(DOY)	(°C)	(DOY)	(°C)	(DOY)
Year	SST at Initiation									
2003	-0.92	110	-0.92	110	2.41	80	1.63	80	0.09	103
2004	-0.82	118	1.22	80	2.93	103	2.55	118	0.51	125
2005	-1.58	72	2.02	87	2.92	95	2.41	80	0.60	80
2006	-1.24	72	2.55	95	2.76	80	1.70	87	-0.70	80
2007	-1.22		2.34	103	2.74	95	1.78	110	-0.55	80
2008	-0.67	103	1.68	110	2.33	87	0.29	72	-1.30	80
2009	-1.08	125	1.84	125	2.71	110	1.54	118	-0.22	118
2010	-1.23	118	1.37	87	2.24	72	2.95	80	0.16	95
2011	-0.82	103	1.90	87	2.64	110	1.59	148	-0.02	156
2012	-1.30	103	1.53	110	1.74	80	0.35	80	-0.97	103
2013	-1.36	103	1.74	103	2.54	95	2.36	95	-0.34	87
	SST at Inflexion Point									
2003	5.20	186	5.20	186	6.70	179	5.61	179	3.46	186
2004	5.43	186	7.00	186	6.62	186	5.34	186	2.65	194
2005	3.94	171	6.79	179	7.23	186	3.56	118	2.31	163
2006	4.31	171	6.95	186	7.60	186	4.97	194	1.29	179
2007	4.63	186	6.16	179	6.73	179	4.24	186	2.20	202
2008	6.45	186	7.70	194	6.99	179	3.25	148	1.70	179
2009	4.37	186	5.47	194	5.77	186	4.54	194	1.86	194
2010	5.93	194	6.90	179	7.40	179	6.30	186	3.46	194
2011	5.02	186	6.06	186	6.33	194	4.99	202	1.53	209
2012	5.94	186	7.15	194	7.10	179	4.94	186	2.53	186
2013	3.36	194	5.84	194	6.07	186	4.64	186	1.55	179

Table 30. PCA loadings of the phytoplankton bloom and warming sea surface temperature indices, for the pooled five regions in the Labrador Sea (W, WC, C, EC and E), between 2003 and 2013.

Variable	Comp. 1	Comp. 2	Comp. 3	Comp. 4	Comp. 5	Comp. 6
Initiation Chl	0.314	-0.511	0.211	0.440	0.550	-0.317
Maximum Chl	-0.368	-0.462		0.384	-0.655	-0.266
End Chl	-0.354	-0.331	0.749	-0.305		0.331
Initiation Time	0.204	-0.615	-0.507	-0.269		0.500
Maximum Time	0.543	-0.139	0.203	-0.543	-0.355	-0.473
End Time	0.552	0.135	0.303	0.445	-0.377	0.495
Initiation SST	-0.281	0.869	-0.195	-0.357		
Sampling SST	0.599	0.448		0.660		
Initiation Time	-0.556	-0.115	-0.645	0.511		
Sampling Time	0.503	-0.174	-0.735	-0.419		

Table 31. PCA loadings of the phytoplankton bloom and warming sea surface temperature indices, for the pooled five regions in Western Greenland (1A, 1B, 1C 1D and 1E), between 1998 and 2010.

Variable	Comp. 1	Comp. 2	Comp. 3	Comp. 4	Comp. 5	Comp. 6
Initiation Chl	0.562			0.498	0.556	-0.343
Maximum Chl	0.512	-0.109	-0.410	-0.156	-0.637	-0.357
End Chl	0.210	-0.388	0.681	0.345	-0.414	0.225
Initiation Time	0.579			-0.552	0.248	0.541
Maximum Time	0.116	0.579	0.577	-0.285		-0.486
End Time	0.170	0.702	-0.167	0.472	-0.227	0.419
Initiation SST	0.465	-0.611	0.526	-0.367		
Inflex. Point SST	0.127	-0.632	-0.753	0.134		
Initiation Time	0.651	0.151	0.113	0.735		
Inflex. Point Time	0.586	0.452	-0.380	-0.554		

APPENDICES

APPENDIX 1.

Chlorophyll_a concentration anomalies at initiation and at maximum of the bloom, time to reach the maximum concentration and the RITA index by NAFO division from 1998 until 2010 are presented in this section. Trend lines were computed using a moving average of 3 years.

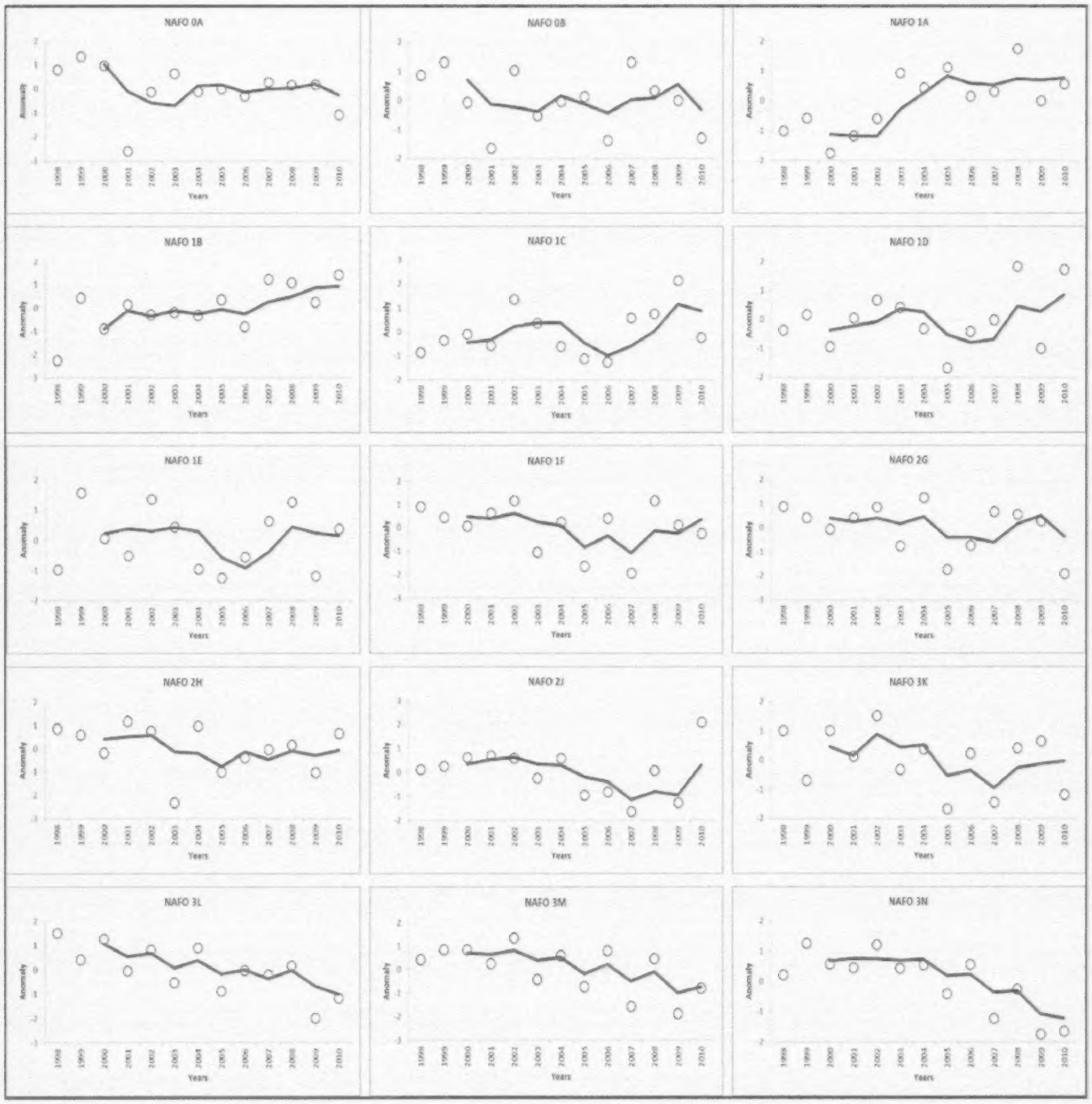

Figure APX1-1. Standardised annual anomalies for chlorophyll_a concentration at the initiation of the bloom (mg m^{-3}), for 28 NAFO divisions between 1998 and 2010. Trend lines computed using 3 year moving averages are also shown.

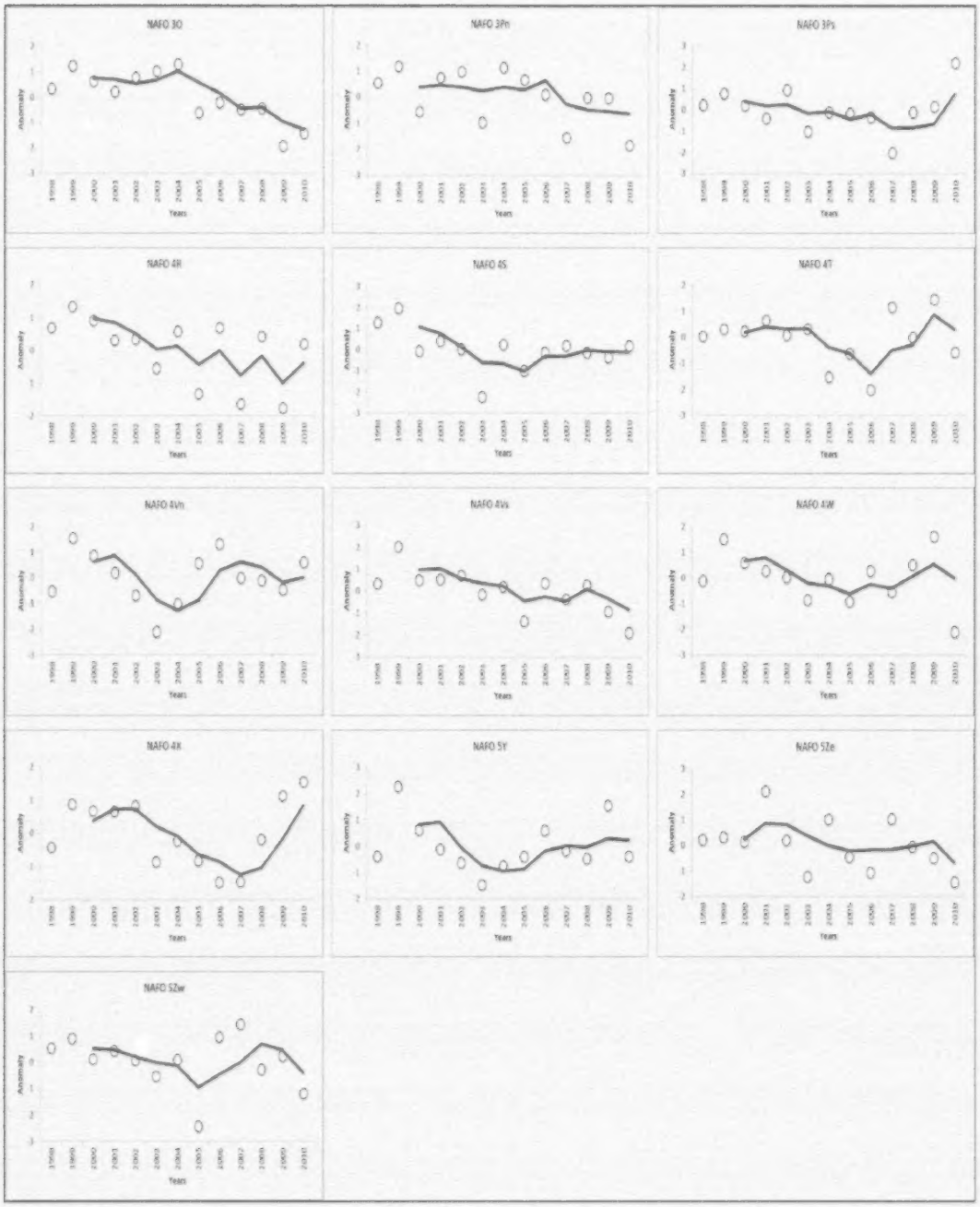

Figure APX1-1. Continued.

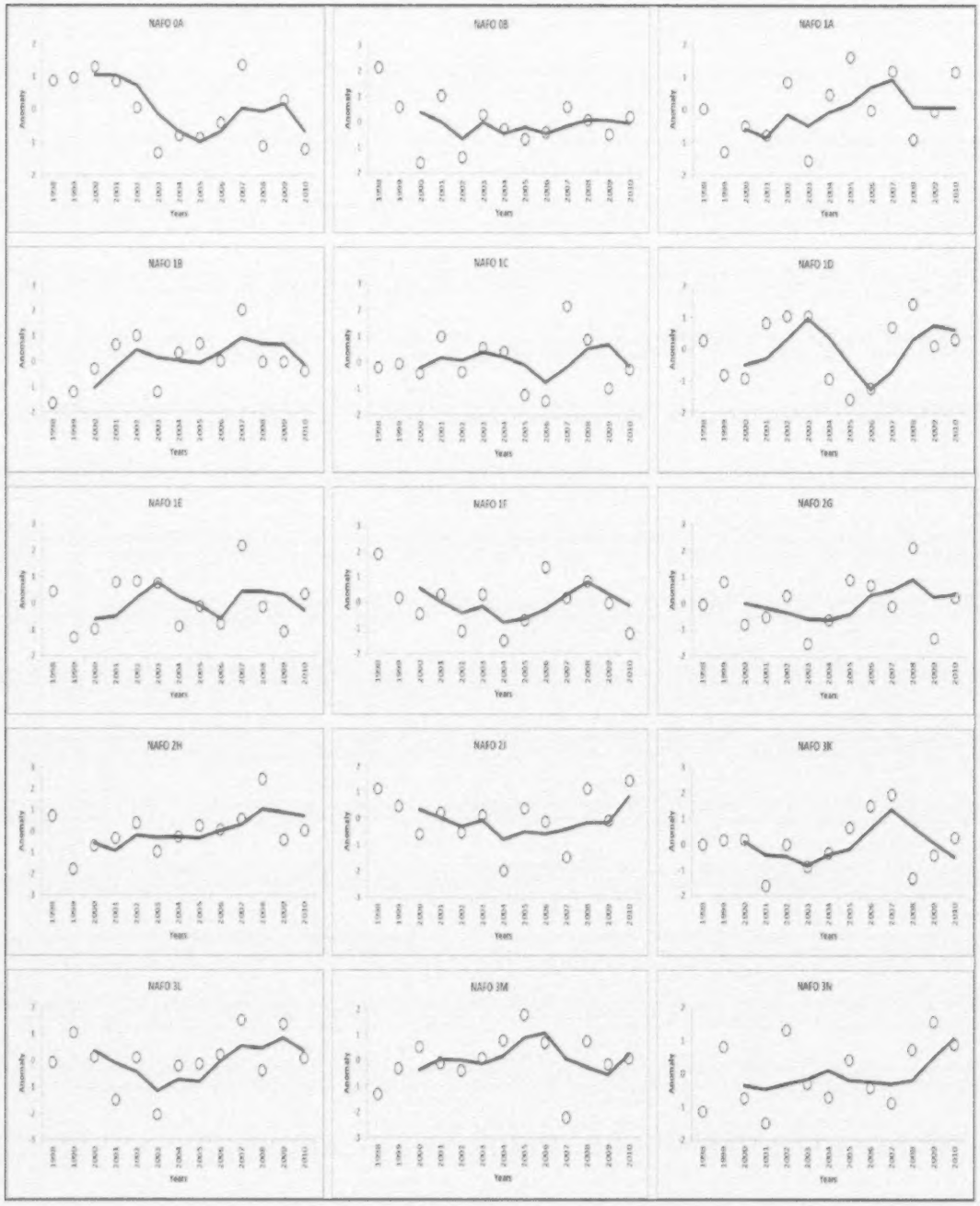

Figure APX1-2. Standardised annual anomalies for chlorophyll_a concentration at the maximum of the bloom (mg m^{-3}), for 28 NAFO divisions between 1998 and 2010. Trend lines computed using 3 year moving averages are also shown.

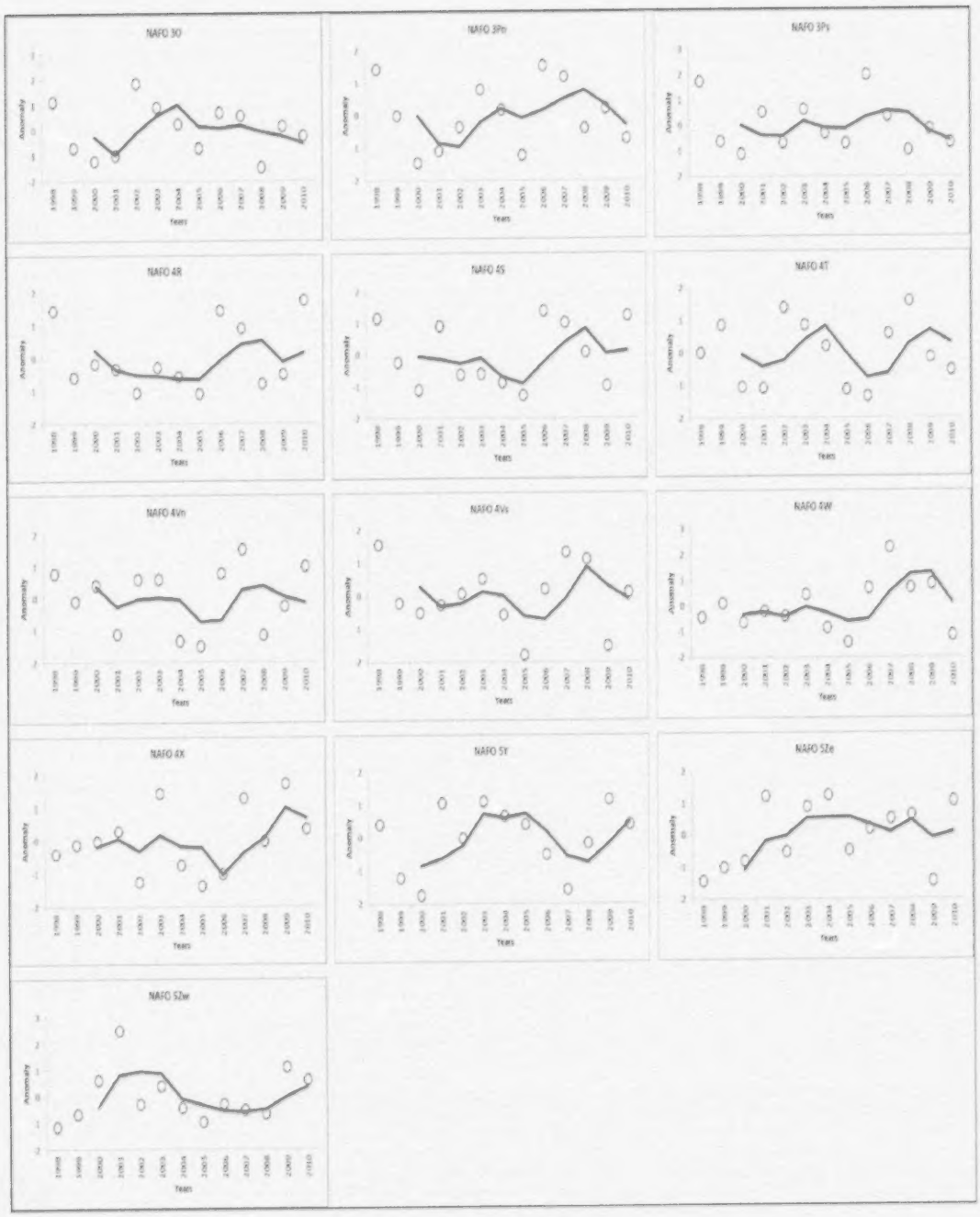

Figure APX1-2. Continued.

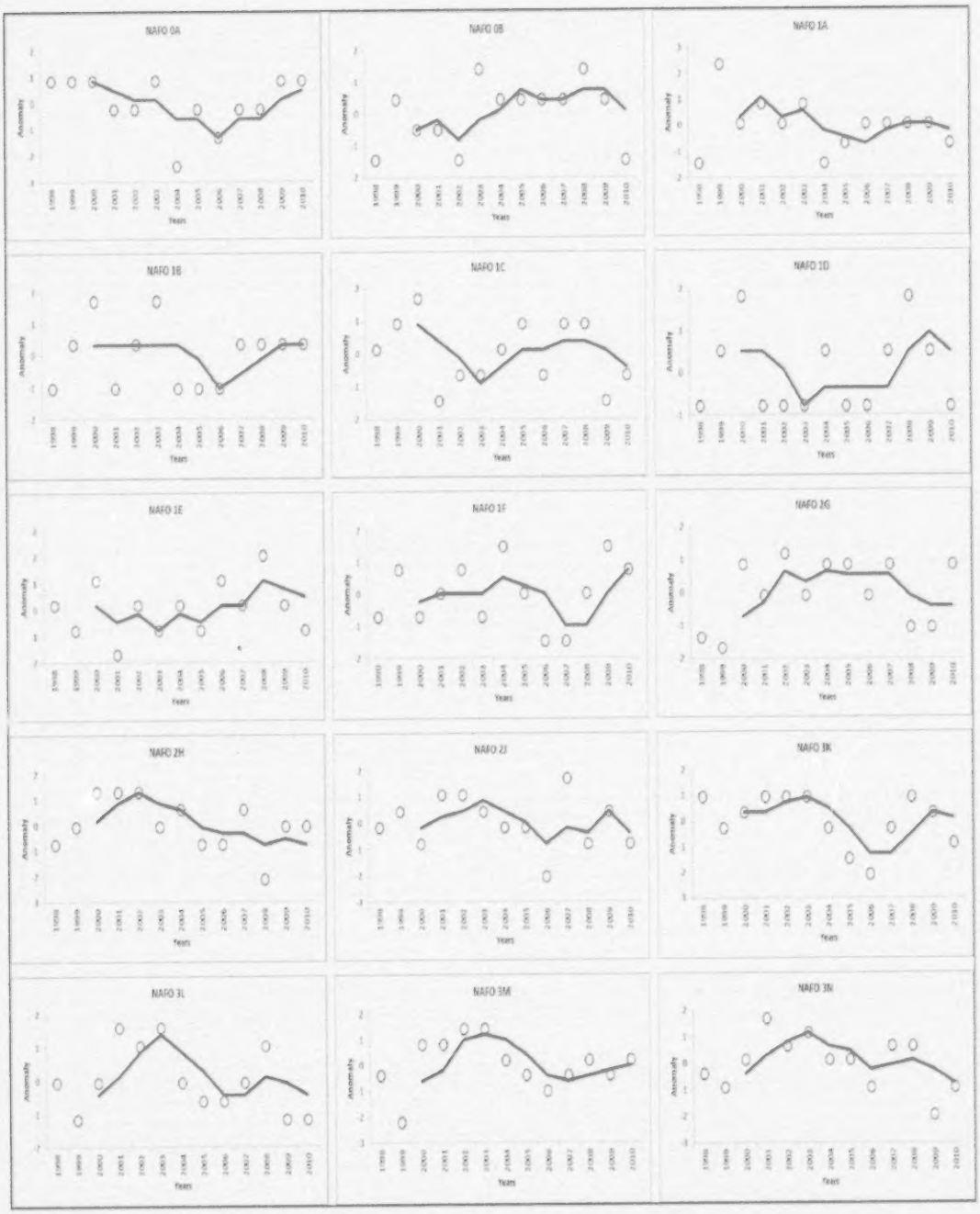

Figure APX1-3. Standardised annual anomalies for the date of the maximum chlorophyll concentration (day of year), for 28 NAFO divisions between 1998 and 2010. Trend lines computed using 3 year moving averages are also shown.

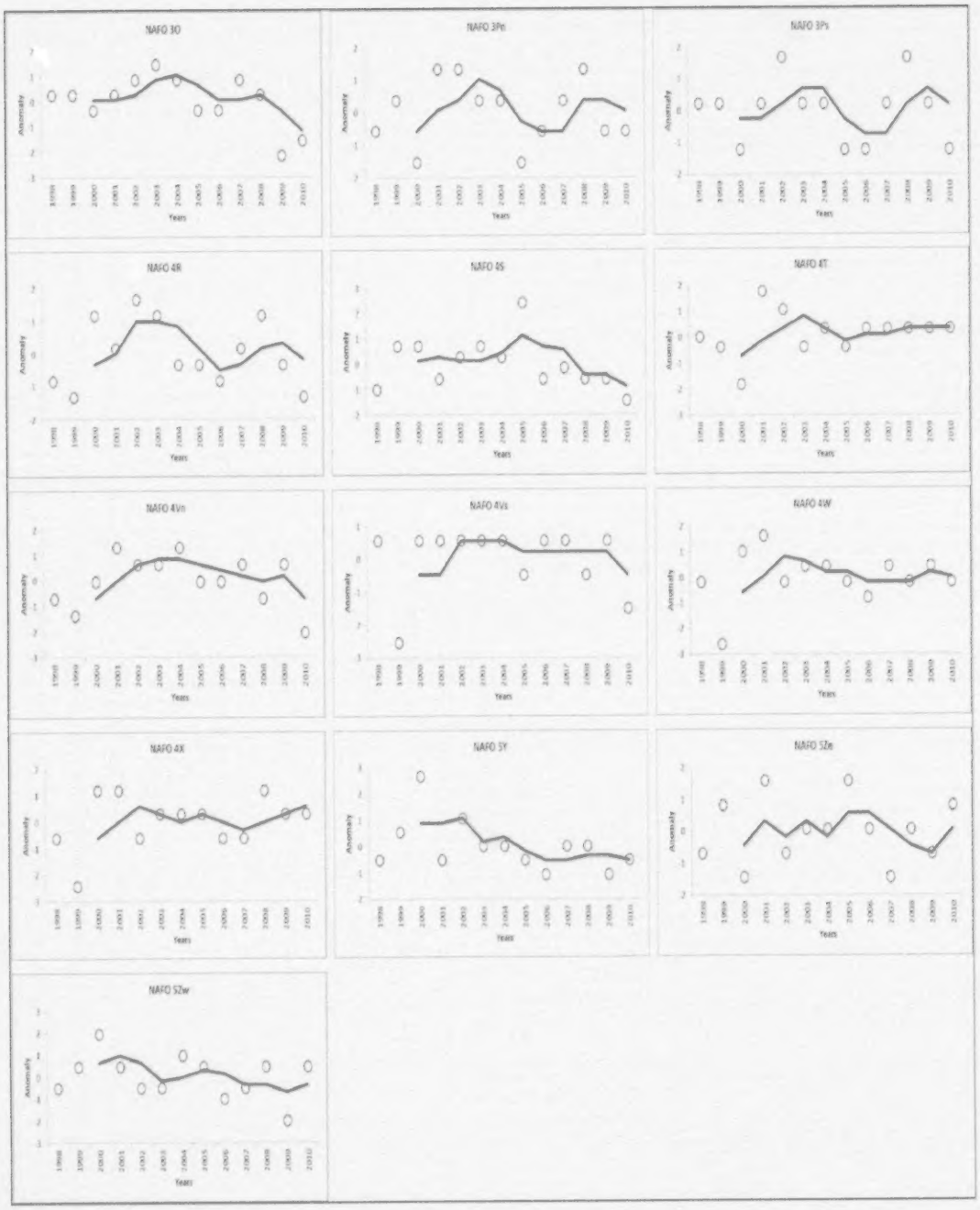

Figure APX1-3.Continued.

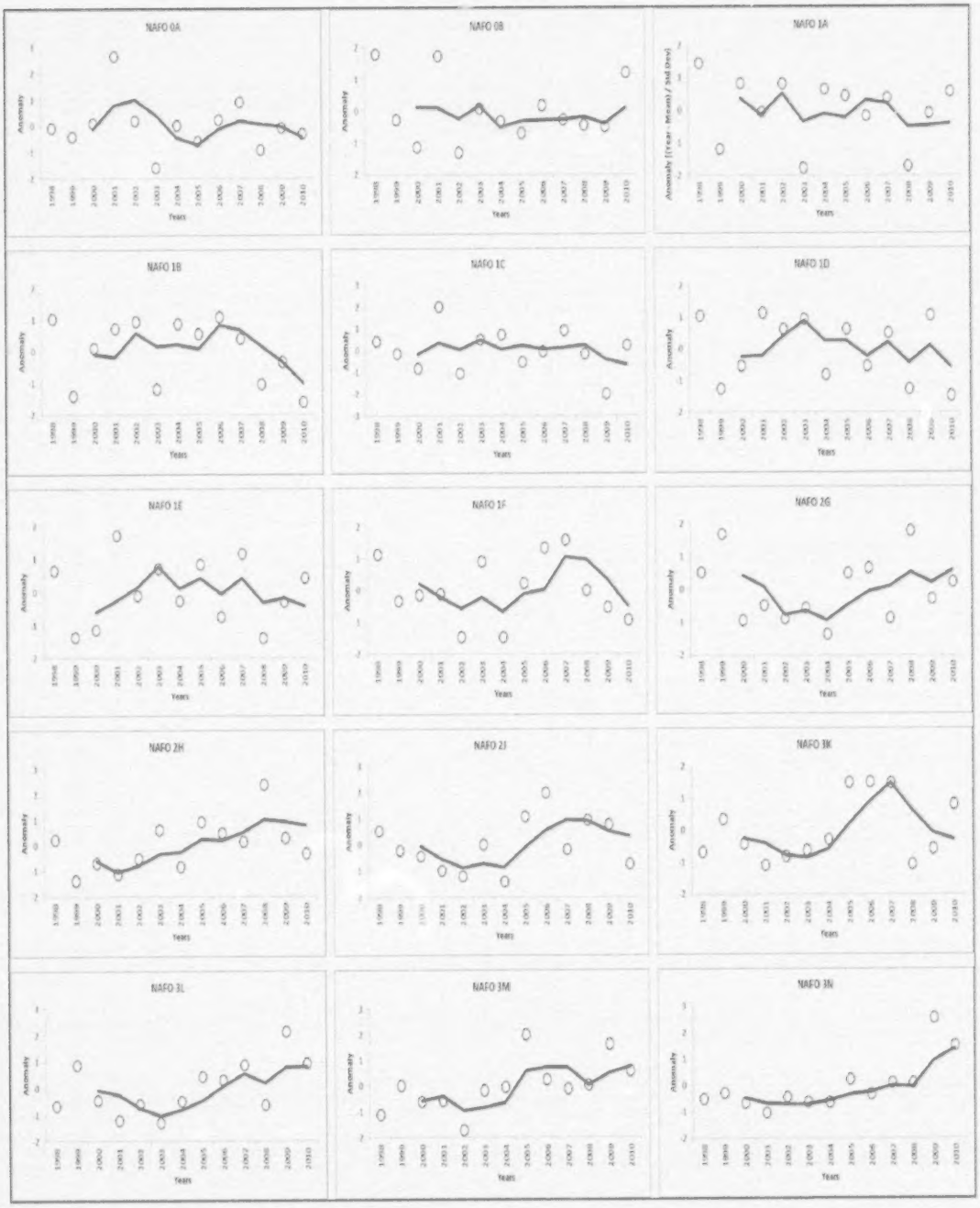

Figure APX1-4. Standardised annual anomalies of the RITA-index (d^{-1}), for 28 NAFO divisions between 1998 and 2010. Trend lines computed using 3 year moving averages are also shown.

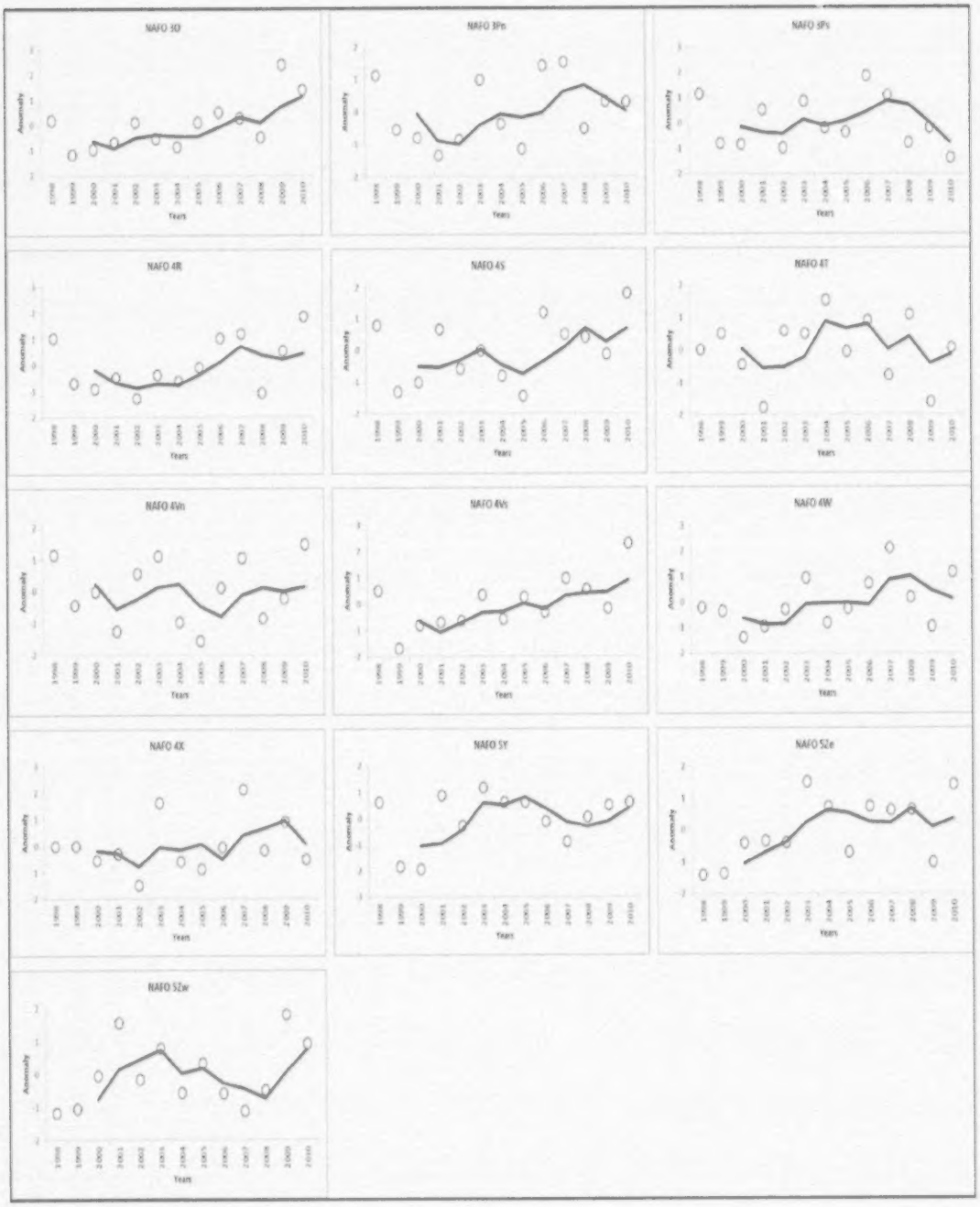

Figure APX1-4. Continued.

APPENDIX 2

Maps of anomalies of RITA index for the twenty-eight NAFO divisions between 1998 and 2010 integrate this appendix.

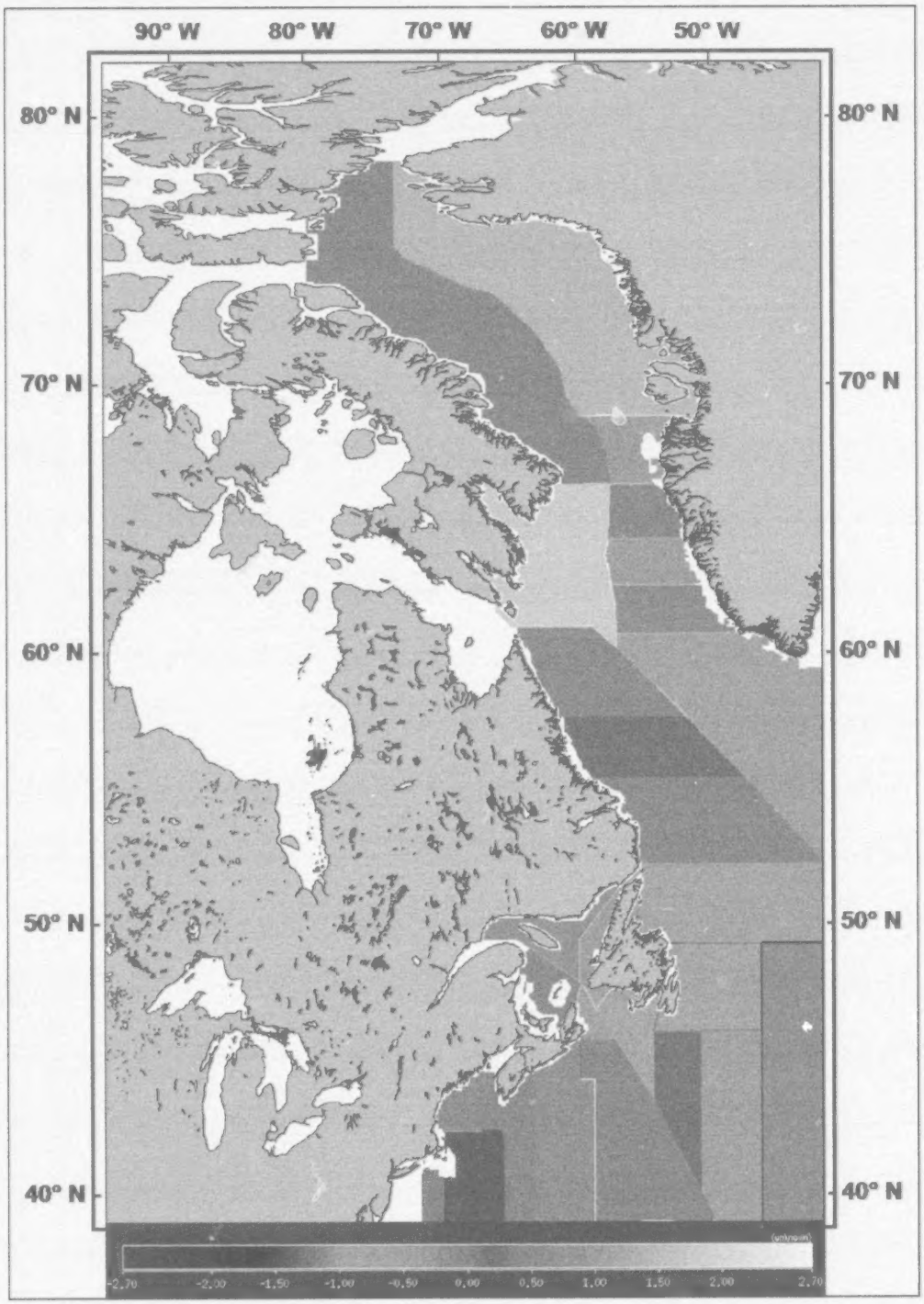

Figure APX2-1. Anomalies for the RITA indexfor NAFO divisions in 1998.

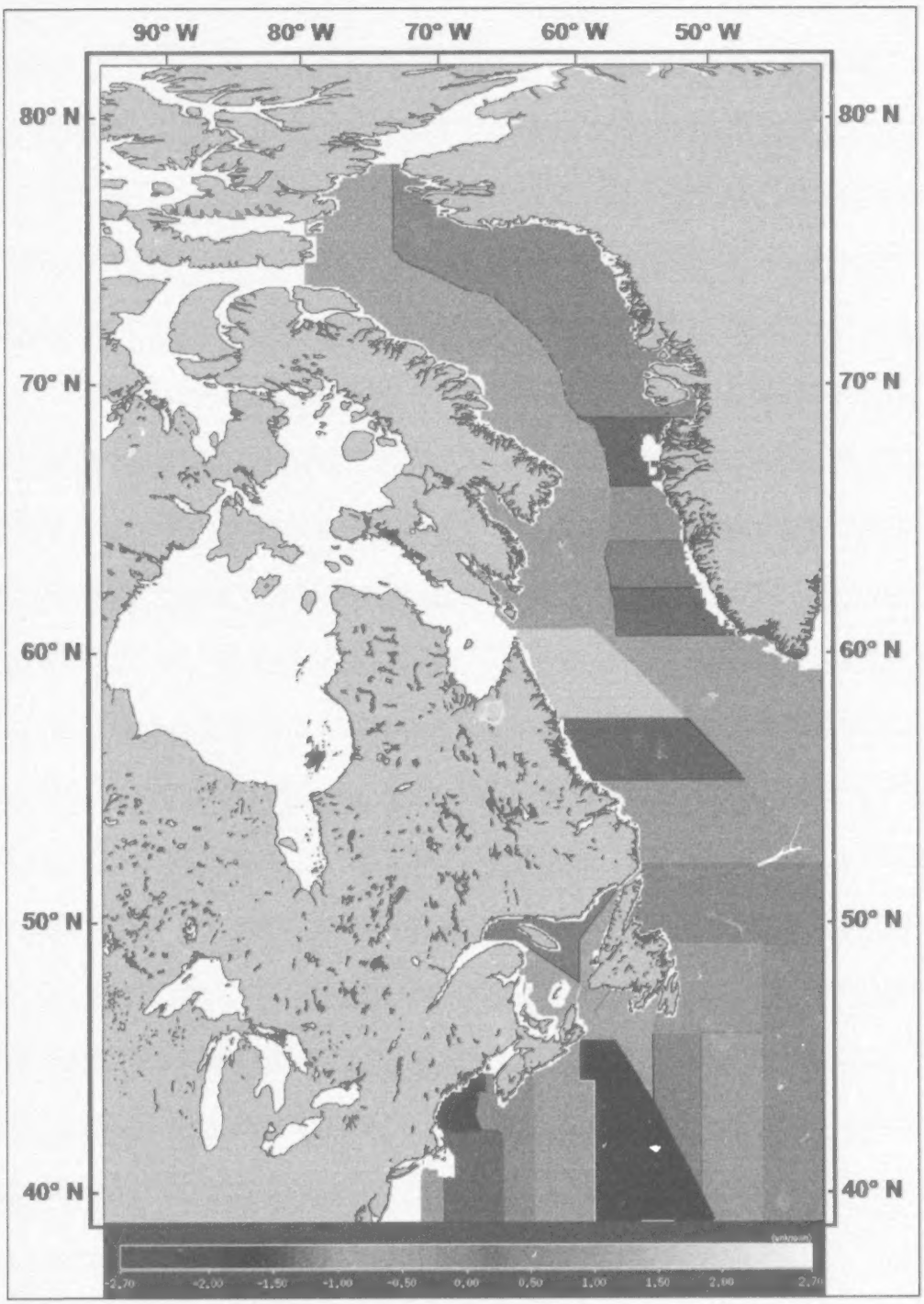

Figure APX2-2. Anomaly of the RITA index by NAFO divisions in 1999.

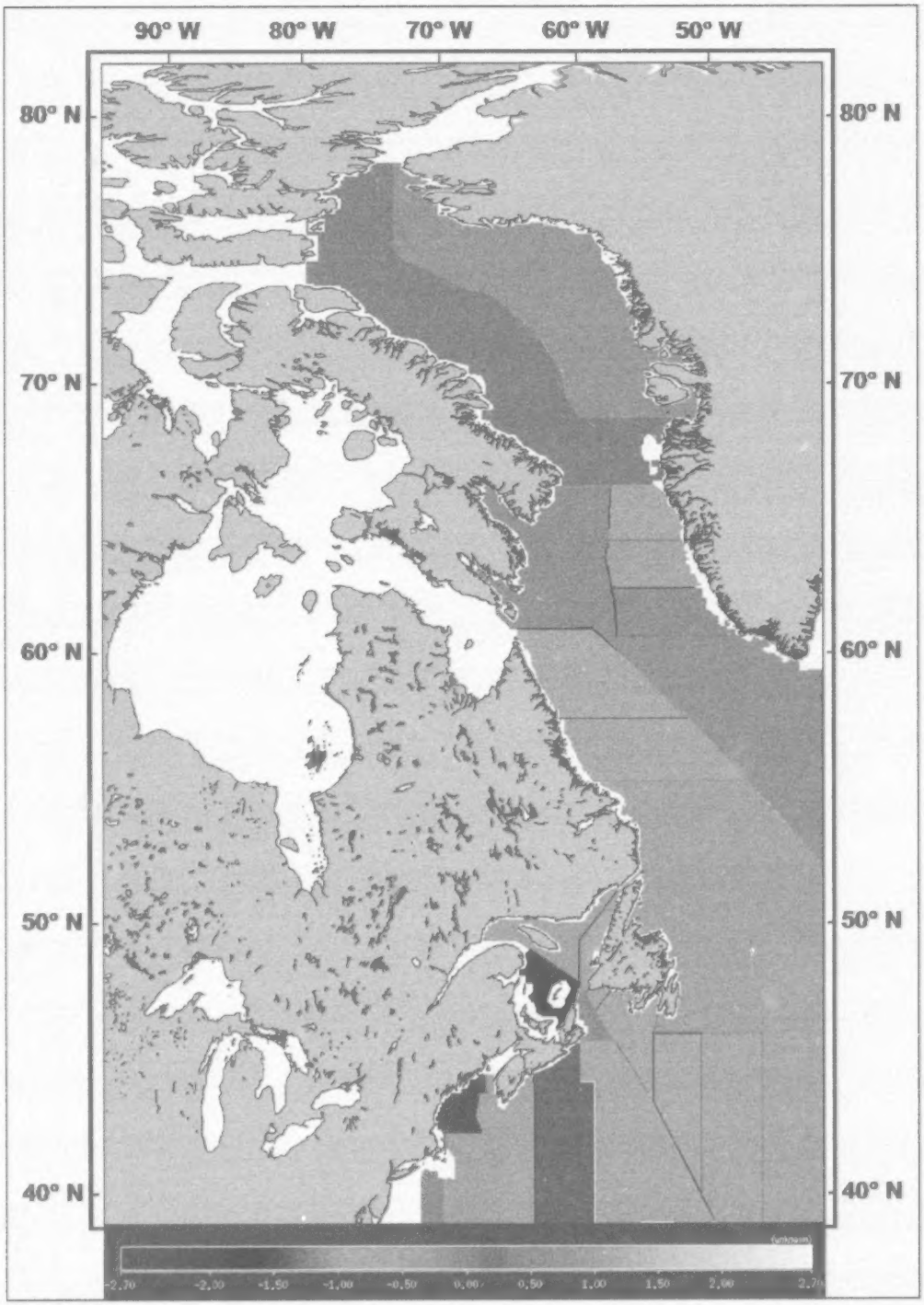

Figure APX2-3. Anomaly of the RITA index by NAFO divisions in 2000.

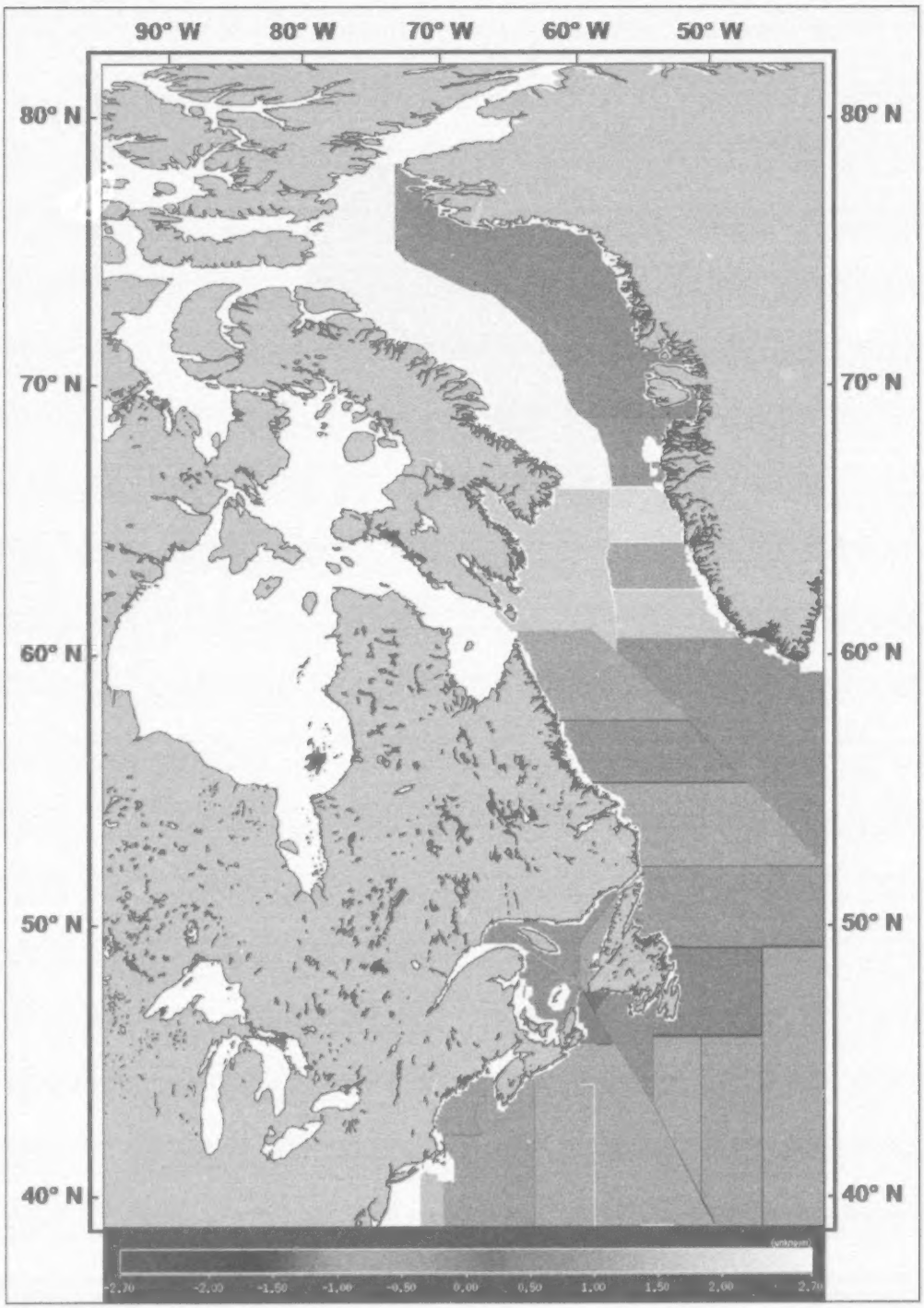

Figure APX2-4. Anomaly of the RITA index by NAFO divisions in 2001.

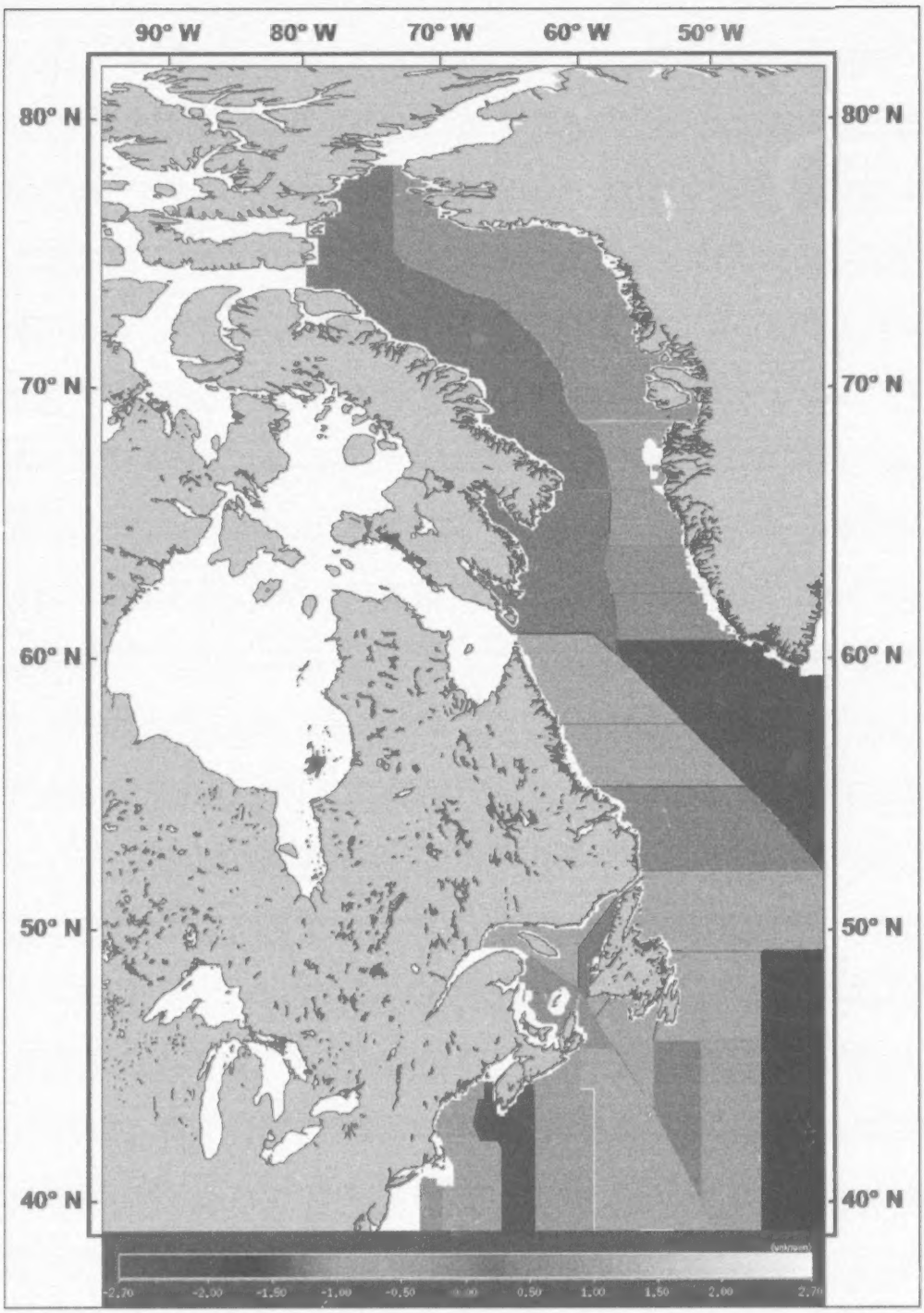

Figure APX2-5. Anomaly of the RITA index by NAFO divisions in 2002.

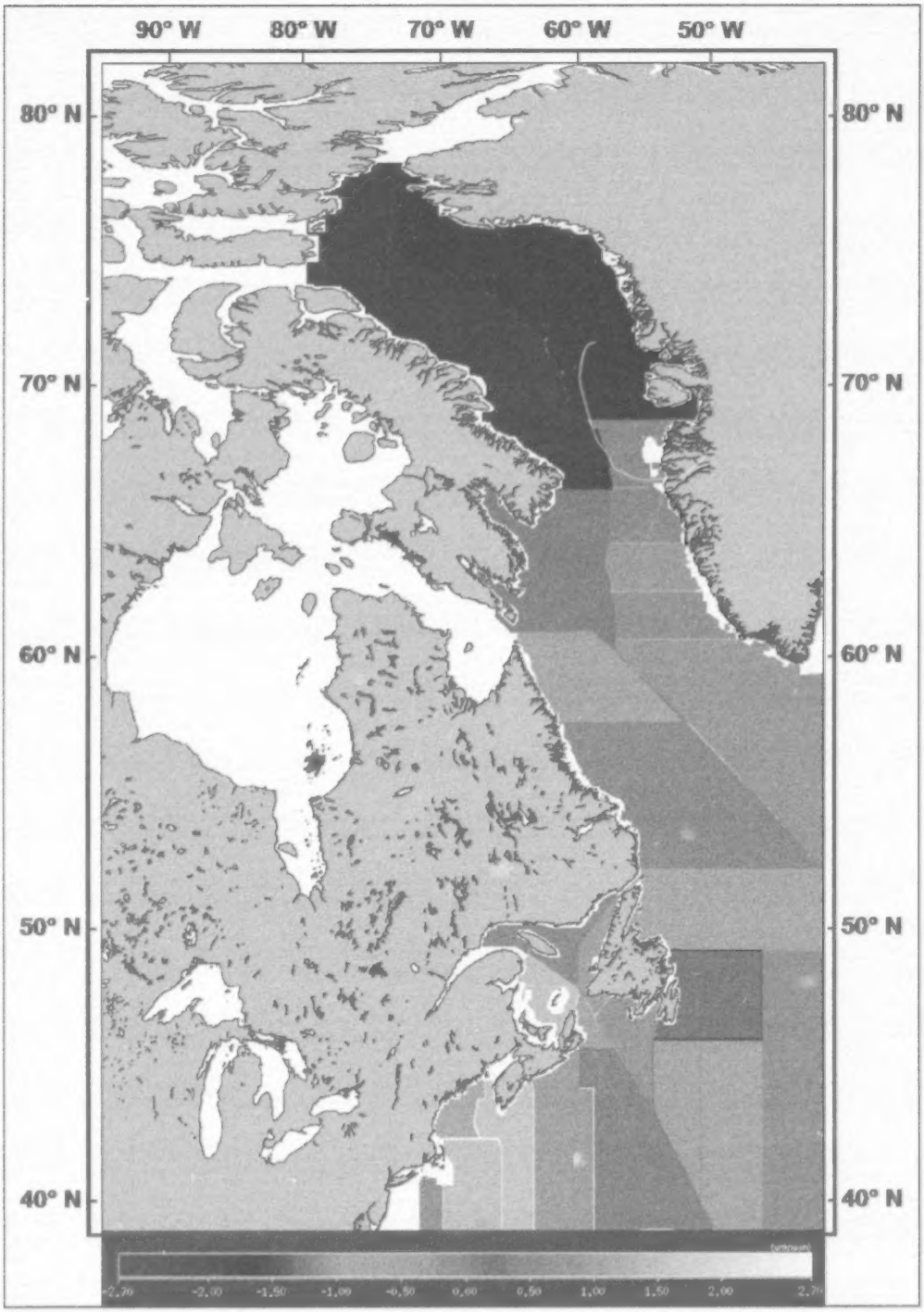

Figure APX2-6. Anomaly of the RITA index by NAFO divisions in 2003.

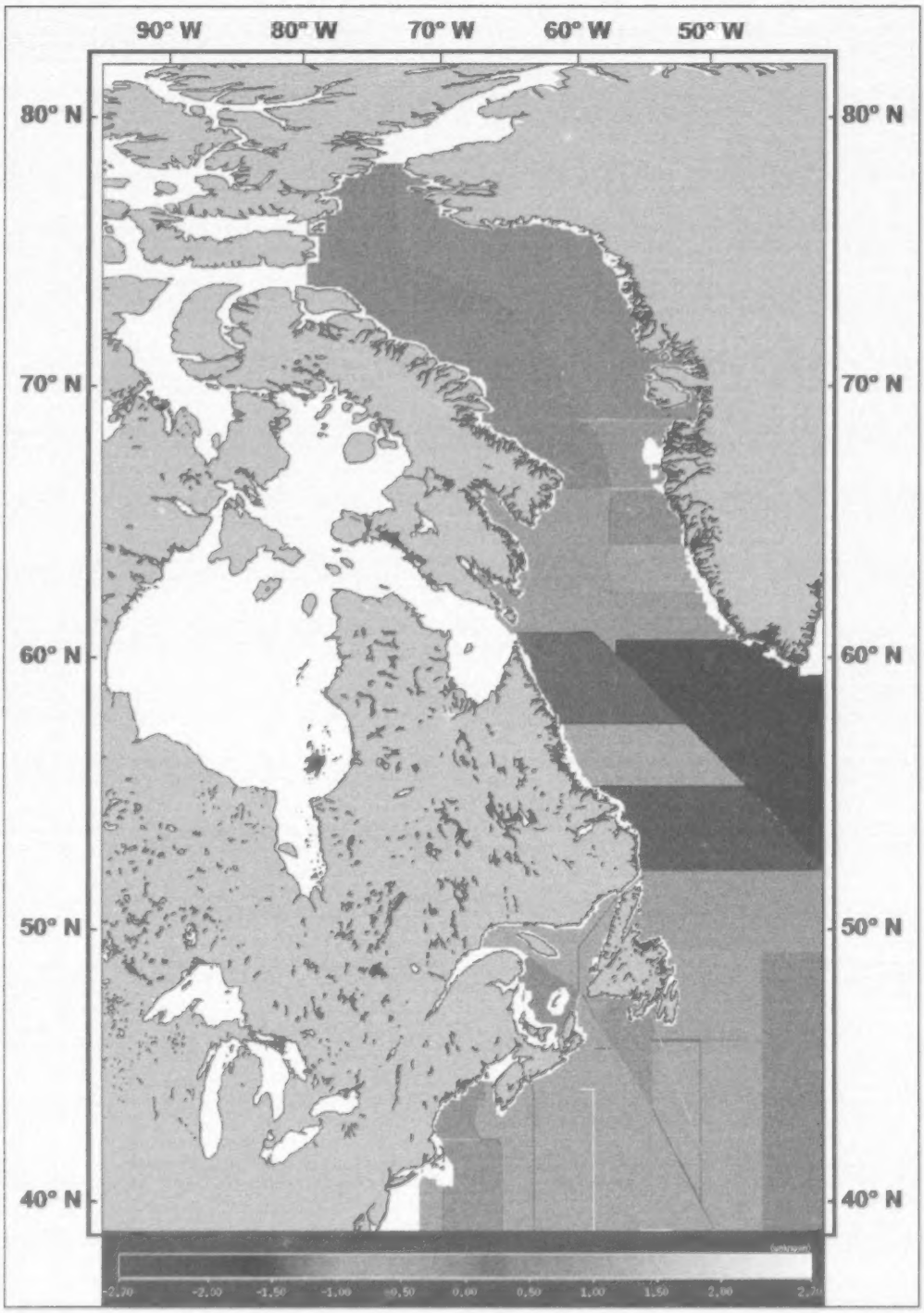

Figure APX2-7. Anomaly of the RITA index by NAFO divisions in 2004.

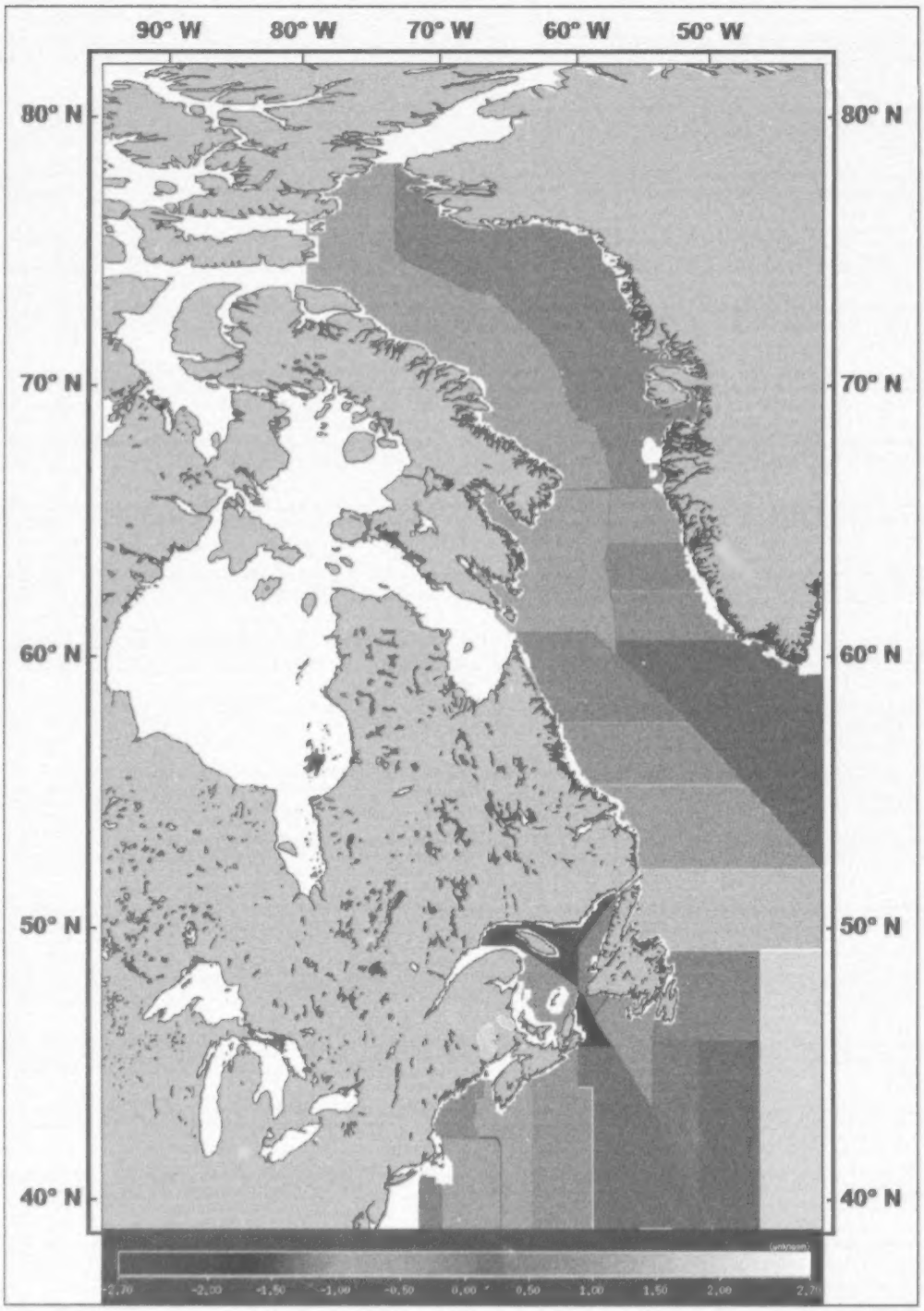

Figure APX2-8. Anomaly of the RITA index by NAFO divisions in 2005.

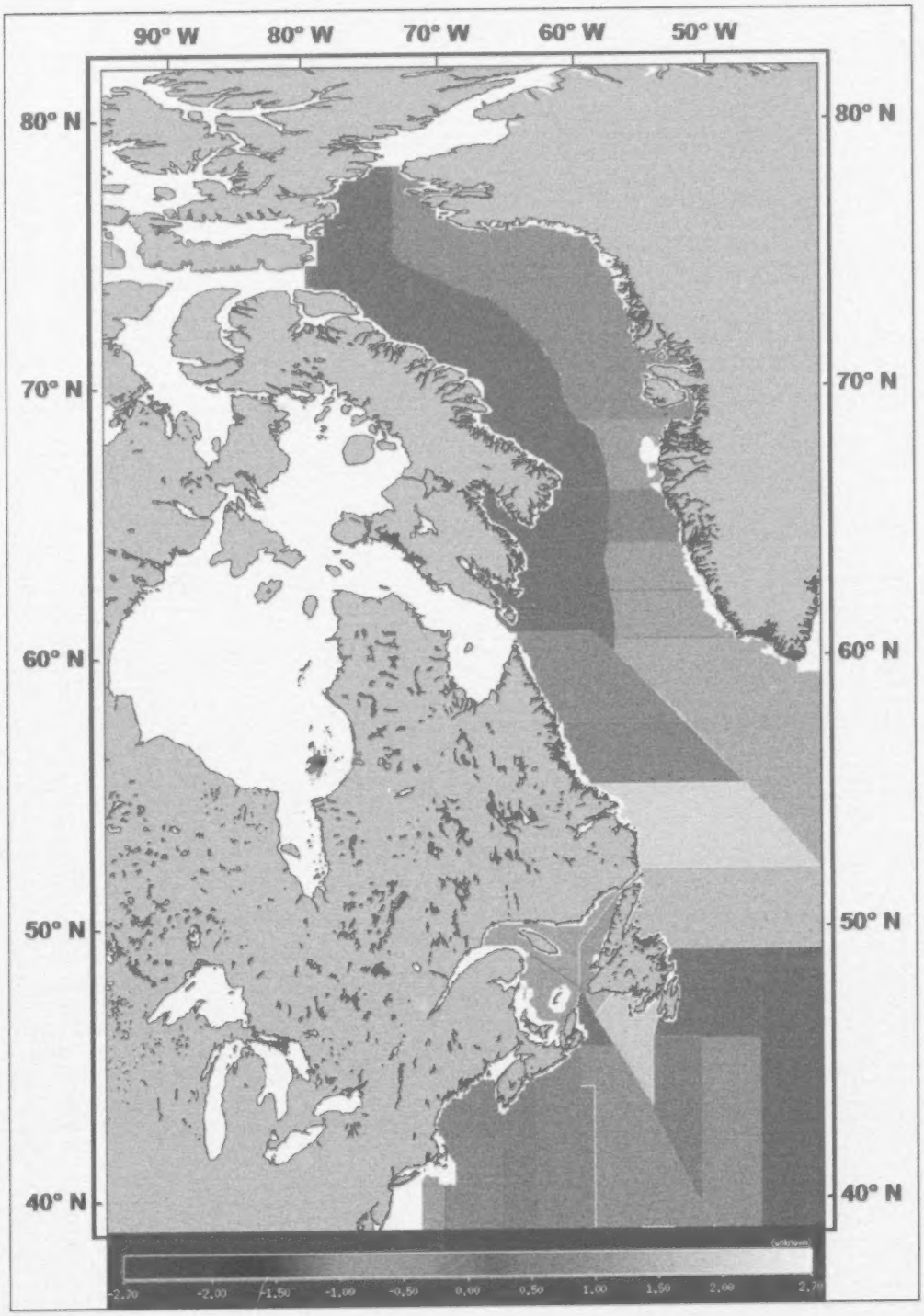

Figure APX2-9. Anomaly of the RITA index by NAFO divisions in 2006.

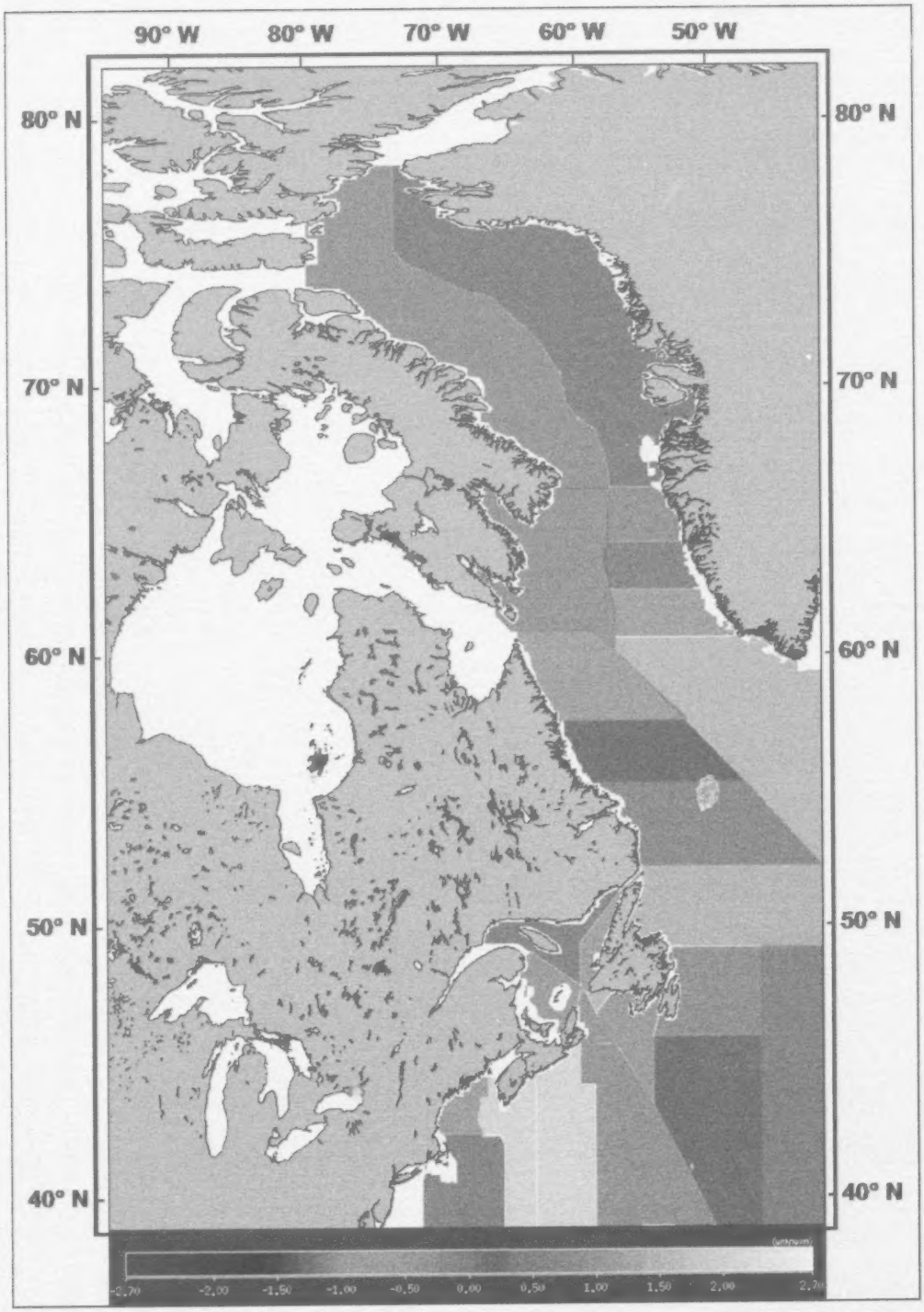

Figure APX2-10. Anomaly of the RITA index by NAFO divisions in 2007.

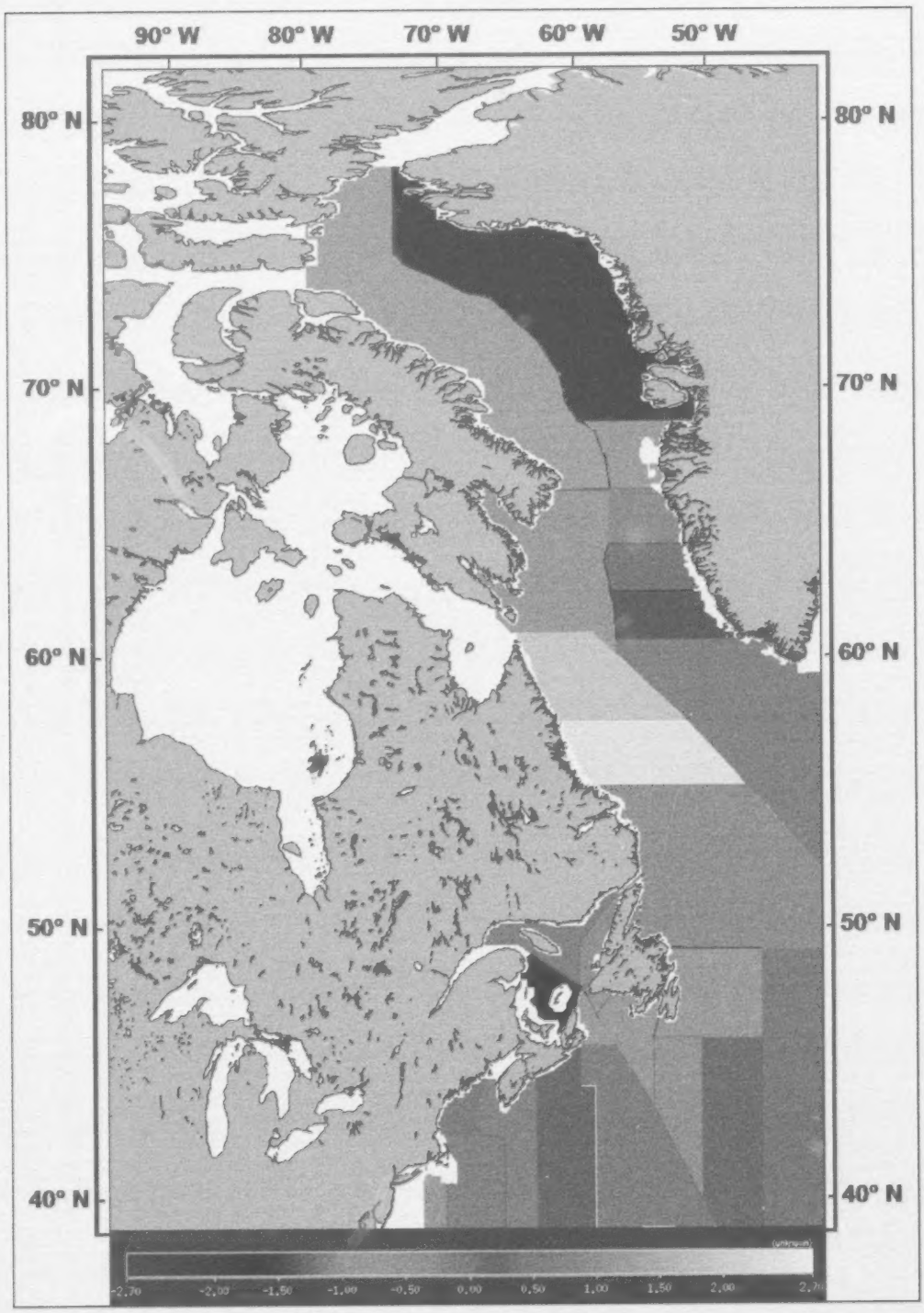

Figure APX2-11. Anomaly of the RITA index by NAFO divisions in 2008.

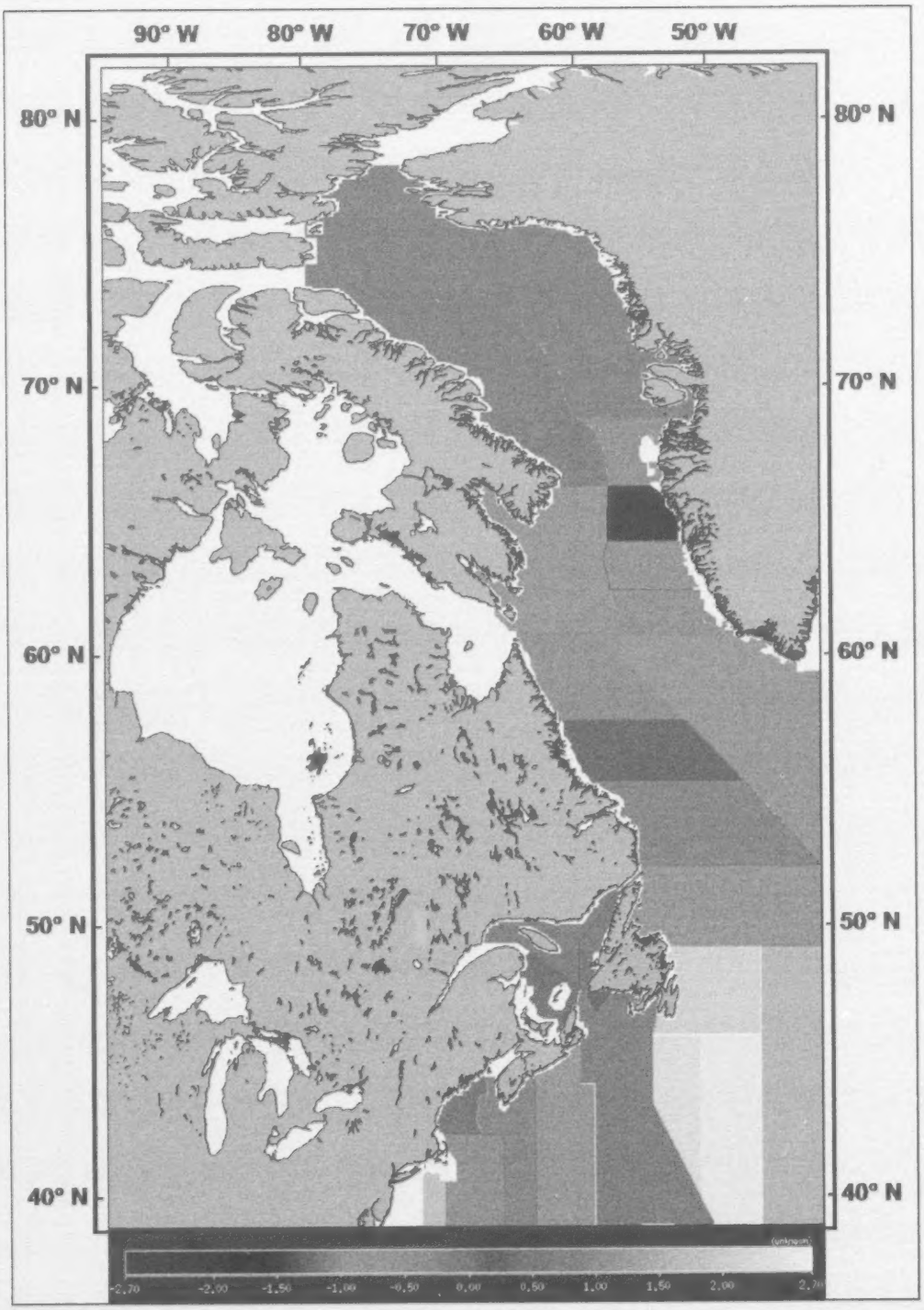

Figure APX2-12. Anomaly of the RITA index by NAFO divisions in 2009.

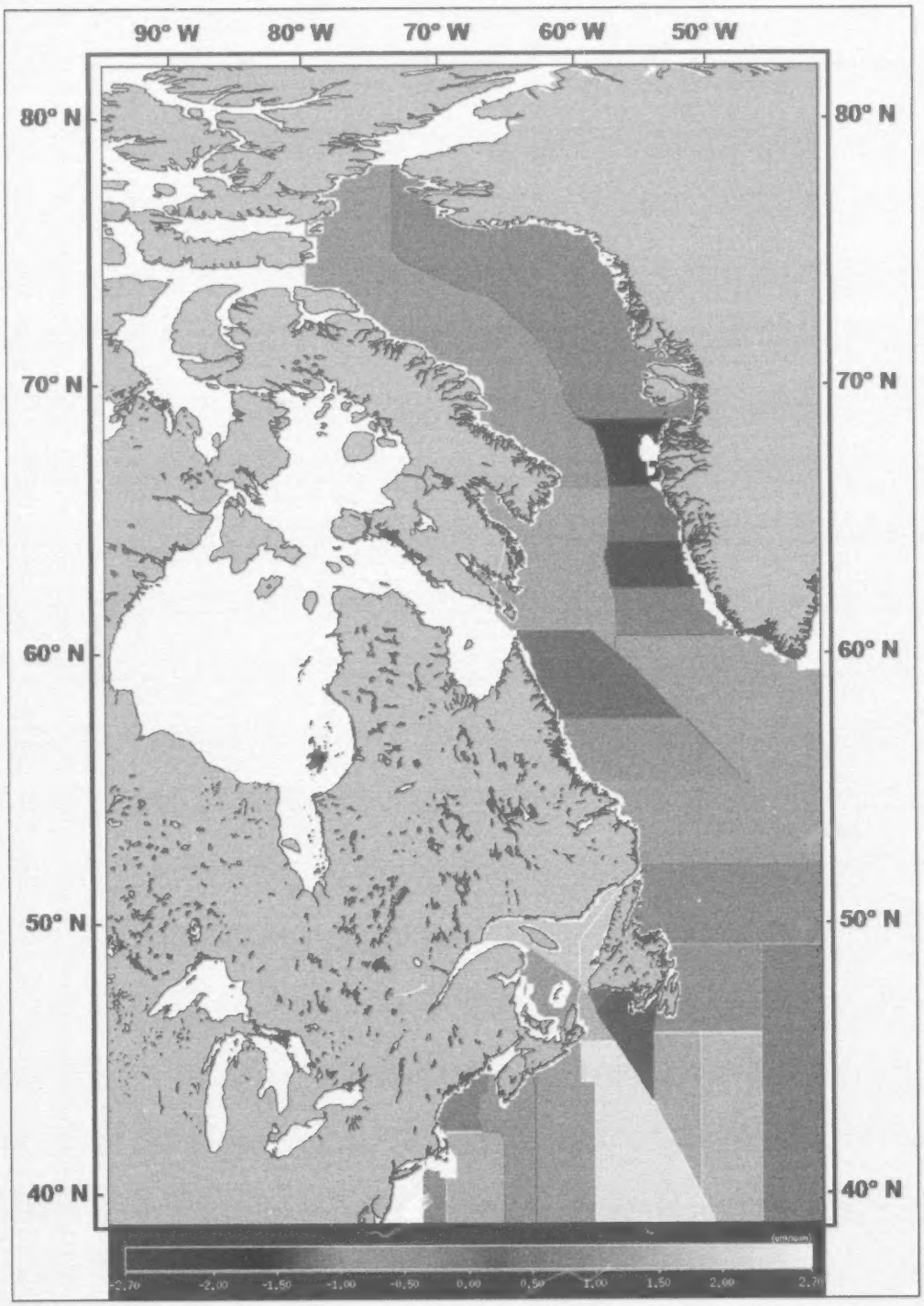

Figure APX2-13. Anomaly of the RITA index by NAFO divisions in 2010.

APPENDIX 3.

Figures APX3-1 until APX-3-5 show chlorophyll_a concentrations and abundance of *Calanus finmarchicus*, copepodites (1+2), for the five regions in the Labrador Sea (W, WC, C, EC, and E), from 2003 until 2013.

Figures APX3-6 until APX-3-10 present the sea surface temperature and copepods abundance from the same period. The figures display satellite measurements, Gaussian fits, as well as the date of sampling of copepods and their abundance.

Figure APX3-11 shows the relative importance of PCA's for the satellite-derived phytoplankton bloom characteristics.

Figure APX3-12 illustrates f-values for the fitted values and the corresponding residuals for the Loess regression on copepod abundance.

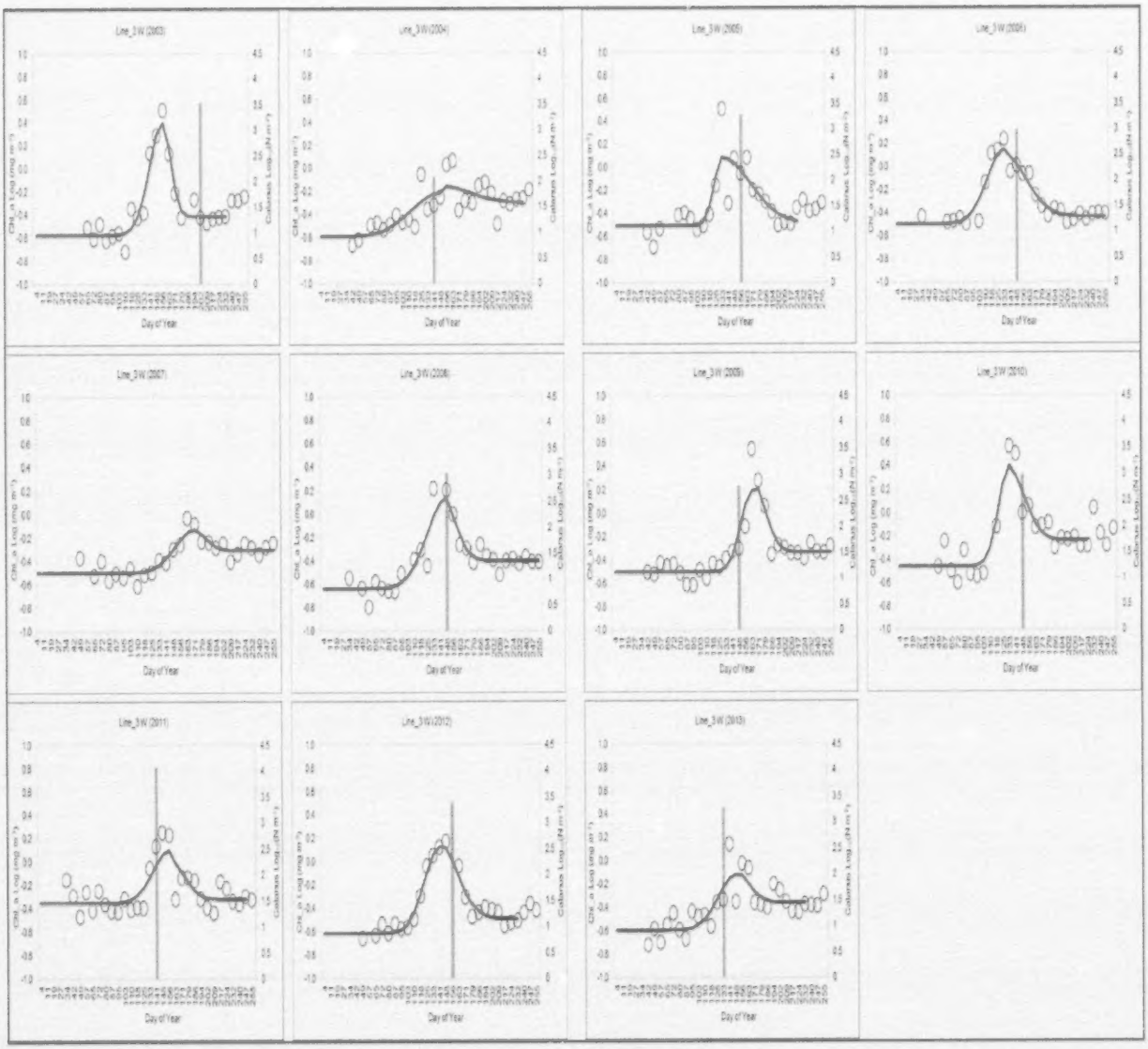

Figure APX3-1. Chlorophyll_a ($Log_{10}(mg\ m^{-3})$) and abundance of copepodites 1 and 2 ($Log_{10}(N\ m^{-2})$ for the Western region from 2003 until 2013. Pigment concentrations (open circles), Gaussian fitted (solid line) and copepods date of sampling and abundance (red line) are shown.

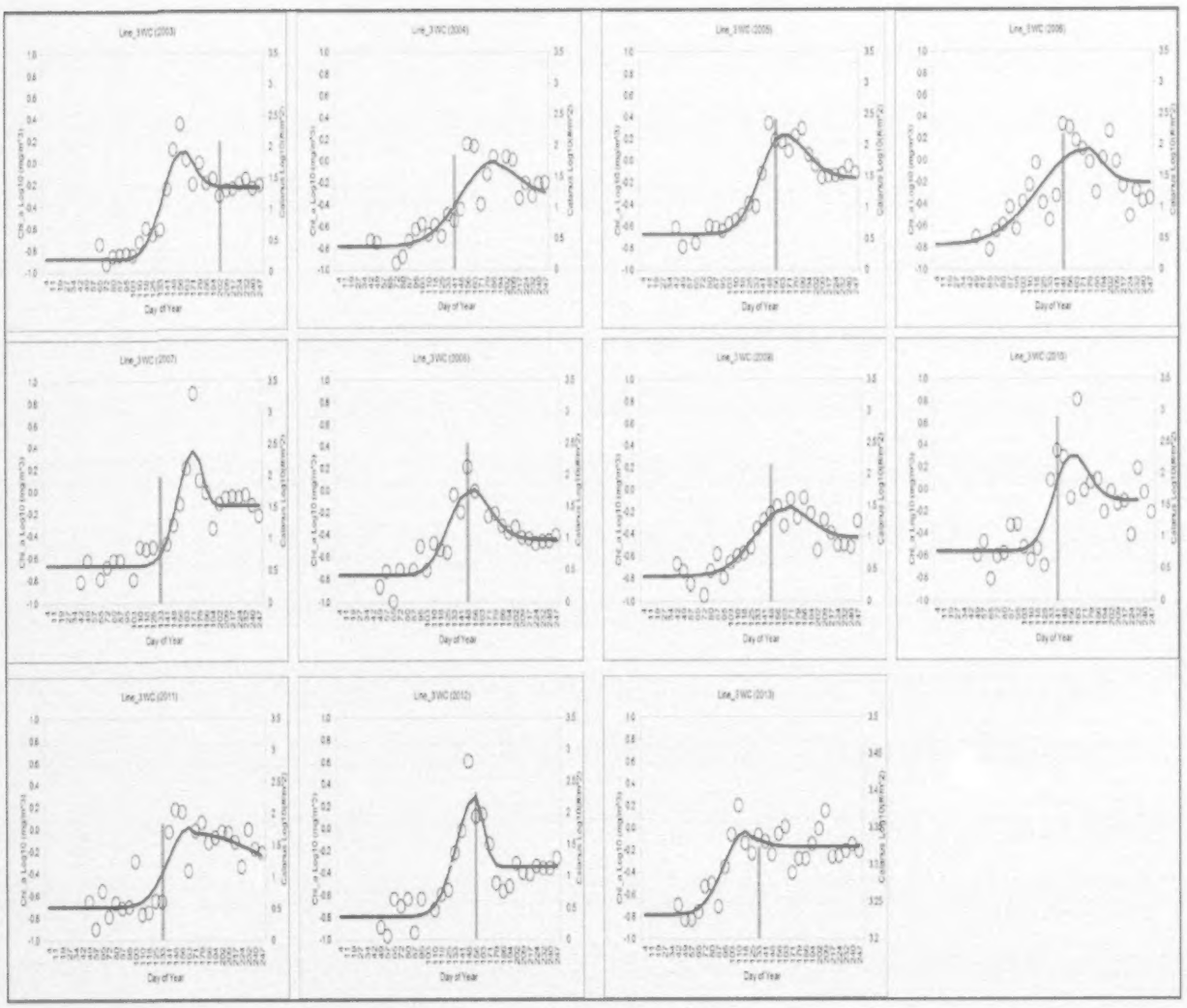

Figure APX3-2. Chlorophyll_a (Log_{10}(mg m^{-3})) and abundance of copepodites 1 and 2 (Log_{10}(N m^{-2})) for the Western-Central region from 2003 until 2013. Pigment concentrations (open circles), Gaussian fitted (solid line) and copepods date of sampling and abundance (red line) are shown.

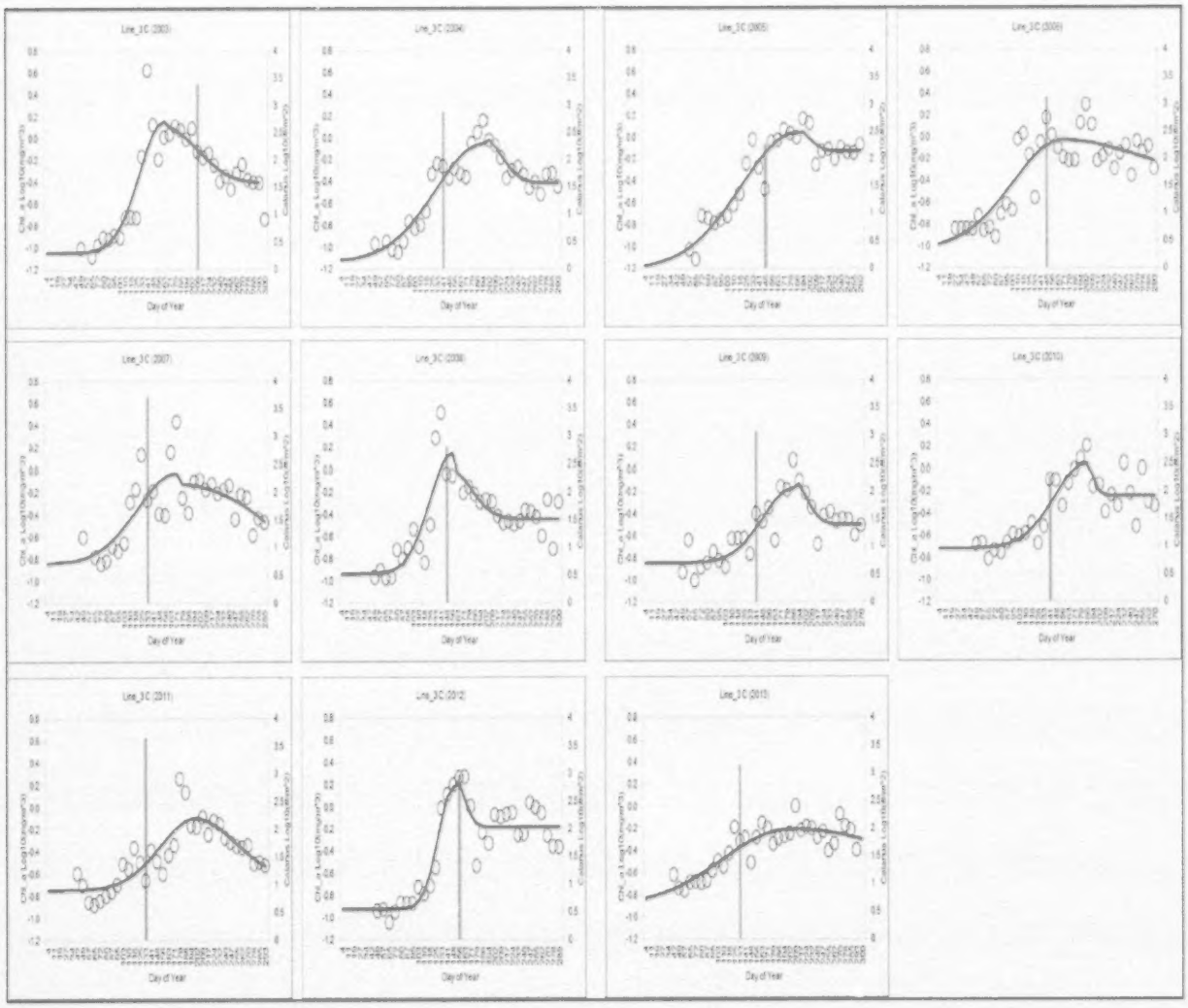

Figure APX3-3. Chlorophyll_a (Log_{10}(mg m^{-3})) and abundance of copepodites 1 and 2 (Log_{10}(N m^{-2})) for the Central region from 2003 until 2013. Pigment concentrations (open circles), Gaussian fitted (solid line) and copepods date of sampling and abundance (red line) are shown.

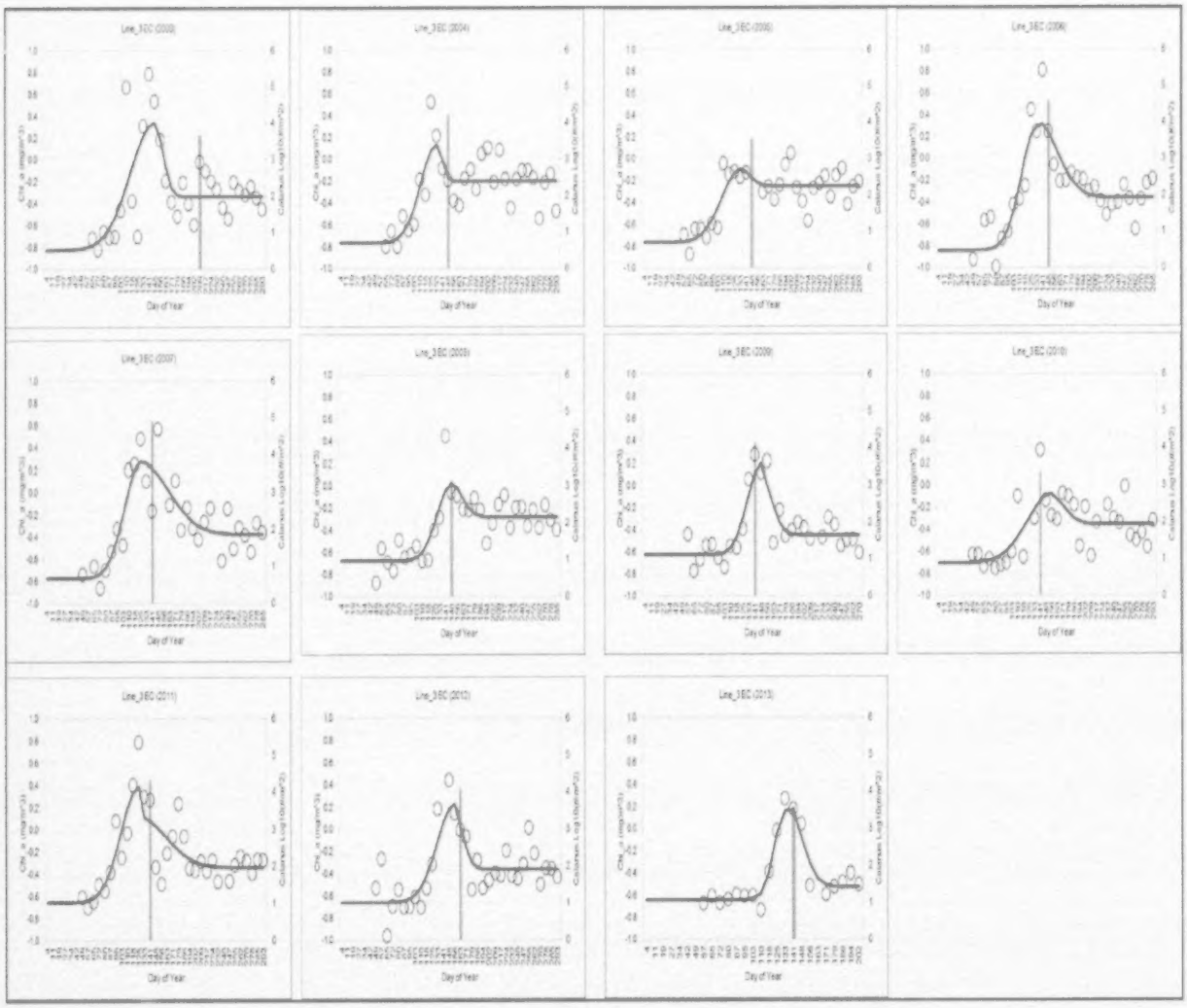

Figure APX3-4. Chlorophyll_a (Log_{10}(mg m^{-3})) and abundance of copepodites 1 and 2 (Log_{10}(N m^{-2}) for the Eastern-Central region from 2003 until 2013. Pigment concentrations (open circles), Gaussian fitted (solid line) and copepods date of sampling and abundance (red line) are shown.

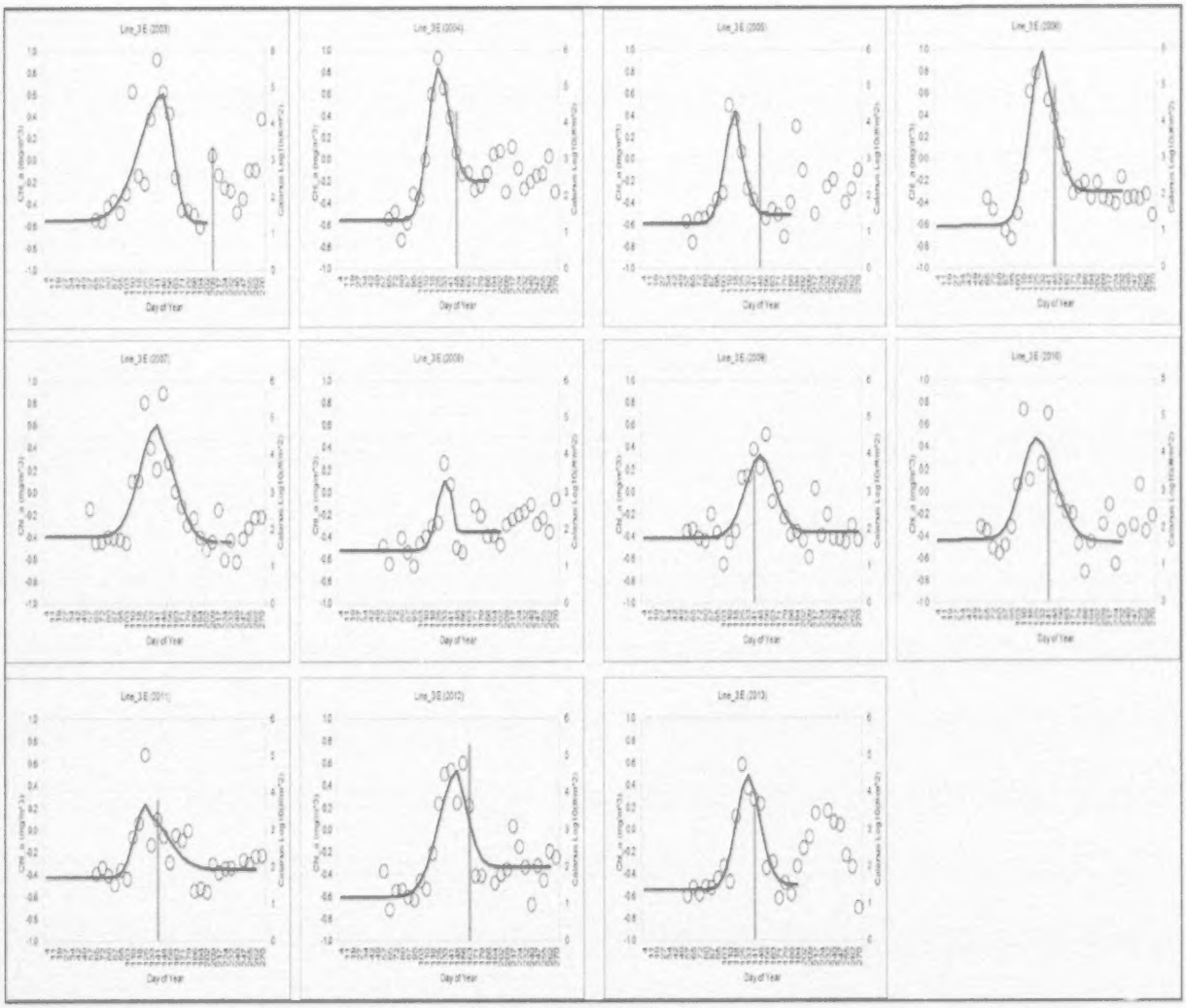

Figure APX3-5. Chlorophyll_a (Log_{10}(mg m^{-3})) and abundance of copepodites 1 and 2 (Log_{10}(N m^{-2}) for the Eastern region from 2003 until 2013. Pigment concentrations (open circles), Gaussian fitted (solid line) and copepods date of sampling and abundance (red line) are shown.

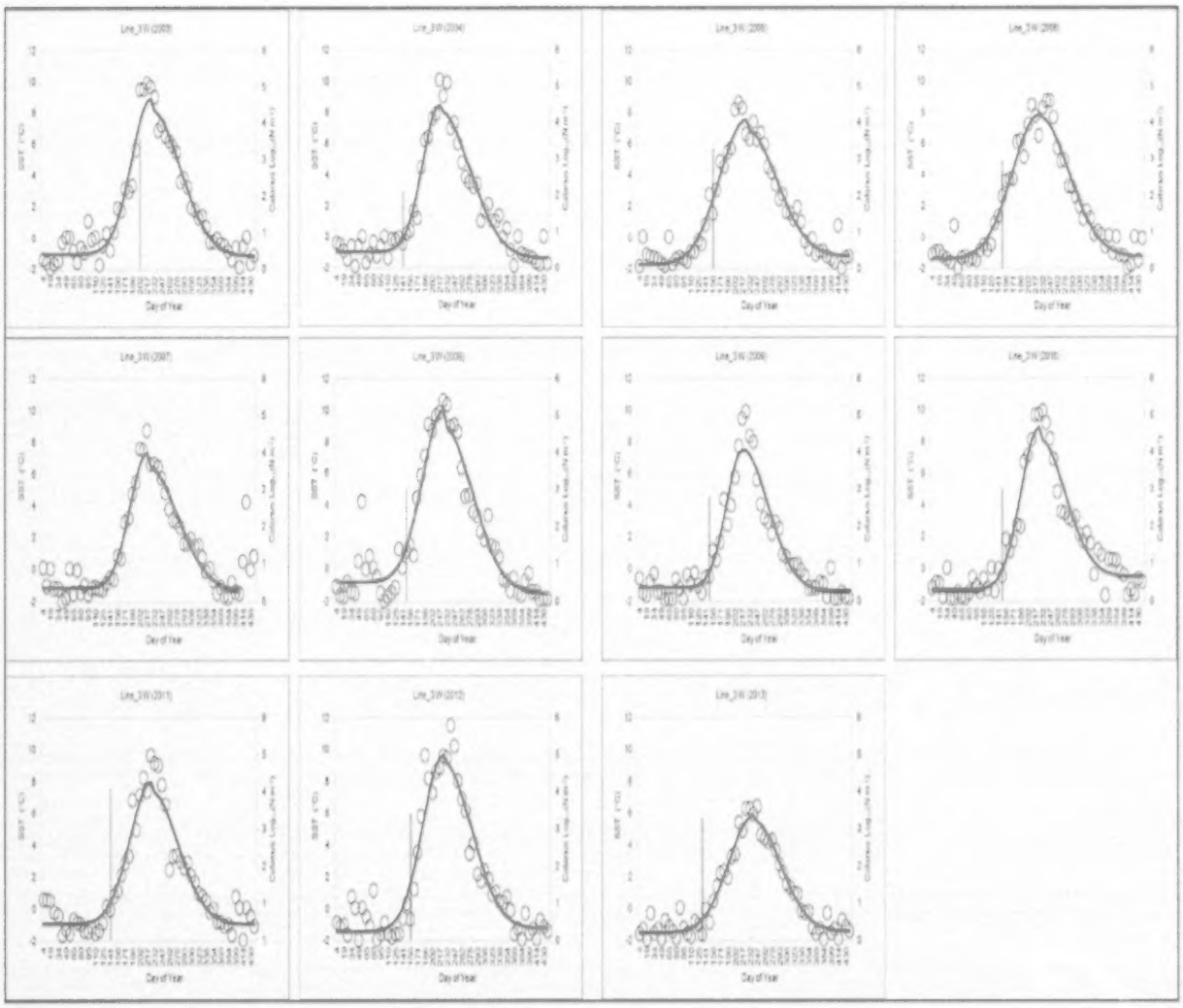

Figure APX3-6. Sea Surface Temperature (°C) and abundance of copepodites 1 and 2 ($Log_{10}(N\ m^{-2})$) for the Western region from 2003 until 2013. SST (open circles), Gaussian fitted (solid line) and copepods date of sampling and abundance (red line) are shown.

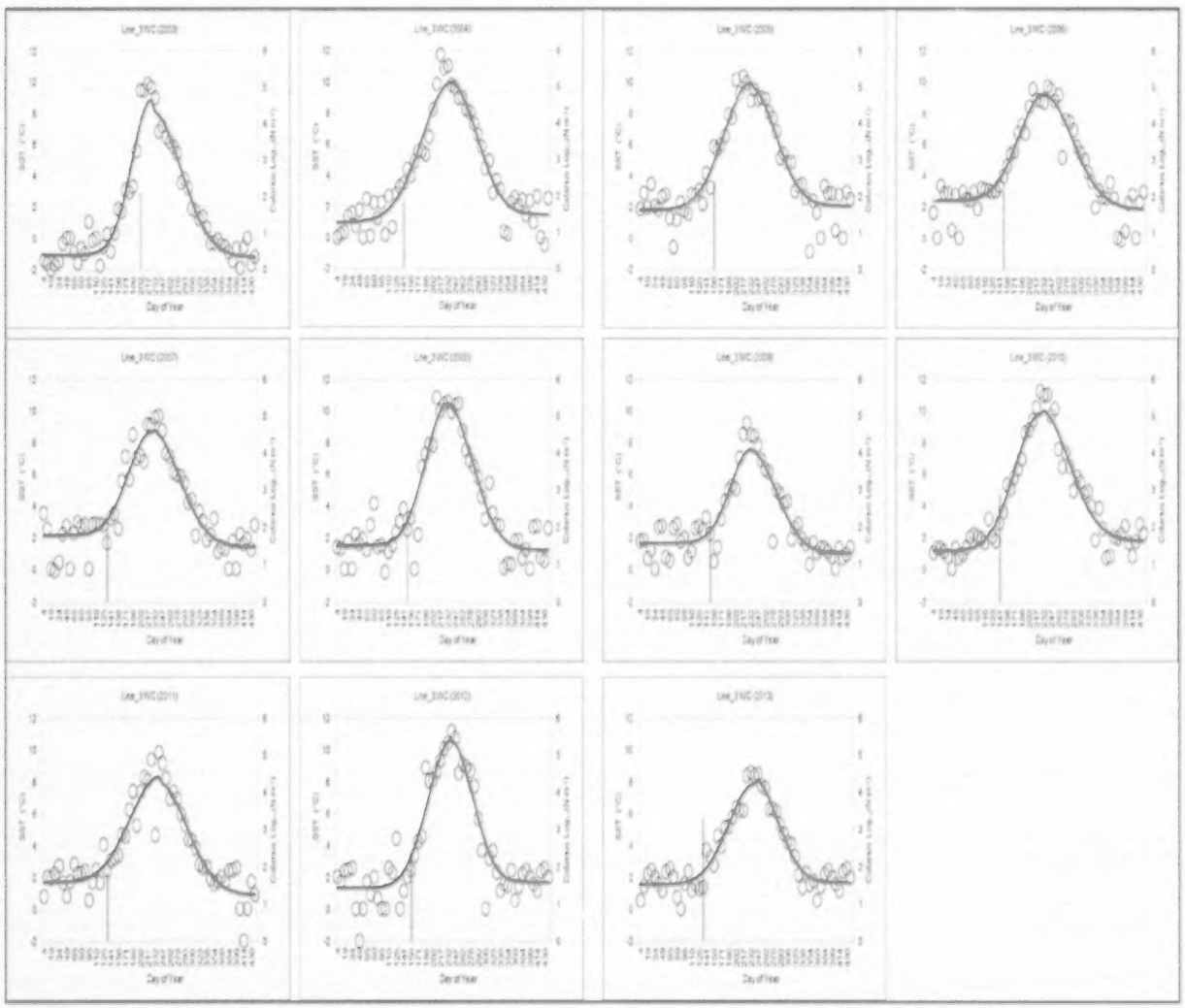

Figure APX3-7. Sea Surface Temperature (°C) and abundance of copepodites 1 and 2 ($Log_{10}(N\ m^{-2})$ for the Western-Central region from 2003 until 2013. SST (open circles), Gaussian fitted (solid line) and copepods date of sampling and abundance (red line) are shown.

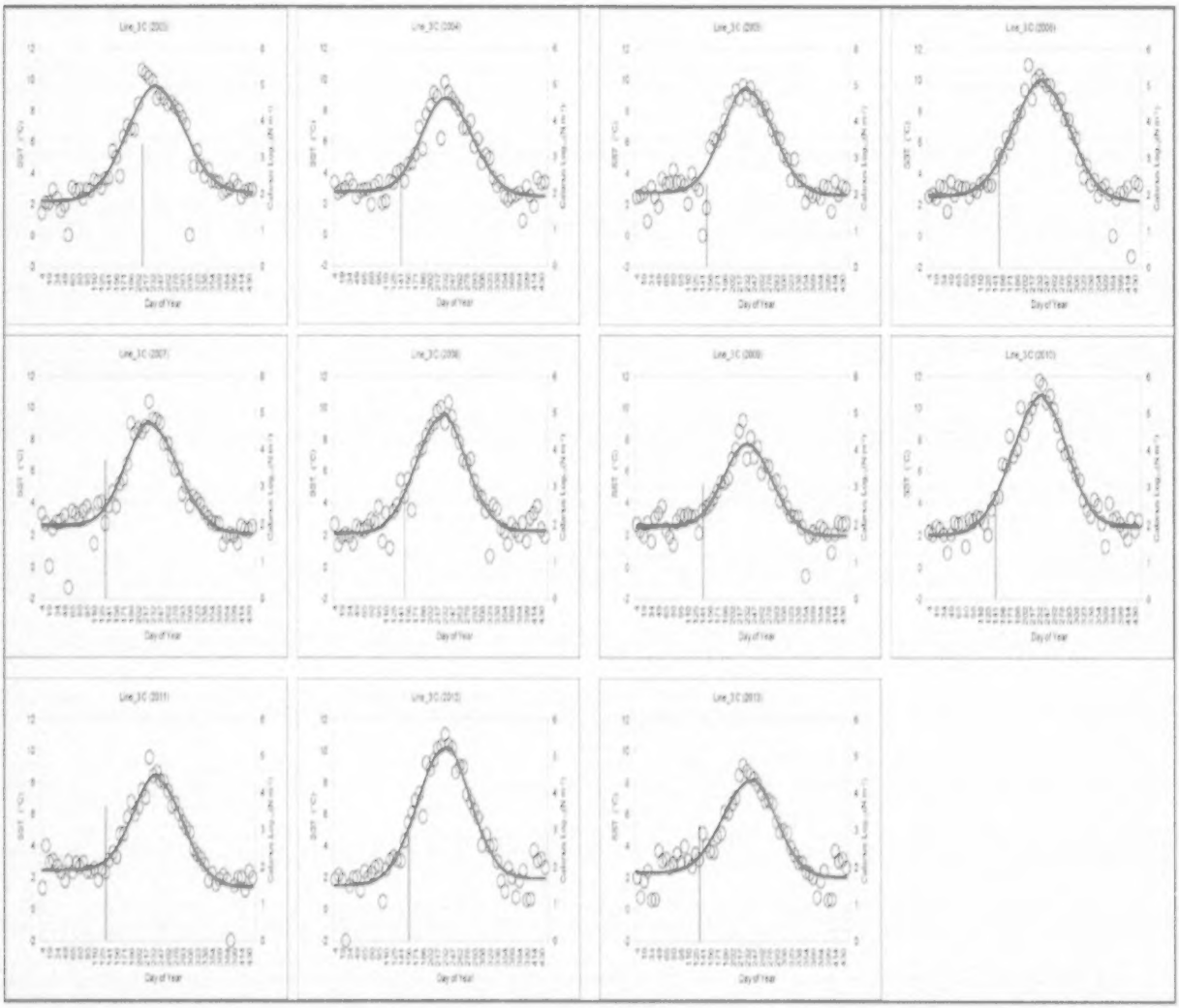

Figure APX3-8. Sea Surface Temperature (°C) and abundance of copepodites 1 and 2 ($Log_{10}(N\ m^2)$) for the Central region from 2003 until 2013. SST (open circles), Gaussian fitted (solid line) and copepods date of sampling and abundance (red line) are shown.

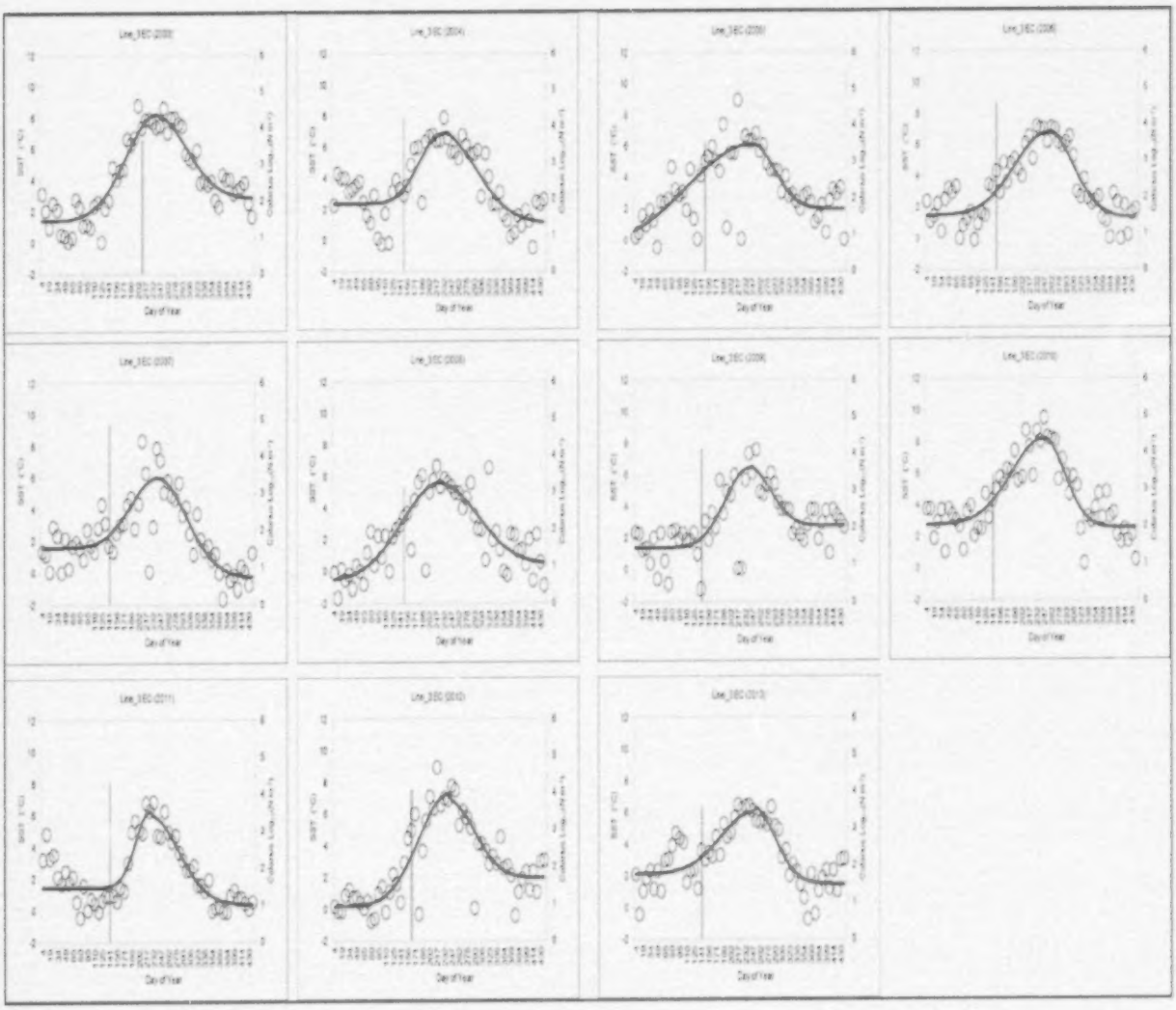

Figure APX3-9. Sea Surface Temperature (°C) and abundance of copepodites 1 and 2 ($Log_{10}(N\ m^{-2})$) for the Eastern-Central region from 2003 until 2013. SST (open circles), Gaussian fitted (solid line) and copepods date of sampling and abundance (red line) are shown.

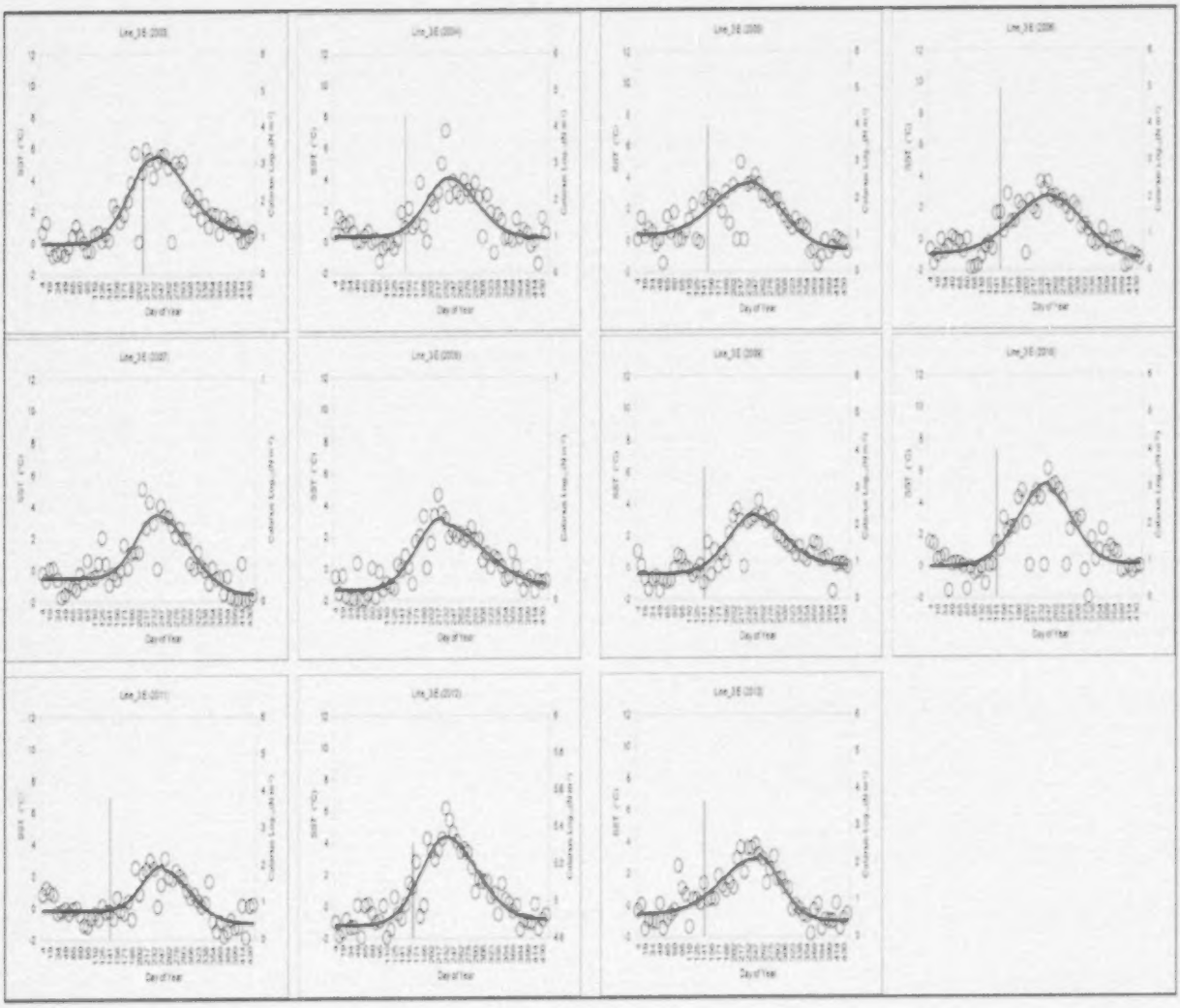

Figure APX3-10. Sea Surface Temperature (°C) and abundance of copepodites 1 and 2 ($Log_{10}(N\ m^{-2})$ for the Eastern region from 2003 until 2013. SST (open circles), Gaussian fitted (solid line) and copepods date of sampling and abundance (red line) are shown.

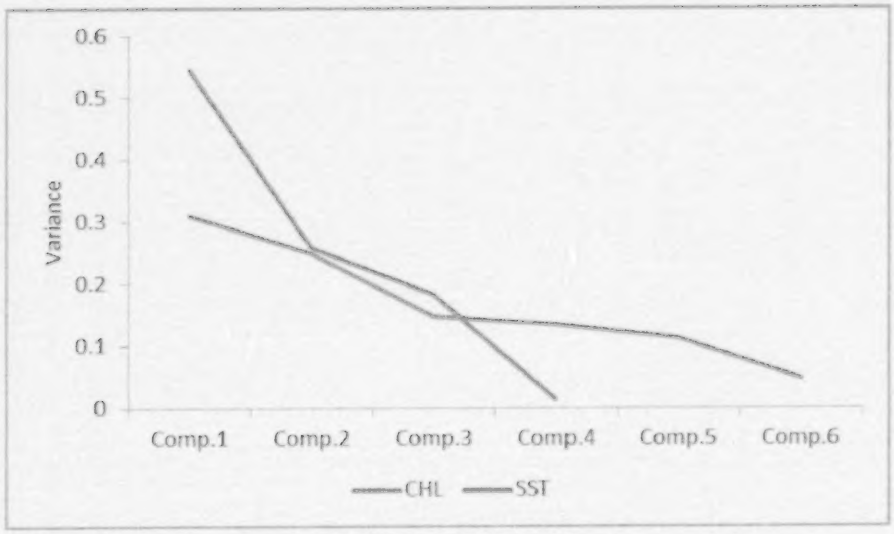

Figure APX3-11. Relative importance of Principal Components of the satellite-derived phytoplankton bloom characteristics (blue line) and warming Sea Surface Temperature (red line) for the pooled five regions in Labrador Sea (W, WC, C, EC and E), and eleven years (2003 until 2013).

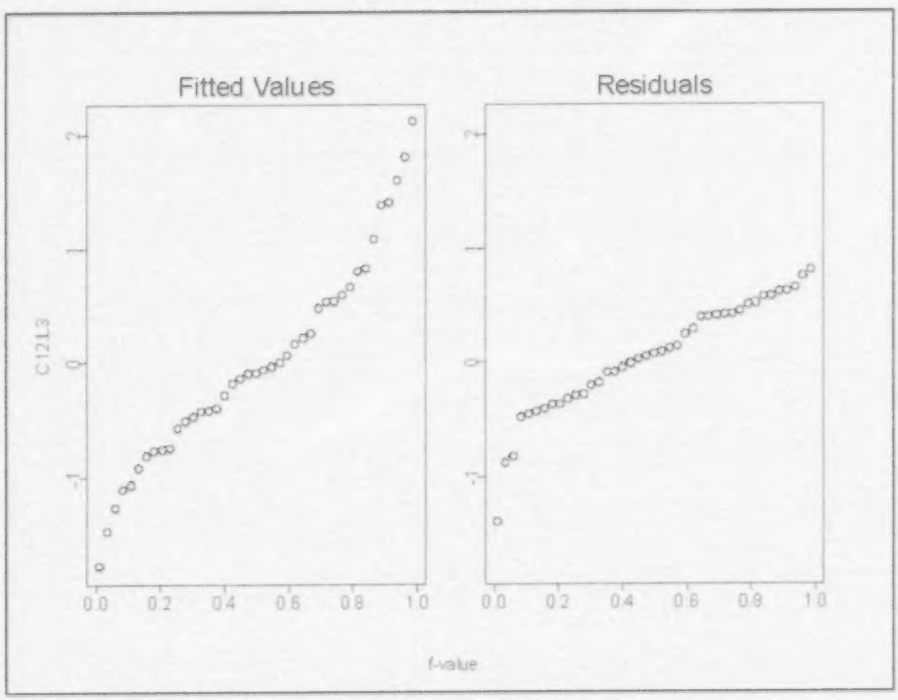

Figure APX3-12. f-values for the fitted values (left) and the corresponding residuals (right) for the Loess regression on Calanus (copepodites 1+2) abundance in the Labrador Sea.

APPENDIX 4.

Graphs APX4-1 shows the relative importance of PCA's of the satellite-derived phytoplankton bloom characteristics for the pooled five regions in Western Greenland (1A, 1B, 1C 1D and 1E), between 1998 and 2010. Figure APX4-2 illustrates f-values of the fitted values and the corresponding residuals for the Loess regression on *Pandalus borealis* (age 2) abundance lagged 2 years.

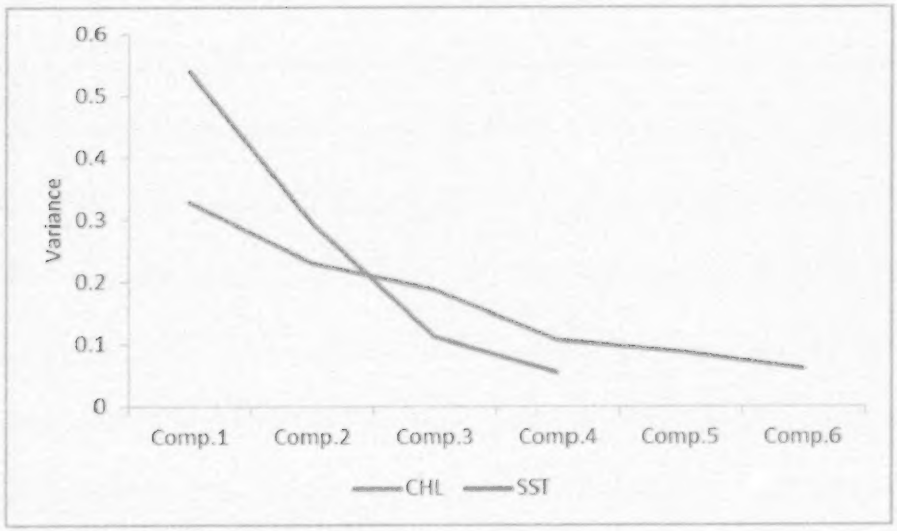

Figure APX4-1. Relative importance of Principal Components of the satellite-derived phytoplankton bloom characteristics (blue line) and warming Sea Surface Temperature (red line), for the pooled five regions in Western Greenland (1A, 1B, 1C, 1D and 1E), and thirteen years (1998 until 2010).

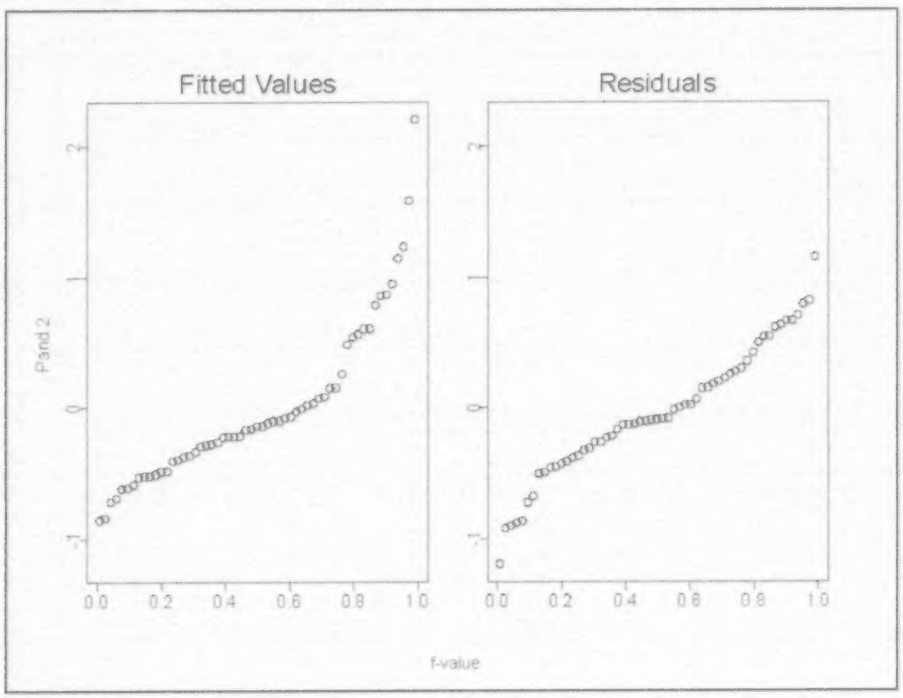

Figure APX4-2. f-values for the fitted values (left) and the corresponding residuals (right) for the Loess regression on Pandalus borealis (age 2) abundance in Western Greenland.